Binding Analysis of Novel Cyclic Naphthalene Diimide with DNA

A THESIS SUBMITTED TO THE GRADUATE SCHOOL OF ENGINEERING AT KYUSHU INSTITUTE OF TECHNOLOGY IN PARTIAL FULFILLMENT OF THE REQUIREMENTS FOR THE DEGREE OF DOCTOR OF ENGINEERING IN APPLIED CHEMISTRY

By

Md. Monirul Islam

September, 2015

Department of Applied Chemistry,

Graduate School of Engineering, Kyushu Institute of

Technology, Tobata, Kitakyushu, Fukuoka, Japan

Doctoral thesis supervisor and chair of doctoral thesis approval committee

Shigeori Takenaka, PhD

Professor, Department of Applied Chemistry,

Graduate School of Engineering, Kyushu Institute of Technology,

Tobata, Kitakyushu, Fukuoka, Japan.

The members of doctoral thesis approval committee

Akihiko Tsuge, PhD

Professor, Department of Applied Chemistry,

Graduate School of Engineering, Kyushu Institute of Technology,

Tobata, Kitakyushu, Fukuoka, Japan.

Teruhisa Ohno, PhD

Professor, Department of Applied Chemistry,

Graduate School of Engineering, Kyushu Institute of Technology,

Tobata, Kitakyushu, Fukuoka, Japan.

Shinobu Sato, PhD

Associate Professor, Department of Applied Chemistry,

Graduate School of Engineering, Kyushu Institute of Technology,

Tobata, Kitakyushu, Fukuoka, Japan.

Shyam Sudhir Pandey, PhD

Associate Professor, Department of Biological Functions Engineering

Graduate School of Life Science and Systems Engineering,

Kyushu Institute of Technology, Wakamatsu, Kitakyushu, Fukuoka, Japan.

Dedication

To my beloved Parents

Acknowledgements

First of all, I praise and give thanks to the almighty creator ALLAH for giving me the confidence, the wisdom, the strength and ability to overcome all the obstacles to the completion of this research work.

I would like to express my sincere gratitude and cordial admiration to my supervisor Professor Shigeori Takenaka for giving me the opportunity to engage his group. I appreciate his contributions of valuable time, scientific idea, guidance and encouragement.

I would like to express my gratitude to Associate professor Shinobu Sato for her valuable guidance and suggestions for conducting my doctoral study.

I would like to appreciate to Professor Akihiko Tsuge, Professor Teruhisa Ohno and Associate professor Shyam Sudhir Pandey for their valuable comments to polish this thesis.

I would like to thank all the lab members of Professor Takenaka's group for their kind support.

I acknowledge to Kyushu Institute of Technology for the support, excellent facilities, and aid for conferences, which helped me a lot both scientifically and socially. I am also grateful to the International student office section, Kyushu Institute of technology for their constant help throughout my period of stay in Japan.

I am very grateful to Rotary Yoneyama scholarship foundation for giving me a scholarship to continue my doctoral study.

Finally, I thank my parents, my wife, my brother, my sister, and my friends for their support and encourage to pursue my doctoral degree.

Md. Monirul Islam

September, 2015

Achievements

List of Publications:

1. M.M. Islam, S. Fujii, S. Sato, T. Okauchi, S. Takenaka, Thermodynamics and Kinetic Studies in the Binding Interaction of Cyclic Naphthalene Diimide Derivatives with Double Stranded DNAs, *Bioorg. Med. Chem*. 23 (2015) 4769–4776. doi:10.1016/j.bmc.2015.05.046 (Impact factor: 2.793)
2. M.M. Islam, S. Fujii, S. Sato, T. Okauchi, S. Takenaka, A Selective G-Quadruplex DNA-Stabilizing Ligand Based on a Cyclic Naphthalene Diimide Derivative, *Molecules* 20 (2015) 10963-10979. doi:10.3390/molecules200610963 (Impact factor: 2.416)

Related Publication not included in this thesis:

1. Y. Esaki, M.M. Islam, S. Fujii, S. Sato, S. Takenaka, Design of tetraplex specific ligands: cyclic naphthalene diimide, *Chem. Commun.* 50 (2014) 5967-5969. DOI:10.1039/C4CC01005A (Impact factor: 6.834)
2. M.M. Islam, S. Fujii, S. Sato, T. Okauchi, S. Takenaka, Interaction studies of ferrocenyl cyclic naphthalene diimide (cFND) derivatives with genomic promoter, thrombin binding aptamer and human telomeric DNA G-quadruplexes (to be submitted to RSC advances) (Impact factor: 3.84)

List of conference presentations:

1. M.M. Islam, S. Fujii, S. Sato, S. Takenaka, Thermodynamic investigation of Cyclic Naphthalene Diimides Derivatives with Calf Thymus DNA, Poster presentation at The 41st International Symposium on Nucleic Acid Chemistry, Kitakyushu International Conference center, Kitakyushu, Fukuoka, Japan, November 5-7, 2014.
2. M.M. Islam**,** Y. Esaki, S. Sato, S. Taknaka, Telomerase inhibition by cyclic naphthalene diimide as a tetraplex binder, Oral presentation at 63rd Annual Meeting of The Society of Polymer Science, Japan, Nagoya Congress Center, Japan, May 28-30, 2014.
3. M.M. Islam, S. Sato, S. Takenaka, Cyclic naphthalene diimide aiming at tetraplex DNA specific ligand. Poster presentation at 7th International Symposium on Nanomedicine, Nakamura Centenary Hall of Kyushu Institute of Technology (Kitakyushu), Japan. November 7-9, 2013.
4. M.M. Islam, I. Czerwinska, S. Fujii, S. Sato, S. Takenaka. Interactions of a novel cyclic naphthalene diimide derivative with double stranded DNA bearing different sequences. Oral presentation at the Twelfth Asian Conference on Analytical Sciences (Asianalysis XII), Maidashi campus of Kyushu University (Fukuoka), Japan, September 22-24, 2013.
5. M.M. Islam**,** S. Sato, S, Takenaka, Thermodynamic and kinetic behaviors of cyclic naphthalene diimide derivative under interaction with double stranded DNA. Poster presentation at 50th chemistry related branch joint Kyushu tournament, Kitakyushu International Conference Center and AIM building, Kitakyushu, Japan, July 6, 2013.

Contents

Abstract

In recent times, DNA structures are one of the attractive research targets because of their vital biological roles and remarkable therapeutic applications. Specially, G-quadruplex DNA structures are a very interesting target because of promoter regions, human telomeres and aptemers are closely associated with the genetic integrity, cell proliferation, aging and cancer. Fundamental understanding of the interactions of small-molecule ligands or proteins with DNA sequences and their structural effect, binding affinities, thermodynamic, kinetic and thermal stability are very crucial. This doctoral thesis has uncovered the interaction studies of novel cyclic naphthalene diimide derivatives (cNDIs, **1**,**2**) & non-cyclic naphthalene diimide (NDI **3**) with double stranded DNA (dsDNA) such as calf thymus DNA (CT-DNA), poly[d(A-T)]$_2$, or poly[d(G-C)]$_2$ and G-quadruplexes DNA such as human telomere DNA (a-core & a-coreTT), promoter region's DNA (c-kit & c-myc) and thrombin-binding aptamer (TBA).

Firstly, I have studied the interaction of newly synthesized cNDIs **1,2** with various types of dsDNA to observe the cyclic linker chain effect binding to dsDNA. Secondly, I have studied the interaction of **2** with various types of G-quadruplexes DNA to observe the specific binding to G-quadruplexes DNA structure. I have studied the interaction of NDI **3** with dsDNA and G-quadruplexes DNA as a control.

The interaction of three different types of dsDNA and seven different types G-rich oligonucleotides studied with newly synthesize **1,2** and NDI **3** by the physicochemical and biochemical method such as UV-Vis spectroscopy, Circular dichroism (CD) spectroscopy, Topoisomerase I assay, Stopped-flow kinetics, Thermal melting studies,

TRAP assay and FRET-melting assay experiments.

The binding studies between cNDIs **1**,**2** and DNA duplexes showed affinities in the order of 10^5–10^6 M^{-1} using UV-Vis spectroscopic titration with a stoichiometry of one cNDI molecule covered four DNA base pairs as a bis-threading intercalation mode of binding. The induced CD signal was observed on cNDIs chromophore upon the addition of CT-DNA. Topo I isomerase assay showed that **2** can unwind circular dsDNA, it's also indicated the bis-intercalation binding of cNDIs with dsDNA. According to the van't Hoff and Gibbs free energy equation, thermodynamic parameters (ΔG, ΔH, and ΔS) indicated that entropy-dependent hydrophobic and endothermic interactions played a major role in the reaction between cNDIs and CT-DNA. Stopped-flow analysis showed that **2** slowly dissociate from GC base pairs. The salt ion effect analysis showed that upon the increasing salt concentration reduced cNDIs binding with dsDNA. Compound **1** showed much slower dissociation, a higher binding selectivity and a more entropically favorable interaction to dsDNA than **2** because of its longer linker chain.

The binding interactions between G-quadruplex DNA structure and cNDIs showed the affinities in the range of 10^6–10^7 M^{-1} orders with a 2:1 stoichiometry. Compound **2** showed highest binding affinities to human telomere a-core G-quadruplex DNA with 270 times selectivity than dsDNA. The CD spectra of G-quadruplex DNA changed upon the addition of cNDIs suggesting the end staking interaction of cNDIs on G-tetrad plane. The thermal melting studies indicated that **2** stabilized to G-quadruplexes DNA with preference of human telomeric a-core TT. The FRET melting assay also showed that **2** highly stabilized with F21T which is an ancestor of human telomere G-

quadruplex DNA. Compound **2** revealed an effective inhibitor against telomerase activity with an IC_{50} value of 0.9 μM.

Briefly, the finding of this doctoral thesis will contribute to generate new idea to design and development suitable DNA binding ligands. The interesting data in the chapter 4 indicated that **2** is the suitable candidate drug target to G-quadruplexes DNA, it deserves for further investigation with cancer cell line.

Chapter I

Introduction and Background

1.1. DNA

DNA (deoxyribonucleic acid) is the crucial component and present in all living things, large and small [1]. It is debatably the most complex structure and we are only just in the beginning to understand its function and mechanism. DNA is responsible for the management and conservation of genetic information of each living things, which is transferred genetic information in germ cells from one generation to the next generation. It also carries the essential information for proteins required for the operation of biological systems. In the last half-century, scientists have begun to study the mechanisms of the process surrounding the function of DNA, such as replication, transcription, translation, cell cycle mechanism and DNA damage repair. The processes of replication, transcription and translation are known as the central dogma of molecular biology (Fig. 1.1) [1].

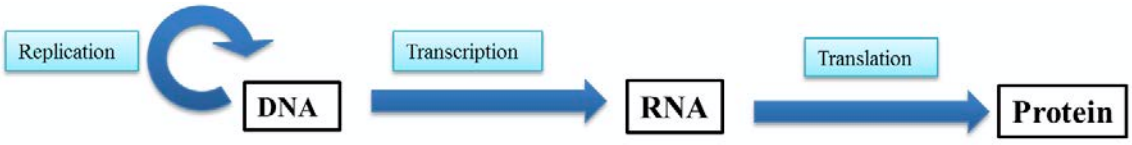

Fig.1.1. Representation of replication, transcription and translation [1].

1.2. Components and structure of DNA

The basic structure of DNA was established by Watson and Crick [2]. DNA consists of two complementary polymer strands that intertwine to give a right handed

double helix running in anti-parallel directions [3,4]. Each strand is made up of a series of units called nucleotides. A nucleotide is made up of a deoxyribose sugar, a phosphate and a nitrogen containing base such as adenine (A), guanine (G), thymine (T) and cytosine (C). The C1′ position of the deoxyribose sugar attaches with N9 position of adenine (A) or guanine (G) or N1 position of thymine (T) or cytosine (C). The deoxyribose sugar connected through the 5′ hydroxyl group and the 3′ hydroxyl group of phosphate. According to Watson-Crick base pairing rules, adenine (A) attaches with thymine (T) by two hydrogen bonds and guanine (G) attaches with cytosine (C) by three hydrogen bonds. The bases are connected through a flexible sugar phosphate chain. The DNA strand chain direction is 5′- to 3′- from top to bottom. The base pairs are not planar, they can twist and roll. Double stranded DNA structure mostly stabilizes by the correct base pairing of hydrogen bonds. It may destabilize by phosphate repulsion because the negative charge of phosphate. High salt concentration protects phosphate repulsion and stabilize the double stranded DNA structure. Cationic ligand molecules may have the same role to stabilize the DNA structure. DNA structure also may stabilize in solution by hydrophilic interactions between the negatively charged phosphate groups and the surrounding solvent [1-4].

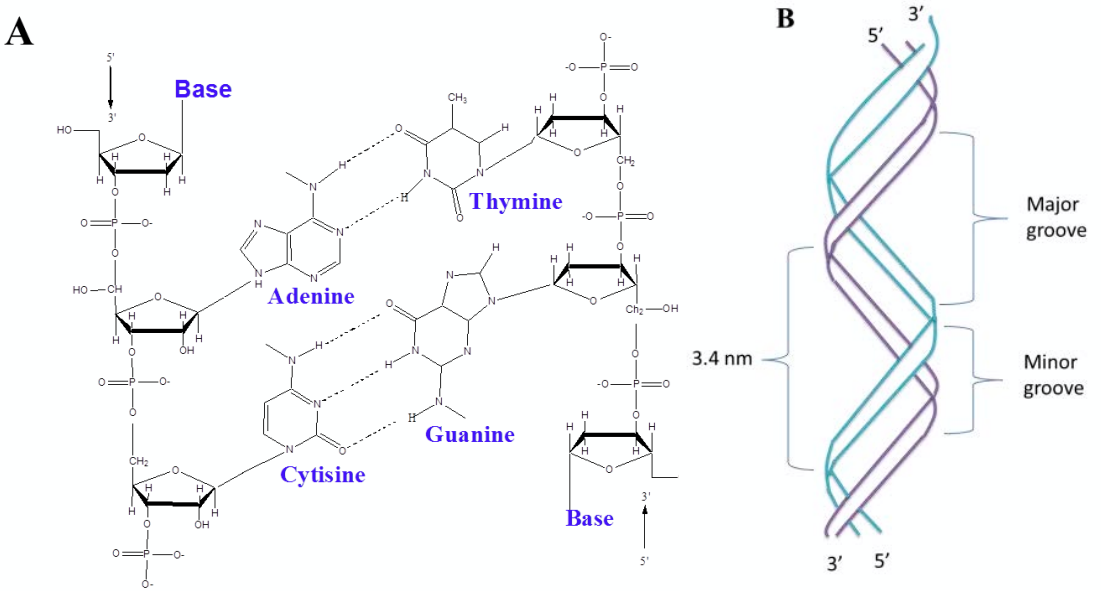

Fig. 1.2. (A) Chemical composition of double stranded DNA and (B) the structure of double stranded DNA [2].

1.3. Double stranded DNA: A-DNA, B-DNA and Z-DNA

A number of different conformations of double helical DNA can be formed by rotating various bonds [3,4]. Although the B-form is the most abundant DNA polymorph, other conformations can exist under appropriate conditions. The structures of A-DNA, B-DNA and Z-DNA are shown in Fig. 1.3 [5].

Under physiological conditions, DNA is generally assumed to be in a B-type conformation DNA [3]. B-DNA and A-DNA are right handed with 10 and 11 bases per turn respectively, Z-DNA is left handed with 12 bases per turn. Z-DNA backbone is not smooth, appearing zig-zag [4].

There are two distinguishable grooves running in the length of the DNA: the major

and the minor groove., The major groove for B-DNA has a depth of ~8Å and a width of ~12Å; the minor groove 8Å and 6Å respectively [4]. This means that only small molecules, that can twist and interact with the minor groove whereas much larger molecules can interact with the major groove. Generally, protein molecules interact with DNA major groove and small molecule drugs bind with minor groove [3].

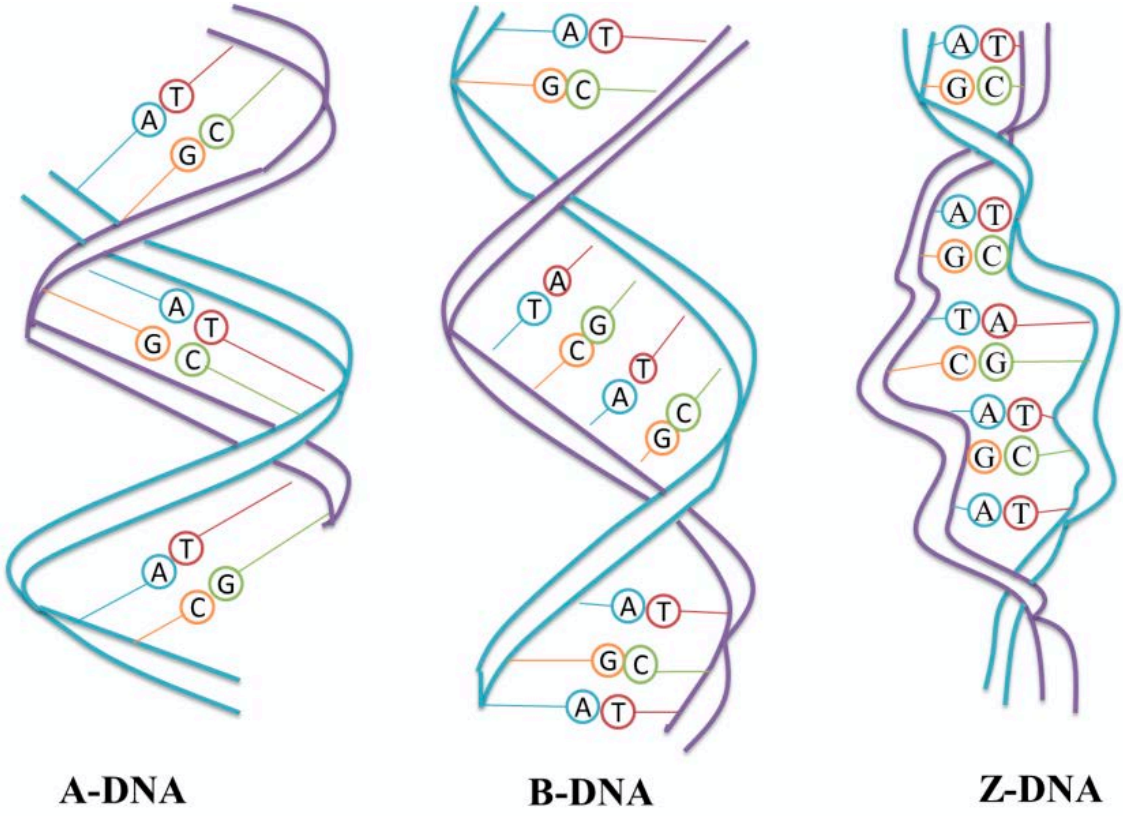

Fig.1.3. The structures of A-DNA, B-DNA and Z-DNA [5].

1.4. G-quadruplex DNA

Unlike Watson-Crick duplex model, nucleic acids are not simple linear polymers in the cell. A fascinating structure is the G-quadruplex DNA composed of four guanines interconnected by Hoogsteen hydrogen bond to form tetrameric units. The formation of G-quadruplex DNA was proposed in the 1960s. In the presence of K^+ or Na^+ mono-

cations, base pairing formed between N_7 and C_6 amino group of the adjacent guanines, and O_6 carbonyl of each guanine by Hoogsteen bond [6-8].

Recently, uncovered the visualization of DNA G-quadruplex structures in human chromosomes have amplified the potential application in therapeutics [6]. G-quadruplex DNA can be folded different quadruplex forms such as parallel, antiparallel, hybrid or mixed hybrid types depending on extrinsic cation and DNA sequence which makes a platform for binding and stabilizing by the small molecule drugs [6-8].

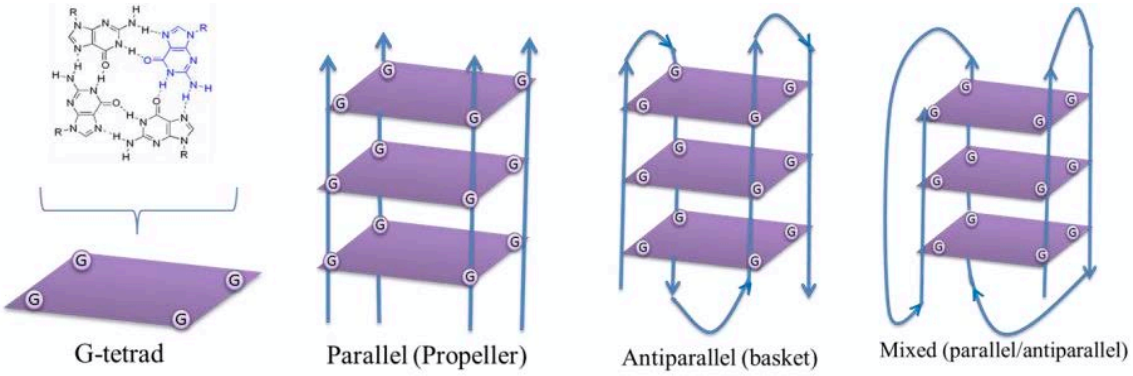

Fig. 1.4. Polymorphism of G-quadruplexes DNA [9].

1.5. Source of G-quadruplexes DNA

There are important regions in the human genome have been described to adopt G-quadruplex structures such as telomere region, promoter region and aptemers etc.

1.5.1. Human Telomere G-quadruplexes DNA

Telomeres are found at the terminus of the chromosomes, which is consisted by a long double stranded DNA sequence and a short G-rich single stranded sequence [10]. Telomeres play a vital role in maintaining genetic stability and cell growth by preventing

gene erosion, non-homologous end-end fusion of chromosomes and attack of nuclease. G-quadruplex structures form in the human telomeric DNA sequences containing four tandem TTAGGG repeats. The G-quadruplexes formed in those sequences have been observed to be highly polymorphic and dynamic in nature. Human telomeric DNA sequence forms a hybrid type G-quadruplex structure in K^+ solution, whereas it forms an antiparallel basket type G-quadruplex structure in Na^+ solution [11].

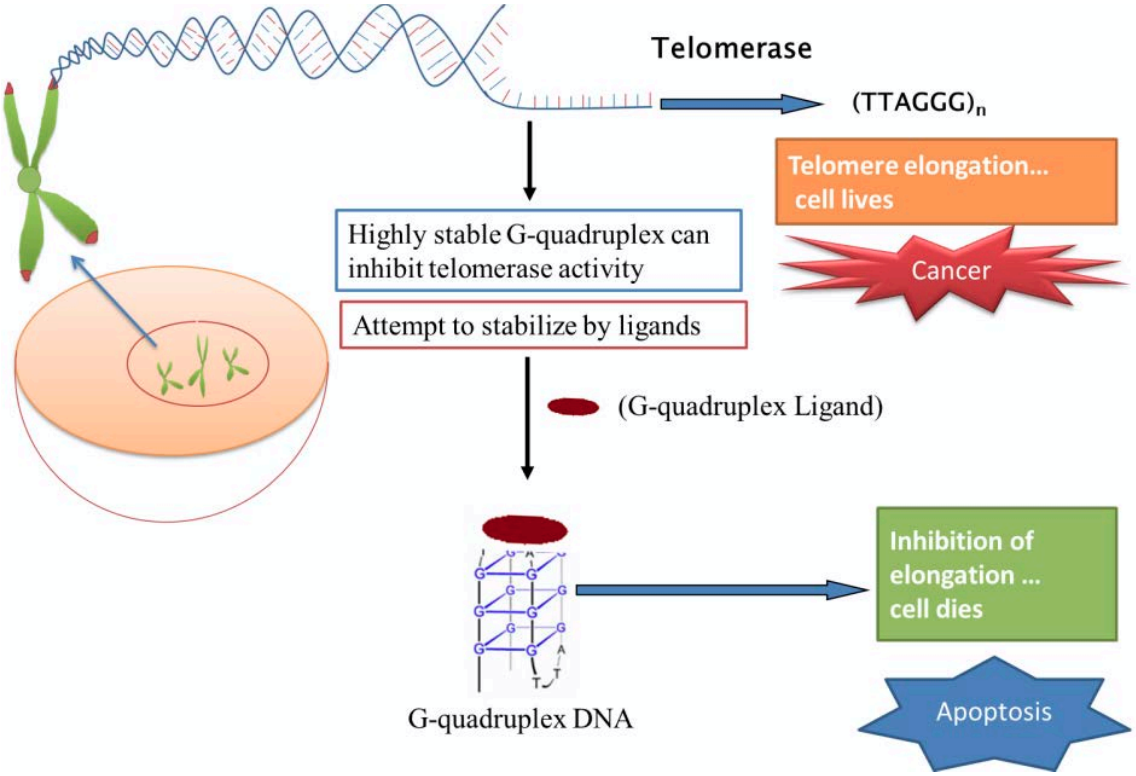

Fig. 1.5. Structure and biological roles of telomeres G-quadruplexes DNA [12].

1.5.2. Promoter region's G-quadruplexes DNA

G-quadruplexes structure have been found in several promoter regions of human genes, including c-myc, c-kit, VEGF etc. The promoter region genes contain the sequence d(GGG GAG GGT GGG GAG GGT GGG GAAGG), which is formed stable G-quadruplex structure. The G-quadruplex structure in promoter regions has a significant

role in transcription regulation [13-15].

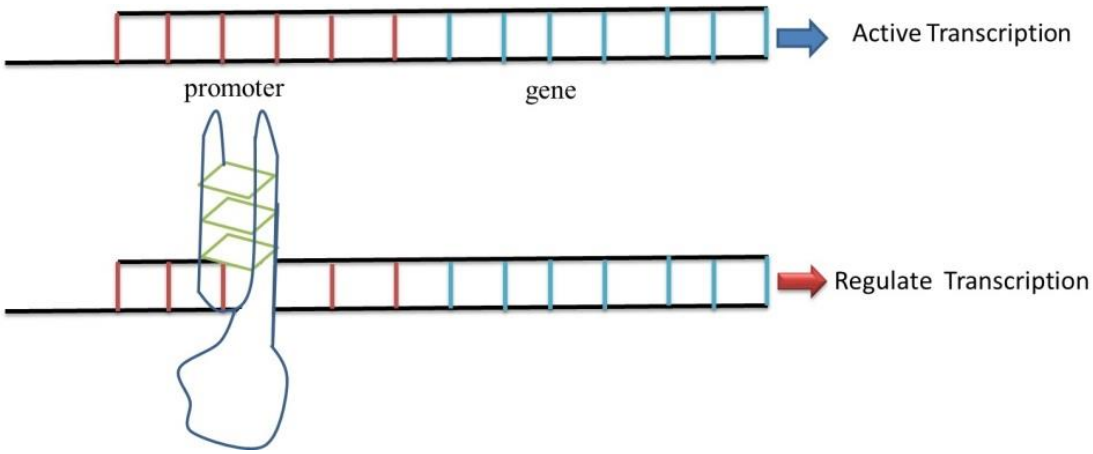

Fig.1.6. The formation of a G-quadruplex DNA in a promoter region [7].

1.5.3. Aptamers G-quadruplexes DNA

Aptamers are RNA or single stranded DNA, which can form G-quadruplexes structure. Aptamers G-quadruplexes DNA shows pharmacological significance such as a 26 mer nucleotide named AS1411 5'-d(GGTGGTGGTGGTTGTGGTGGTGGTGG), which can inhibit cancer cell proliferation [16,17].

1.6. Binding modes of ligands to DNA

1.6.1. Irreversible binding to DNA

The irreversible binding of drugs to DNA ability to bind by cross-linking through a base. One of the examples of irreversible binding of drugs to DNA is cisplatin [18].

1.6.2. Reversible bindings of small molecules with DNA

The small molecule drugs bind to DNA reversibly mainly three ways:

1. Electrostatic binding

2. Groove binding

3. Intercalation

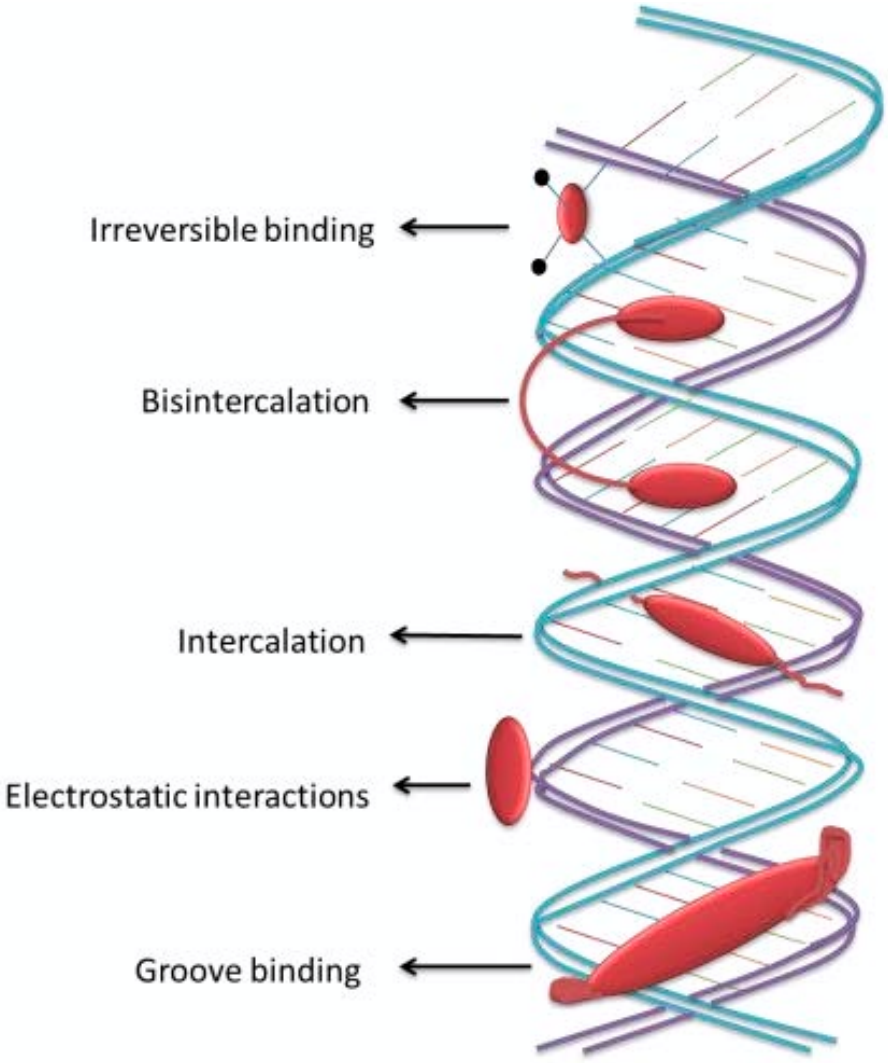

Fig. 1.7. Schematic representations of binding modes for ligand–duplex DNA [3,18].

1.6.2.1. Electrostatic interactions

Because of negatively charged of DNA, the positively charged cationic molecules bind with DNA through external association by the electrostatic interaction (Fig. 1.7) [3]. I have discussed in details at the salt effect analysis section in the chapter 3 about the binding of ligand molecules to DNA depends on the concentration of cations in the solution.

1.6.2.2. Intercalation

The planar aromatic molecules insert to the base pairs of DNA and bind with DNA generally known as DNA intercalation. There are many ligand molecules have been discovered as a DNA intercalator such as proflavine, ethidium bromide, daunomycin etc. (Fig. 1.7) [3]. Bis-intercalation of ligands with DNA is one of the attracted field because bi-functional molecules interact strongly with both DNA grooves (Fig. 1.7) [3].

1.6.2.3. Groove binding

The ligand molecules are associated with DNA at the location of major and/or minor groove and bind through van der Waals, hydrophobic and/or hydrogen bonding interactions known as DNA groove binding (Fig. 1.7) [3].

1.6.3. Binding modes between ligands and G-quadruplexes DNA

The planar aromatic ring molecules can interact with G-quadruplex by end stacking on the terminal G-tetrads as well as groove binding and intercalation binding with G-quadruplex DNA (Fig.1.8) [12,19].

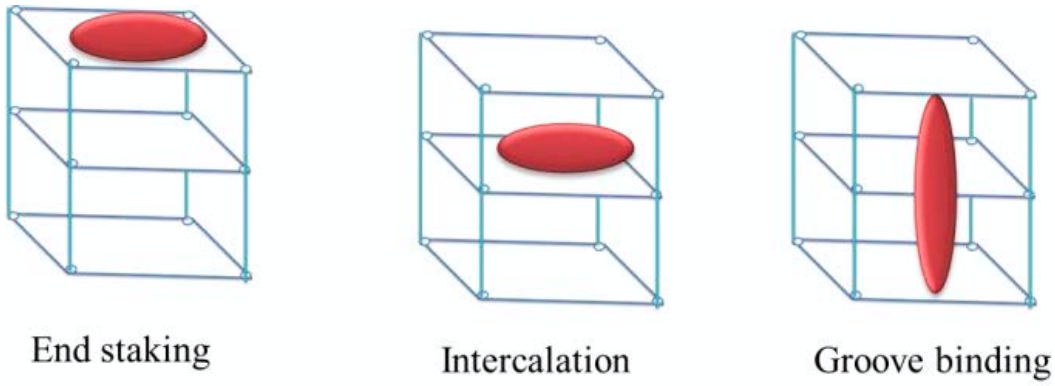

Fig.1.8. Interaction modes between G-Quadruplex DNA structures and ligands [12].

1.7. Binding of small molecules to double stranded DNA and G-quadruplexes DNA

1.7.1. Binding of small molecules to double stranded DNA

The development of small ligand molecules that bind with target DNA sequence selectively are leading to improve anticancer drugs [20,21]. These ligand molecules normally bind to target DNA sequence and controlling gene expression. An example of DNA binding drug is Pentamidine, which is used for the treatment of the disease of pancreatic cancer [22]. This drugs bind non-specifically to DNA, causing damage to normal cells, it displays side effects. However, one of the most challenging goals in this area is the design of molecules, which will bind to DNA with specific targets.

1.7.2. Binding of small molecules to G-quadruplexes DNA structures

G-quadruplex DNA structures form with the assembling of telomeric repeat $(TTAGGG)_3$ by telomerase in the telomeres of chromosomal end [23]. Most of the cancer cells activated by the over expression of telomerase enzyme in cancer cells. So, targeting the controlling of telomeric activity has led to the discovery of a novel anticancer drugs. Small molecule drugs are the main targets for stabilizing G-quadruplex DNA structure. There are a large number of G-quadruplex DNA stabilizing ligands has been discovered such as Anthraquinone [24], acridines [25], perylenes [26], berberine [27], porphyrins [28], and telomestatin derivatives [29]. These molecules are potential telomerase inhibitor. Most of the G-quadruplex DNA stabilizing ligands allows binding through π-π overlap on the terminal of G-tetrad [30]. Anthraquinone derivatives such as 2,6-disubstituted aminoalkylamido anthraquinone BSU-1051 is the first G-quadruplex DNA interactive ligands. It shows telomerase inhibition activity with IC_{50} values 23 μM [31]. The 3,6,9-trisubstituted acridines shows 30-40 times higher folding to G-quadruplex than duplex DNA and telomerase inhibition activity with IC_{50} values 10-20 nM. A cyclic acridine (BOQ1) also shows a potent telomerase inhibitor with IC_{50} values 0.33 μM [32]. The Perelene derivatives such as PIPER shows effective telomerase inhibitor at low micro-molar concentration. It shows a potent G-quadruplex DNA binding ligands with the stoichiometry of 2:1 than DNA duplex [33]. The Berberine derivatives reveal a stronger binding affinity to G-quadruplex and highly inhibit telomerase at low micromolar concentration [27]. The Napthalene diimide derivatives, NDIs shows high binding affinity to G-quadruplex over duplex DNA and telomerase inhibition of at low micromolar concentration [34]. The porphyrin derivatives are widely used macrocyclic ligands, shows high binding affinity to G-quadruplex DNA than duplex DNA [13,35,36].

Mn-TMPyP4 shows 10,000 fold selectivity to G-quadruplex DNA over duplex DNA and a potential telomerase inhibitor with IC_{50} value 580 nM. It's also shows the inhibitory effect on cancer cell line [37]. Telomestain is a natural compound isolated from *Streptomyces anulatus,* shows telomerase inhibition activity at 5 nM concentration. It's also able to reduce tumor cell growth [38]. Telomestain derivatives such as cyclic oxazoles shows structure specific selectivity with parallel c-kit G-quadruplex DNA than antiparallel telomeric G-quadruplex DNA [39]. The telomestain derivatives such as hexaoxazole containing macrocycle (HXDV) selectively stabilize telomeric G-quadruplexes DNA structure, whereas it did not show affinity to duplex DNA [40].

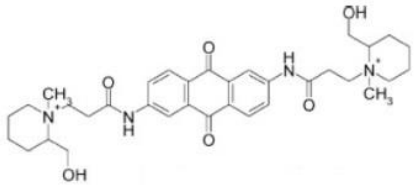

2,6-disubstituted anthraquinone [31]

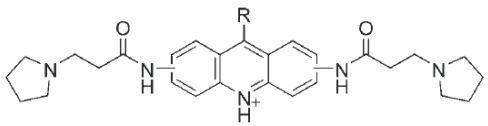

3,6,9-trisubstituted acridines [32]

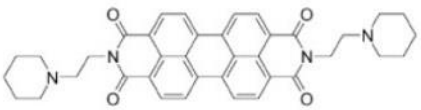

PIPER [33]

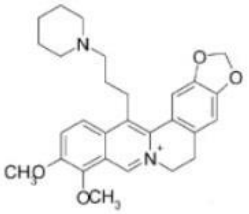

Piperidino berberine [27]

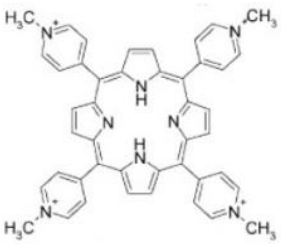

TMPyP4 porphyrin [35]

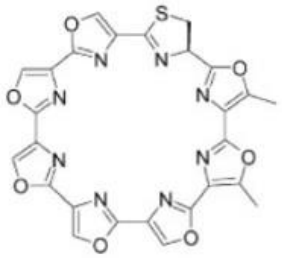

Telomestain [39]

Fig.1.9. Structures of known G-quadruplex ligands.

1.8. Methods for the study of ligand interactions with G-quadruplex and duplex DNA

The understanding in detail mechanisms of drug-DNA interactions are very crucial to the design and discovery of DNA targeting drugs [41]. There are several techniques which have been used to investigate drug–DNA interactions, including absorption spectroscopy [42], circular dichroism (CD) [43], emission spectroscopy [44], calorimetry [45], nuclear magnetic resonance (NMR) [46], surface plasmon resonance (SPR) [47], mass spectrometry [48], X-ray diffraction [49], competition dialysis [50], TRAP assay [23] and Molecular modeling [51].

In particular, the UV-Vis absorption titration have been developed for the binding studies to measure binding constant (K) and binding site size (n) [42]. The Stopped flow kinetics method have been sued to understand the dissociation constant (k_d) and association constant (k_a) of DNA-ligand interactions [42]. The CD has been used to study for characterizing the DNA structure and DNA structural change upon the binding of ligands molecules [52]. The Thermal melting studies have been used to know the stabilization of DNA-ligand interactions. The Fluorescence Resonance Energy Transfer (FRET) assays also have been widely used to study competitive thermal stabilization of different types of DNA binding with ligand or different types of ligand binding with DNA [53,54]. The Topo I isomerase assay is a powerful technique to study intercalation of ligands with circular double stranded DNA. The Telomere repeat amplification protocol (TRAP) assay is a widely used technique to know the inhibitory activity of telomerase enzyme by the ligand molecules [23]. Nowadays, Computer modeling, simulation is a popular technique to study of the interaction of ligands with G-quadruplexes DNA and

double stranded DNA [51].

1.9. Binding of naphthalene diimide derivatives to DNA

Naphthalene diimide derivatives are important DNA binder due to their large conjugated planer structure. Napthalene diimide binds with double stranded DNA as a threading intercaator. Recently, the several concept has been explored for bis-intercalating or polycyclic intercalating or cyclic intercalating derivatives of naphthalene diimide [55-60]. The interaction of a cyclic naphthalene diimide (cNDI) with DNA shows a unique catenated structure that dramatically stabilizes the duplex complex. Over the last few years a number of NDI based compounds have been developed in part by exploiting the available NDI-G-quadruplexes structures. A new type of macrocyclic naphthalene diimide, which is connected through the benzene ring with its substituent, showed stabilization and high affinity to G-quadruplexes DNA [61].

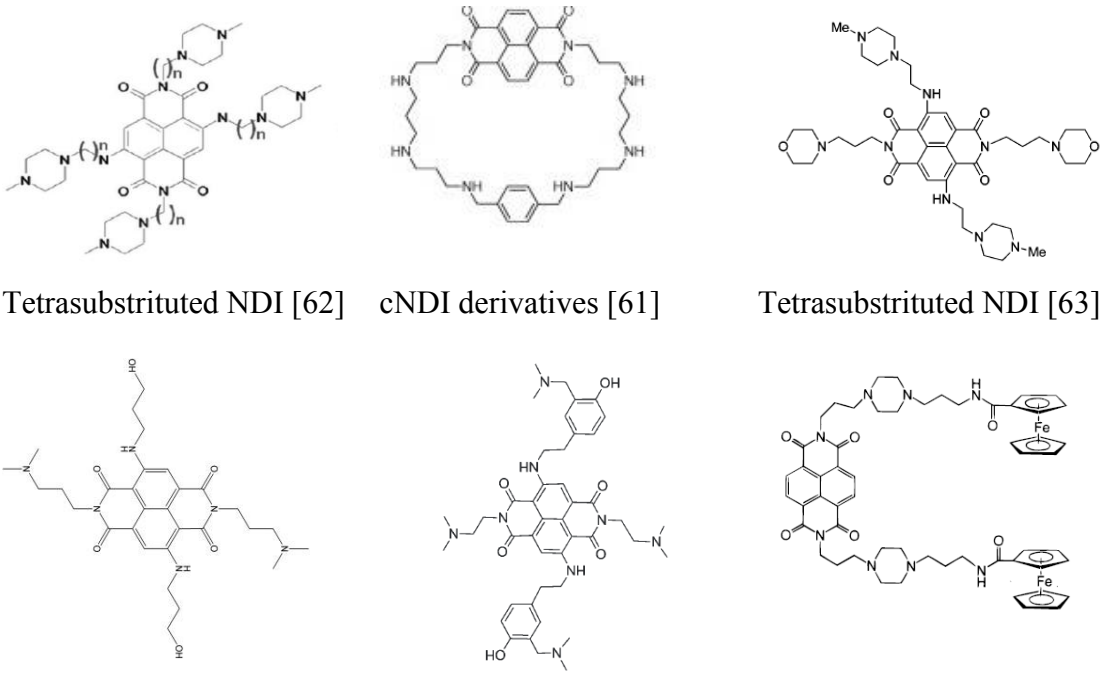

Tetrasubstituted NDI [62] cNDI derivatives [61] Tetrasubstituted NDI [63]

Tetrasubstitute NDI [64] Tetrasubstituted NDI [65] Ferrocinyl NDI [66]

Fig.1.10. Naphthalene diimide derivatives studied the interactions with DNA

1.10. Why cyclic naphthalene diimide derivatives (cNDI)?

Recently, researchers are searching stabilizing ligands for capable of specific binding with a G-quadruplexes DNA. Napthalene diimide (NDI) backbone can intercalate to dsDNA. Cyclization of NDI with linker chain through benzene ring, seems to be a wonderful idea for the stabilization of G-quadruplexes DNA. Because NDI moiety can be stacked on G-tetrad plane and bind with π-π interaction. The cNDI molecule would be reduced binding to dsDNA because linker chain and benzene part will protect to bind to dsDNA.

So, I have synthesized a series of cNDI derivatives and investigated the interaction with various types of DNA targeting to develop G-quadruplexes DNA specific binder

whereas reducing the binding to dsDNA.

1.11. The aim of the thesis

My doctoral research deals with the design and synthesis of new DNA interactive compounds and the evaluation of their efficiency in binding and stabilizing the double stranded and G-quadruplex DNA structures. In particular, my efforts have been directed towards the synthesis of macrocyclic naphthalene diimide derivatives (cNDI), where cNDI derivatives are designed by different length of linker chain through benzene.

In the last few years, several macrocycles were synthesized for binding with DNA specially G-quadruplexes DNA. A natural macrocyclic Telomestsian strongly stabilized G-quadruplexes DNA and inhibit telomerase in low concentration [29]. Porphyrins derivatives showed 10,000 times selectivity to G-quadruplexes DNA over duplex DNA [37]. Recently, NDI based macrocyclic compound showed high stabilization with G-quadruplexes DNA [61].

In this context, our interest has been devoted to the design of new cNDI macrocycles, considering the structure based stabilization with G-quadruplexes DNA and reducing the binding with dsDNA. In particular, I have targeted to optimize stacking interactions between the cNDI and terminal G-tetrad. So, I have deigned a shorter chain cNDI to specific binding model for G-tetrad.

An array of biophysical and biochemical techniques, ultraviolet-visible (UV-Vis), Circular Dichroism (CD), Stopped-flow, FRET melting assay, Topo I isomerase assay,

TRAP assay and Computer modeling were utilized. The mode of binding, binding affinities, thermodynamics, kinetics, thermal melting, telomerase inhibition assay and Computer modeling with various DNA sequences are discussed. This dissertation is divided into five chapters which are described below:

Chapter 1 is the current chapter, gives a general introduction to targeting DNA with small molecules as an effective strategy for drug design.

Chapter 2 is a reproduce work from M.M. Islam, S. Fujii, S. Sato, T. Okauchi, S. Takenaka, *Bioorganic Med. Chem.* 23 (2015**)** 4769–4776 and describes the synthesis of cNDI derivaties **1**-**3**.

Chapter 3 is a reproduce work from M.M. Islam, S. Fujii, S. Sato, T. Okauchi, S. Takenaka, *Bioorganic Med. Chem.* 23 (2015**)** 4769–4776 and describes the binding studies, kinetic and thermodynamic analysis of cNDIs with ds DNA.

Chapter 4 is a reproduce work from M.M. Islam, S. Fujii, S. Sato, T. Okauchi, S. Takenaka, *Molecule* 20 (2015) 10963-10979 and describes the binding studies, thermal stability and telomerase inhibition of cNDIs with different types of G-quadruplexes DNA.

Chapter 5 is a reproduce work from M.M. Islam, S. Fujii, S. Sato, T. Okauchi, S. Takenaka, *Bioorganic Med. Chem.* 23 (2015**)** 4769–4776 & M.M. Islam, S. Fujii, S. Sato, T. Okauchi, S. Takenaka, *Molecule,* 20 (2015) 10963-10979 and described the conclusion and the perspective of this thesis.

1.12. References

1. B. Alberts, A. Johnson, J. Lewis, M. Raff, K. Roberts, P. Walter, *Molecular Biology of the Cell*, 5th Ed., Garland Science, Taylor & Francis Group, LLC, an informa business, 270 Madison Avenue, New York, NY 10016, USA. 2008.
2. J.D. Watson and F.H.C. Crick, Molecular Structure of Nucleic Acids: A Structure for Deoxyribose Nucleic Acid, *Nature* 171 (1953) 737-378.
3. G.M. Blackburn, M.J. Gait, D. Loakes, D.M. Williams, *Nucleic Acids in Chemistry and Biology*, 3rd Ed., RSC Publication, Thomas Graham House, Science Park, Milton Road, Cambridge CB4 0WF, UK, 2006.
4. C. R. Calladine and H. R. Drew, *Understanding DNA: The molecule and how it works*, 2nd Ed, Academic Press: Cambridge, UK, 1997.
5. J. Muller, Functional metal ions in nucleic acids, *Metallomics* 2 (2010) 318–327.
6. D. Tannahill, J. McCafferty, S. Balasubramanian, Quantitative visualization of DNA G-quadruplex structures in human cells, *Nat. Chem.* 5 (2013) 182-186.
7. J.L. Huppert, Four-stranded nucleic acids: structure, function and targeting of G-quadruplexes, *Chem. Soc. Rev.* 37 (2008) 1375–1384.
8. S.M. Haider, S. Neidle, G.N. Parkinson, A structural analysis of G-quadruplex/ligand interactions, *Biochimie* 93 (2011) 1239–1251.
9. G. Song, J. Ren, Recognition and regulation of unique nucleic acid structures by small molecules, *Chem. Commun.* 46 (2010) 7283-7294
10. E.H. Blackburn, C.W. Greider, J.W. Szostak, Telomeres and telomerase: the path from maize, Tetrahymena and yeast to human cancer and aging, *Nat. Med.* 12 (2006) 1133-1138.
11. K.N. Luu, A.T. Phan, V. Kuryavyi, L. Lacroix, D.J. Patel, Structure of the human

telomere in K+ solution: an intramolecular (3 + 1) G-quadruplex scaffold, *J. Am. Chem. Soc.* 128 (2006) 9963-9970.

12. T. Ou, Y. Lu, J. Tan, Z. Huang, K. Wong, L. Gu, G-Quadruplexes: Targets in Anticancer Drug Design, *Chem. Med. Chem.* 3 (2008) 690–713.
13. A. Siddiqui-Jain, C.L. Grand, D.J. Bearss, L.H. Hurley, Direct evidence for a Gquadruplex in a promoter region and its targeting with a small molecule to repress c-MYC transcription, *Proc. Natl. Acad. Sci. USA* 99 (2002) 11593–11598.
14. D. Sun, K. Guo, J.J. Rusche, L.H. Hurley, Facilitation of a structural transition in the polypurine/polypyrimidine tract within the proximal promoter region of the human VEGF gene by the presence of potassium and G-quadruplex-interactive agents, *Nucleic Acids Res.* 33 (2005) 6070-6080.
15. S. Rankin, A.P. Reszka, J. Huppert, M. Zloh, G.N. Parkinson, A.K. Todd, S. Ladame, S. Balasubramanian, S. Neidle, Putative DNA quadruplex formation within the human ckit oncogene, *J. Am. Chem. Soc.* 127 (2005) 10584–89.
16. T. Mashima, A. Matsugami, F. Nishikawa, S. Nishikawa, M. Katahira, Unique quadruplex structure and interaction of an RNA aptamer against bovine prion protein, *Nucleic Acids Res.* 37 (2009) 6249–6258.
17. Y. Teng, A.C. Girvan, L.K. Casson, J.W.M. Pierce, M. Qian, S.D. Thomas, P.J. Bates, AS1411 alters the localization of a complex containing protein arginine Methyltransferase 5 and nucleolin, *Cancer Res.* 67 (2007) 10491-500.
18. P.M. Takahara, C.A. Frederick, S.J. Lippard, Crystal Structure of the Anticancer Drug Cisplatin Bound to Duplex DNA, *J. Am. Chem. Soc*. 118 (1996) 12309.

19. T. Shalaby, G. Fiaschetti, K. Nagasawa, K. Shin-ya, M. Baumgartner, M. Grotzer, G-Quadruplexes as Potential Therapeutic Targets for Embryonal Tumors, *Molecules* 18 (2013) 12500-12537.
20. P.G. Baraldi, A. Bovero, F. Fruttarolo, D. Preti, M.A. Tabrizi, M.G. Pavani, R. Romagnoli, DNA minor groove binders as potential antitumor and antimicrobial agents, *Med. Res. Rev.* 24 (2004) 475-528..
21. R. Palchaudhuri, P.J. Hergenrother, DNA as a target for anticancer compounds: methods to determine the mode of binding and the mechanism of action, *Curr. Opin. Biotechnol.* 18 (2007) 497-503.
22. M.K. Pathak, D. Dhawan, D.J. Lindner, E.C. Borden, C. Farver, T.L. Yi, Pentamidine is an inhibitor of PRL phosphatases with anticancer activity, *Mol. Cancer Ther.* 1 (2002) 1255-1264.
23. D. Gomez, J.L. Mergny, J.F. Riou, Detection of telomerase inhibitors based on gquadruplex ligands by a modified telomeric repeat amplification protocol assay, *Cancer Res.* 62 (2002) 3365–3368.
24. J.M. Zhou, X.F. Zhu, Y.J. Lu, R. Deng, Z.S. Huang, Y.P. Mei, Y. Wang, W.L. Huang, Z.C. Liu, L.Q. Gu, Y.X. Zeng, Senescence and telomere shortening induced by novel potent G-quadruplex interactive agents, quindoline derivatives, in human cancer cell lines, *Oncogene* 25 (2005) 503–511.
25. S.M. Gowan, Heald, R. M.F. Stevens, L.R. Kelland, Potent inhibition of telomerase by smallmolecule pentacyclic acridines capable of interacting with g-quadruplexes, *Mol. Pharmacol.* 60 (2001) 981–988.
26. M. Franceschin, A. Alvino, V. Casagrande, C. Mauriello, E. Pascucci, M. Savino, G. Ortaggi, A. Bianco, Specific interactions with intra- and intermolecular G-quadruplex

DNA structures by hydrosoluble coronene derivatives: a new class of telomerase inhibitors, *Bioorg. Med. Chem.* 15 (2007) 1848-1858.

27. M. Franceschin, L.D. Rossetti, A. Ambrosio, S. Schirripa, A. Bianco, G. Ortaggi, M. Savino, C. Schultes, S. Neidle, Natural and syntetic G-quadruplex interactive berberine derivatives, *Bioorg. Med. Chem. Let.* 16 (2006) 1707-1711.
28. R.T. Wheelhouse, D.K. Sun, H.Y. Han, F.X. Han, L.H. Hurley, Cationic porphyrins as telomerase inhibitors: the interaction of tetra-(N-methyl-4- pyridyl)porphine with quadruplex DNA, *J. Am. Chem. Soc.* 120 (1998) 3261–3262.
29. K. Shin-Ya, K. Wierzba, K. Matsuo, T. Ohtani, Y. Yamada, K. Furihata, Y. Hayakawa, H. Seto, Telomestatin, a novel telomerase inhibitor from Streptomyces anulatus. *J. Am. Chem. Soc.* 123 (2001) 1262–1263.
30. A.D. Cian, L. Lacroix, C. Douarre, N. Temime-Smaali, C. Trentesaux, J.F. Riou, J.L. Mergny, Targeting Telomeres and Telomerase, *Biochimie* 90 (2008) 131-155.
31. D. Sun, B. Thompson, B.E. Cathers, M. Salazar, S.M. Kerwin, J.O. Trent, T.C. Jenkins, S. Neidle, L.H. Hurley, Inhibition of human telomerase by a G-quadruplex-interactive compound, *J. Med. Chem.* 1997, 40, 2113–2116.
32. M.J.B. Moore, C.M. Schultes, J. Cuesta, F. Cuenca, M. Gunaratnam, F.A. Tanious, W.D. Wilson, S. Neidle, Trisubstituted Acridines as G-quadruplex Telomere Targeting Agents. Effects of Extensions of the 3,6- and 9-Side Chains on Quadruplex Binding, Telomerase Activity, and Cell Proliferation, *J. Med. Chem.* 49 (2006) 582–599.
33. O.Y. Fedoroff, M. Salazar, H. Han, V.V. Chemeris, S.M. Kerwin, L.H. Hurley, NMR-Based Model of a Telomerase-Inhibiting Compound Bound to G-Quadruplex DNA, *Biochemistry* 37 (1998) 12367–12374.

34. I. Czerwinska, S. Sato, B. Juskowiak, S.Takenaka, Interactions of cyclic and non-cyclic naphthalene diimide derivatives with different nucleic acids, *Bioorg. Med. Chem.* 22 (2014) 2593–2601.

35. D.F. Shi, R.T. Wheelhouse, D.Y. Sun, L.H. Hurley, Quadruplex interactive agents as telomerase inhibitors: Synthesis of porphyrins and structure-activity relationship for the inhibition of telomerase, *J. Med. Chem.* 44 (2001) 4509-4523.

36. C.L. Grand, H. Han, R.M. Munoz, S. Weitman, D.D. Von Hoff, L.H. Hurley,; D.J. Bearss, The cationic porphyrin TMPyP4 downregulates c-MYC and human telomerase reverse transcriptase expression and inhibits tumor growth in vivo, *Mol. Cancer Ther.* 1 (2002) 565-73.

37. I.M. Dixon, F. Lopez, A.M. Tejera, J.P. Esteve, M.A. Blasco, G. Pratviel, B. Meunier, A G-quadruplex ligand with 10000-fold selectivity over duplex DNA, *J. Am. Chem. Soc.* 129 (2007) 1502-1503.

38. T. Tauchi, K. Shin-ya, G. Sashida, M. Sumi, S. Okabe, J.H. Ohyashiki, K. Ohyashiki, Telomerase inhibition with a novel G-quadruplex-interactive agent, telomestatin: in vitro and in vivo studies in acute leukemia, *Oncogene* 25 (2006) 5719–25.

39. K. Jantos, R. Rodriguez, S. Ladame, P.S. Shirude, S. Balasubramanian, Oxazole-based peptide macrocycles: a new class of G-quadruplex binding ligands, *J. Am. Chem. Soc.* 128 (2006) 13662–3.

40. D.S. Pilch, C.M. Barbieri, S.G. Rzuczek, E.J. LaVoie, J.E. Rice, Targeting human telomeric G-quadruplex DNA with oxazole containing macrocyclic compounds, *Biochimie* 90 (2008) 1233-1249.

41. J. Jaumot, R. Gargallo, Experimental methods for studying the interactions between G-quadruplex structures and ligands, *Curr. Pharm. Des.* 18 (2012) 1900-1916.

42. C. Wei, G. Jia, J. Yuan, Z. Feng, C. Li, A spectroscopic study of the interactions of porphyrin with G-quadruplex DNAs, *Biochemistry* 45 (2006) 6681–6691.
43. S, Paramasivan, I. Rujan, P.H. Bolton, Circular dichroism of quadruplex DNAs: applications to structure, cation effects and ligand binding, *Methods* 43 (2007) 324–331.
44. L.R. Keating, V.A. Szalai, Parallel-stranded guanine quadruplex interactions with a copper cationic porphyrin, *Biochemistry* 43 (2004) 15891–15900.
45. E. Erra, L. Petraccone, V. Esposito, A. Randazzo, L, Mayol, J, Ladbury, G. Barone, C. Giancola, Interaction of porphyrin with G-quadruplex structures. Nucleosides Nucleotides, *Nucleic Acids Res.* 24 (2005) 753–756.
46. C. Hounsou, L. Guittat, D. Monchaud, M. Jourdan, N. Saettel, J.L. Mergny, M.P. Teulade-Fichou, G-quadruplex recognition by quinacridines: a SAR, NMR, and biological study, *Chem. Med. Chem.* 2 (2007) 655–666.
47. J.E. Redman, Surface plasmon resonance for probing quadruplex folding and interactions with proteins and small molecules, *Methods* 43 (2007) 302–312.
48. C.L. Mazzitelli, J.S. Brodbelt, J.T. Kern, M. Rodriguez, S.M. Kerwin, Evaluation of binding of perylene diimide and benzannulated perylene diimide ligands to DNA by electrospray ionization mass spectrometry, *J. Am. Soc. Mass Spectrom.* 17 (2006) 593-604.
49. N.H. Campbell, G.N. Parkinson Crystallographic studies of quadruplex nucleic acids, *Methods* 43 (2007) 252– 263.
50. P. Ragazzon, J.B. Chaires, Use of competition dialysis in the discovery of G-quadruplex selective ligands, *Methods* 43 (2007) 313–323.

51. P. Murat, Y. Singhb, E. Defrancq, Methods for investigating G-quadruplex DNA/ligand interactions, *Chem. Soc. Rev.* 40 (2011) 5293–5307

52. T. Yamashita, T. Uno, Y. Ishikawa, Stabilization of guanine quadruplex DNA by the binding of porphyrins with cationic side arms, *Bioorg. Med. Chem.* 13 (2005) 2423–2430.

53. J.L. Mergny, Ethidium derivatives bind to G-quartets, inhibit telomerase and act as fluorescent probes for quadruplexes, *Nucleic Acids Res.* 29 (2001) 1087–1096.

54. A. DeCian, L. Guittat, M. Kaiser, B. Saccà, S. Amrane, A. Bourdoncle, P. Alberti, M.P. Teulade-Fichou, L. Lacroix, J.L. Mergny, Fluorescence-based melting assays for studying quadruplex ligands, *Methods* 42 (2007)183-95.

55. R.S. Lokey, Y. Kwok, V. Guelev, C.J. Pursell, L.H. Hurley, B.L. Iverson, A New Class of Polyintercalating Molecules, *J. Am. Chem. Soc.* 119 (1997) 7202-7210.

56. G.G. Holman, M. Zewail-Foote, A.R. Smith, K.A. Johnson, B.L. Iverson, A sequence-specific threading tetra-intercalator with an extremely slow dissociation rate constant, *Nat Chem.* 3 (2011) 875-881.

57. A.R. Smith, B.L. Iverson, Threading Polyintercalators with Extremely Slow Dissociation Rates and Extended DNA Binding Sites, *Am. Chem. Soc.* 135 (2013) 12783–12789.

58. Y. Chu, D.W. Hoffman, B.L. Iverson, A Pseudocatenane Structure Formed between DNA and A Cyclic Bisintercalator, *J. Am. Chem. Soc.* 131 (2009) 3499–3508.

59. Y. Chu, S. Sorey, D.W. Hoffman, B.L. Iverson, Structural Characterization of a Rigidified Threading Bisintercalator, *J. Am. Chem. Soc.* 129 (2007) 1304-1311.

60. J. Lee, V. Guelev, S. Sorey, D.W. Hoffman, B.L. Iverson, NMR Structural Analysis of a Modular Threading Tetraintercalator Bound to DNA, *J. Am. Chem. Soc.* 126 (2004) 14036-14042.

61. C. Marchetti, A. Minarini, V. Tumiatti, F. Moraca, L. Parrotta, S. Alcaro, R. Rigo, C. Sissi, M. Gunaratnam, S.A. Ohnmacht, S. Neidle, A. Milelli, Macrocyclic naphthalene diimides as G-quadruplex binders, *Bioorg. Med. Chem.* 23 (2015) 3819-3830.

62. G.W. Collie, R. Promontorio, S.M. Hampel, M. Micco, S. Neidle, G.N. Parkinson, Structural Basis for Telomeric G-Quadruplex Targeting by Naphthalene Diimide Ligands, *J. Am. Chem. Soc.* 134 (2012) 2723–2731.

63. M. Micco, G.W. Collie, A.G. Dale, S.A. Ohnmacht, I. Pazitna, M. Gunaratnam, A.P. Reszka, S. Neidle, Structure-Based Design and Evaluation of Naphthalene Diimide G-Quadruplex Ligands As Telomere Targeting Agents in Pancreatic Cancer Cells, *J. Med. Chem.* 56 (2013) 2959–2974.

64. G.N. Parkinson, F. Cuenca, S. Neidle, Topology Conservation and Loop Flexibility in Quadruplex–Drug Recognition: Crystal Structures of Inter- and Intramolecular Telomeric DNA Quadruplex–Drug Complexes *J. Mol. Biol.* 381 (2008) 1145–1156.

65. F. Doria, M. Nadai, M. Folini, M.D. Antonio, L. Germani, C. Percivalle, C. Sissi, N. Zaffaroni, S. Alcaro, A. Artese, S.N. Richter, M. Freccero, Hybrid ligand–alkylating agents targeting telomeric G-quadruplex Structures, *Org. Biomol. Chem.* 10 (2012) 2798–2806.

66. S. Takenaka, K. Yamashita, M. Takagi, Y. Uto, H. Kondo, DNA Sensing on a DNA Probe-Modified Electrode Using Ferrocenylnaphthalene Diimide as the Electrochemically Active Ligand, *Anal. Chem.* 72 (2000) 1334-1341.

Chapter II

Synthesis of cyclic naphthalene diimide 1, 2 and 3

Contents of this chapter have been published in the Bioorgamic & Medicinal chemistry Journal (M.M. Islam, S. Fujii, S. Sato, T. Okauchi, S. Takenaka, Bioorganic Med. Chem. 23 (2015) 4769–4776). The materials of the chapter have been reproduced with the permission of the Bioorgamic & Medicinal chemistry Journal [1].

2.1.1. Synthesis of cyclic naphthalene diimide 1 and 2

As precursors of **1** and **2**, N,N'-bis[[4-(3-aminopropyl)piperazinyl]propyl]-naphthalene-1,4,5,8-tetracarboxylic acid diimide (**4**) and N, N'-bis[3-(3-aminopropyl)methylaminopropyl] naphthalene-1,4,5,8-tetracarboxylic acid diimide (**5**) were synthesized according to the procedure reported previously [2].

2.1.2. Synthesis of 1 (cNDI 1)

A solution of **4** 1.0 g (1.5 mmol), terephthalic acid 0.25 g (1.5 mmol), triethylamine 12 mL, 1-hydroxybenzotriazole (HOBt) 0.60 g (4.5 mmol), 1H-Benzotriazol-1-yloxy-tri(pyrrolidino) phosphonium hexafluorophosphate (PyBOP) 2.3 g (4.5 mmol) in $CHCl_3$ 500 mL was stirred at room temperature and the progress of this reaction was monitored by TLC on silica gel with mixture of $CHCl_3$:

diethylamine = 10: 1.0 as developing agent. After 48 h stirring where the TLC spot of NDI (R_f=0) was disappeared, the reaction mixture was evaporated under reduced pressure and the residue was dissolved with 20 mL $CHCl_3$. After filtration and subsequently evaporation under reduced pressure, the residue was chromatographed on a silica gel column (Merck 60) using the eluent consisted of $CHCl_3$: diethylamine = 10: 1.0. The fraction of R_f= 0.33 was collected and the solvent was removed under reduced pressure. The obtained residue was recrystallized from ethyl acetate, and **1** was obtained as brown crystal with 0.11 g (yield, 10%). MALDI-TOFMS (positive mode, α-CHCA) m/z =763.73 (theory for $C_{42}H_{50}N_8O_6$+H^+= 763.90). ^{1}H NMR (250 MHz, $CDCl_3$, TMS) δ1.54 (8H, m), 1.98 (4H, t, *J* = 6.0 Hz), 2.15 (6H, m), 2.29 (12H, m), 2.48 (4H, t, *J*=6.5 Hz), 3.44 (4H, m), 4.35 (4H, m, *J* = 6.0 Hz), 7.80 (4H, s), and 8.77(4H, s) ppm; HRMS Calcd. for $C_{42}H_{50}N_8O_6$+H^+: M, 763.55. Found: m/z 763.55. 1 mM **1** aqueous solution was prepared as estimated from the molar absorptivity of 28800 $cm^{-1}M^{-1}$ at 384 nm.

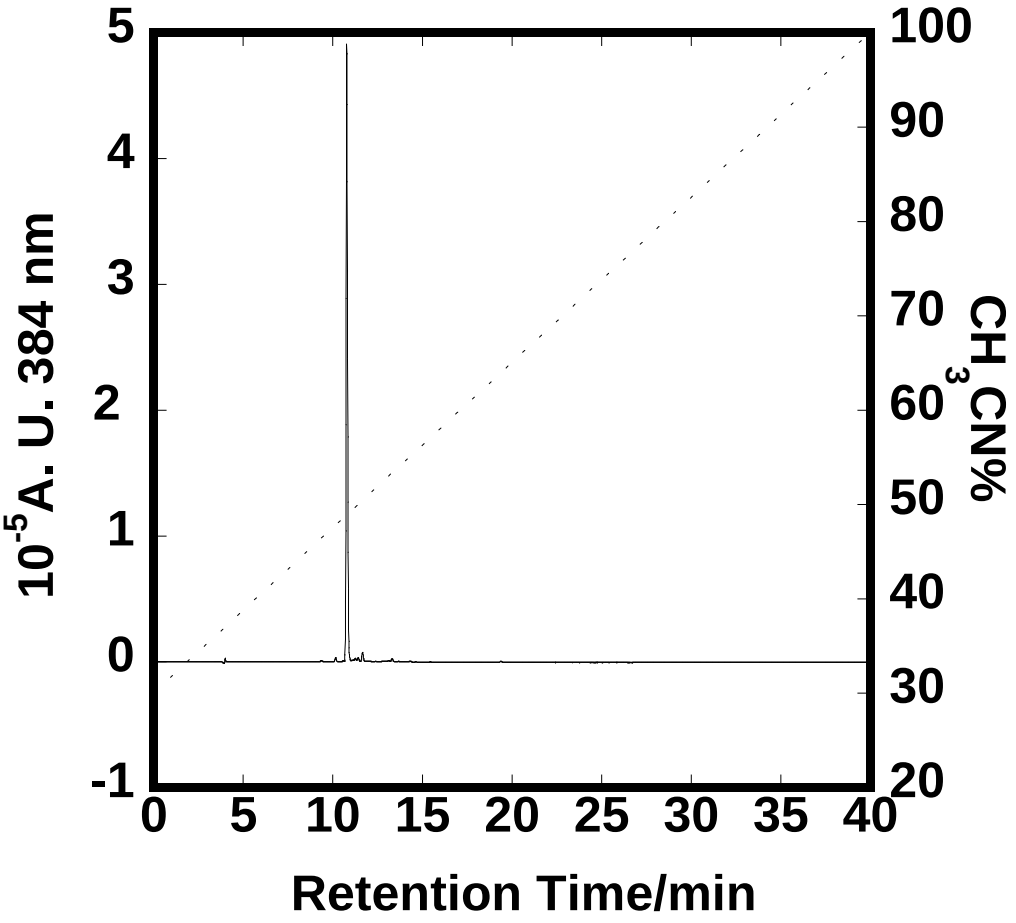

Fig. 2.1. Reversed phase HPLC of **1**. The concentration of acetonitrile was changed linearly to 100% from 28% in water containing 0.1% trifluoroacetic acid over 40 min at 40 ˚C.

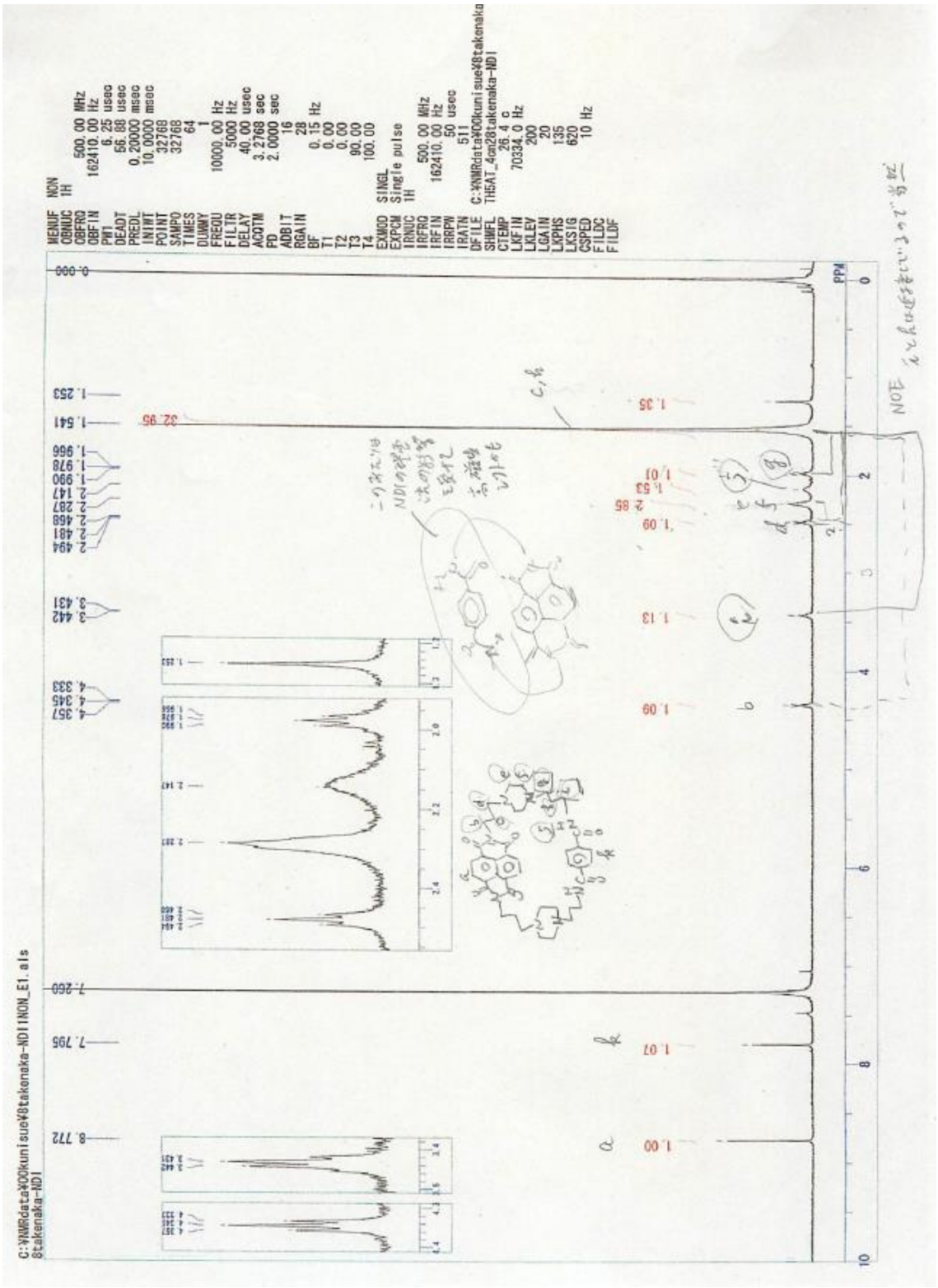

Fig. 2.2. ^{1}H-NMR chart of **1** in $CDCl_3$ using TMS as internal standard.

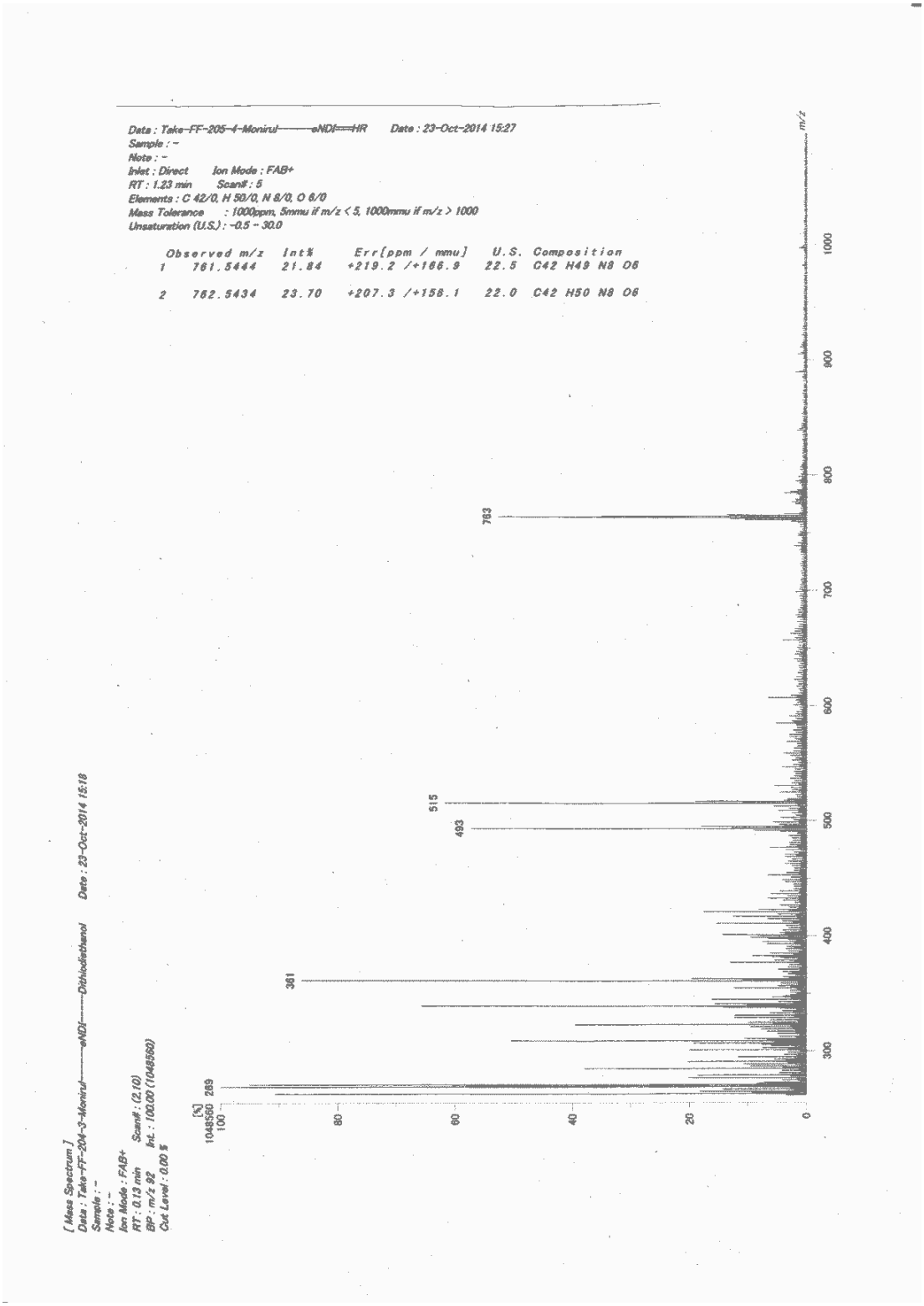

Fig. 2.3. High-resolution mass spectra (HRMS-FAB) of **1**.

2.1.3. Synthesis of 2 (cNDI 2)

A solution of **5** 1.1 g (0.9 mmol), terephthalic acid 0.15 g (0.9 mmol), triethylamine 15 mL, 1-hydroxybenzotriazole (HOBt) 0.12 g (0.9 mmol), 1-Ethyl-3-(3-dimethylaminopropyl)-carbodiimide hydrochloride 0.17 g (0.09 mmol) in $CHCl_3$ 400 mL was stirred at room temperature and the progress of this reaction was monitored by TLC on silica gel with mixture of $CHCl_3$: diethylamine : Methanol = 10 : 0.2 : 1.0 as developing agent. After 48 h stirring, the reaction mixture was evaporated under reduced pressure and the residue was dissolved with 100 mL $CHCl_3$. After filtration and subsequently washed with sat. $NaHCO_3$ aq. (80 ml×5), and dried over magnesium sulfate. The solvent was removed and the residue was chromatographed on a silica gel column (Merck60) using the eluent of $CHCl_3$: diethylamine : Methanol = 10 : 0.2 : 1.0. The fraction of R_f= 0.41 was collected and the solvent was removed under reduced pressure. The obtained residue was recrystallized from ethyl acetate, and **2** was obtained as brown crystal with 17 mg (yield, 3%). MALDI-TOFMS (positive mode, α-CHCA) m/z =653.54 (theory for $C_{36}H_{40}N_6O_6+H^+$= 653.302). ^{1}H NMR (500 MHz, $CDCl_3$, TMS) δ 1.34 (4H, m), 1.5 (4H, t, J=5.9), 1.87 (4H, m), 2.09 (6H, s), 2.31 (4H, m) 3.16 (4H, m), 4.12 (4H, t, J=6.8), 7.12 (2H, s), 7.56 (4H, s), 8.71 (4H, s) ppm. HRMS Calcd. for $C_{36}H_{40}N_6O_6+H^+$: M, 653.302. Found: m/z 653.302. 1 mM **2** aqueous solution was prepared as estimated from the molar absorptivity of 28800 $cm^{-1}M^{-1}$ at 384 nm.

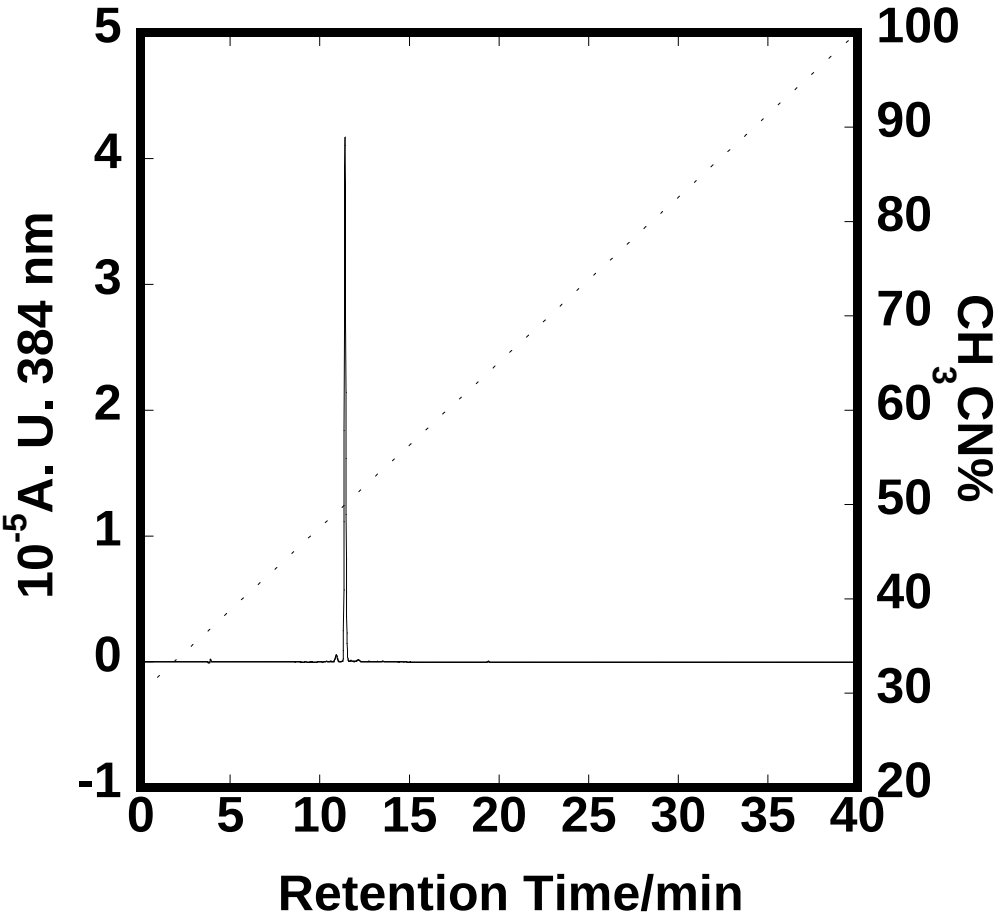

Fig. 2.4. Reversed phase HPLC of **2**. The concentration of acetonitrile was changed linearly to 100% from 29% in water containing 0.1% trifluoroacetic acid over 40 min at 40 ˚C.

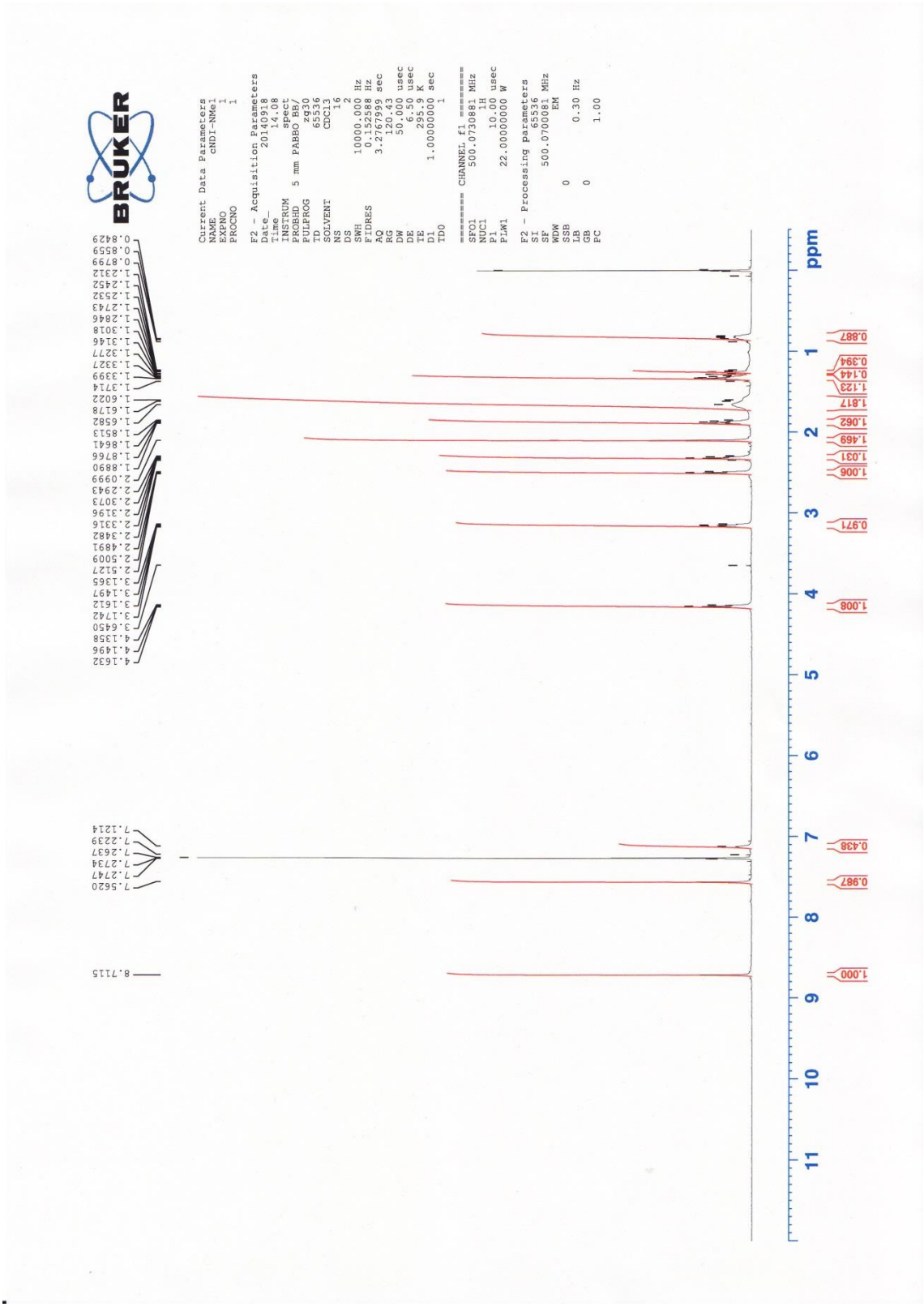

Fig. 2.5. ^{1}H-NMR chart of **2** in $CDCl_3$ using TMS as internal standard.

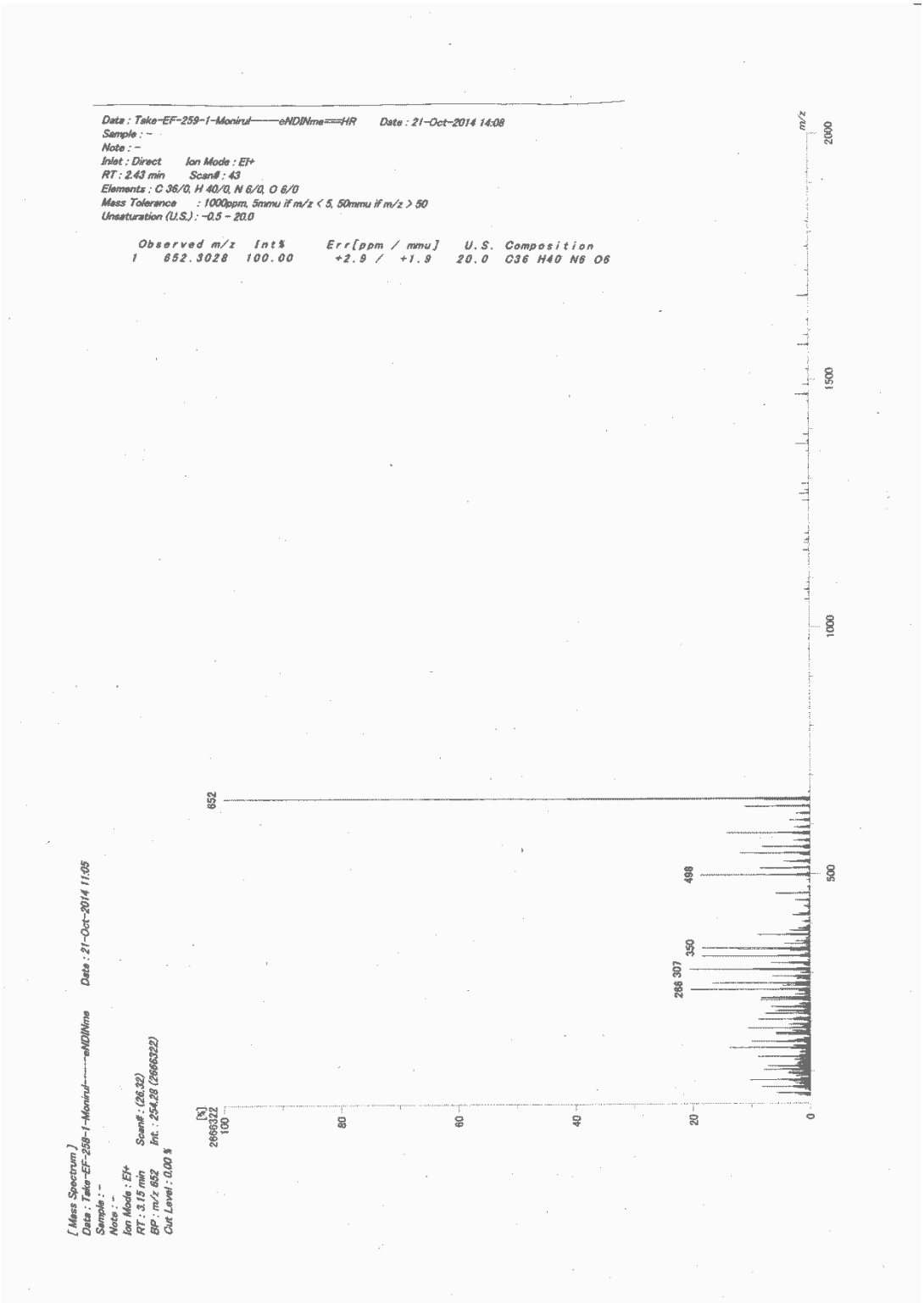

Fig. 2.6. High-resolution mass spectra (HRMS-EI$^+$) of **2**.

2.2. Synthesis of NDI 3

Details of non-cyclic NDI **3** synthesis was asper method previously described [3].

2.3. References

1. M.M. Islam, S. Fujii, S. Sato, T. Okauchi, S. Takenaka, Thermodynamics and kinetic studies in the binding interaction of cyclic naphthalene diimide derivatives with double stranded DNAs, *Bioorganic Med. Chem.* 23 (2015) 4769–4776.
2. S, Sato, S. Takenaka, Linker effect of ferrocenylnaphthalene diimide ligands in the interaction with double stranded DNA, *J. Organomet. Chem.* 693 (2009) 1177-1185.
3. F.A. Tanious, S.F. Yen, W.D. Wilson, Kinetic and Equilibrium Analysis of a Threading Intercalation Mode: DNA Sequence and Ion Effects, *Biochemistry* 30 (1991) 1813–1819.

Chapter III

Thermodynamics and Kinetic Studies in the Binding Interaction of Cyclic Naphthalene Diimide Derivatives with Double Stranded DNAs

Contents of this chapter have been published in the Bioorgamic & Medicinal chemistry Journal (M.M. Islam, S. Fujii, S. Sato, T. Okauchi, S. Takenaka, Bioorg. Med. Chem. 23 (2015) 4769–4776). The materials of the chapter have been reproduced with the permission of the Bioorgamic & Medicinal chemistry Journal [1].

3.1. Introduction

Small molecules that bind to DNA affect numerous functions of living organisms, such molecules have potential as therapeutic agents that function by controlling gene expression. Thus, the study of interactions between DNA and small molecules is vital in chemical and biological drug discovery research [2,3]. It is important to study the thermodynamics and kinetics of the interactions between small molecules and DNA in order to understand the binding modes of these molecules and develop new, effective, DNA-targeted drugs [2]. Accordingly, many small molecule drugs that interact with DNA have been investigated [4]. A classical intercalating drug slides between adjacent base pairs of a DNA duplex and forms a stable complex, resulting to mutations, such as frameshift [6]. A threading intercalating drug is a new type of intercalator; in its

interaction with DNA, two substituents of the molecule are located on the major and minor grooves of the DNA duplex, preventing dissociation [3]. Nogalamycin is a typical threading intercalator, and its antitumor activity is correlated with its DNA dissociation rate constant [3]. This exemplifies the relationship between physical data and biological activity. It also shows the importance of physical studies of the interactions between small molecules and DNA duplexes.

Expanding on threading intercalating drugs, bis-intercalators have also been utilized to stabilize the DNA complex [2-5]. Chaires et al. developed the bis-intercalating drug daunomycin [3]. Like nogalamycin, this molecule's slower dissociation rate correlates with its biological activity. Recently, the same concept has been explored for bis-intercalating or cyclic intercalating derivatives of naphthalene diimide [6-11]. The interaction of a cyclic naphthalene diimide with DNA shows a unique catenated structure that dramatically stabilizes the complex. A new type of cyclic naphthalene diimide, **1**, which is connected with its substituent through the benzene ring, can stabilize both a DNA duplex and a DNA tetraplex [12,13]. In recent years, the synthesis of bis-intercalators has drawn considerable attention because of the drugs' potential superiority over mono-intercalators. Higher DNA-binding constants, slower dissociation rates, and substantial sequence selectivity can be expected from the incorporation of two or more intercalating units into a polyfunctional ligand [7,8].

Researchers have already reported that naphthalene diimide derivatives act as DNA-targeting anticancer agents, and such derivatives have shown potent activity against cancer cell lines and telomerase [14,15]. Depending on the substituents, naphthalene

diimide derivatives have shown selectivity toward AT- or GC-rich regions of DNA [5,7]. Our group previously published our synthesis and evaluation of the binding of G-quadruplex and dsDNA with **1** and other cNDIs [12,13]. In the present study, the interaction of **1** and the newly designed **2** with dsDNA was analyzed by UV-Vis spectroscopy, CD spectroscopy, a topoisomerase I assay, and stopped-flow kinetics to characterize differences in binding mode and binding selectivity.

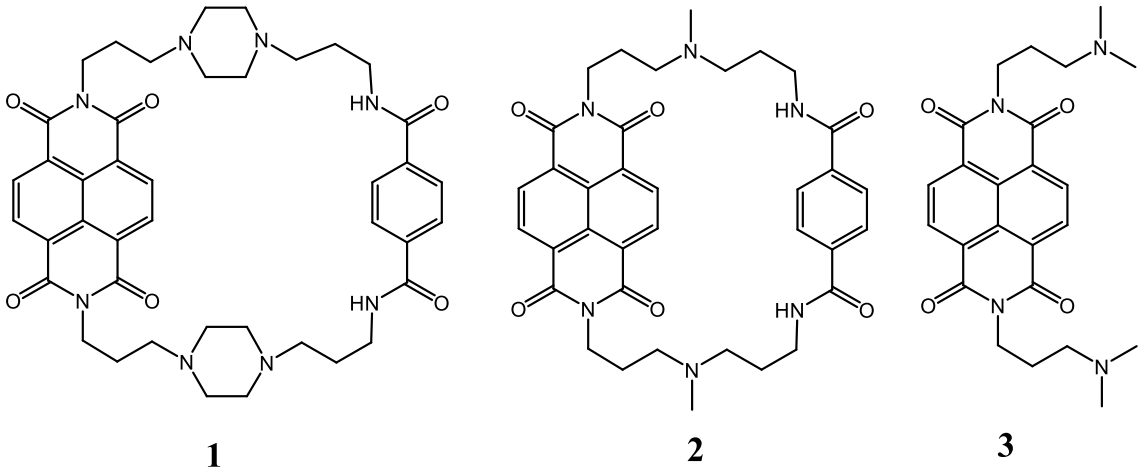

Fig. 3.1. Chemical structure of cNDI **1, 2** and NDI **3**

3.2. Experimental procedure

3.2.1. Materials

CT-DNA, poly[d(A-T)]$_2$, and poly d[(G-C)]$_2$ synthetic polymers were obtained from Sigma-Aldrich (St. Louis, MO). Following the extinction coefficients (ε) were used for quantification of the nucleic acid solutions: 12824 M^{-1} cm^{-1} for CT-DNA, 13200 M^{-1} cm^{-1} for poly[d(A-T)]$_2$, and 16800 M^{-1} cm^{-1} for poly[d(G-C)]$_2$. Details of the synthesis procedure for **1** and **2** are described in the supplementary data, and **3** was synthesized as

previously described [16]. I obtained 2.0 M KCl and 5.0 M NaCl aqueous solutions from Life Technologies (Carlsbad, CA), 1.0 M Tris-HCl (pH 7.4) buffer from Sigma-Aldrich (St. Louis, MO), and 2-Morpholinoethanesulfonic acid (MES) from Dojindo (Japan).

3.2.2. UV-Vis titration experiments

Absorption spectra were measured using the Hitachi U-3310 spectrophotometer with a 1-cm path-length quartz cell and were recorded in the 200–600 nm range at 25°C. UV-Vis absorption titrations were carried out by the stepwise addition of 3 mM/base pair of CT-DNA, poly[d(A-T)]$_2$, or poly[d(G-C)]$_2$ to a UV cell containing 6.7 μM solutions of **1–3**. The measurements were performed in 10 mM MES buffer (pH 6.25) containing 100 mM NaCl and 1 mM EDTA. Binding data, which were obtained by spectrophotometric titration of increasing concentrations of each drug to a fixed concentration of DNA, were analyzed by Scatchard plot analysis of r/C versus r, according to the excluded-site model of the McGhee-von Hippel equation [17] (Eq. 3.1). The binding data were analyzed with KaleidaGraph software, using the Levenberg-Marquardt algorithm to determine parameters K_b and n.

3.2.3. Thermodynamics analysis

The effect of temperature on ligand binding affinity was investigated to derive the thermodynamic functions of ligand-DNA complex formation. Absorption spectra were measured at 20, 22.5, 25, and 27.5°C. Titrations were performed under conditions similar to those used in the UV-Vis titration experiments. Enthalpy change (ΔH) and entropy change (ΔS) were measured by the van't Hoff equation plotted against ln$K$ versus 1/T (Eq. 3.2). The free energy change (ΔG) was estimated by the Gibbs free energy equation (Eq. 3.3).

3.2.4. Salt effect analysis

Salt-dependent Scatchard analysis was conducted at five different concentrations of sodium salt: 50, 75, 100, 125, and 150 mM. Titrations were performed under similar conditions as those used for the UV-Vis titration experiments. The strength of electrostatic interactions of the ligand was determined by plotting the negative logarithm of the sodium salt concentration (log [Na^+]) against the binding constant (log K) (Eq. 3.4).

3.2.5. Stopped flow kinetics experiments

Stopped-flow kinetic experiments were performed with the SF-61 DX2 double mixing stopped-flow system (Hi-Tech Scientific Inc., Salisbury, UK) equipped with a Lauda RF206 temperature controller. Samples were prepared in a buffer solution (10 mM MES, 1 mM EDTA, and 0.1 M NaCl; pH 6.25). Absorbance was measured at the maximum absorption of the cNDI derivatives. Association rate constants of the ligand-dsDNA interactions were obtained by fitting the exponential traces of absorbance observed after mixing the ligand solution with DNA at a 10-fold excess of the ligand concentration. The dual-exponential equation was used for nonlinear fitting: $A_1 \exp(k_1 t) + A_2 \exp(k_2 t)$, where A and k refer to the fractional amplitudes and rate constants, respectively. The intrinsic second-order association rate constant (k_a) and the dissociation rate constants (k_d) were obtained from the slope and intercept of a plot of the apparent association rate constant ($k_{app} = A_1 k_1 + A_2 k_2$) against the DNA concentration, according to the equation $k_{app} = k_a[DNA] + k_d$. The dissociation rate constant (k_d) of the ligand from DNA was independently determined by sodium dodecyl sulfate (SDS)-driven dissociation measurements, as described previously [15,16]. Equal volumes of 1% SDS solution and the DNA-ligand complex were mixed instantaneously using a piston pump. Changes in absorbance over time were recorded. When the DNA-ligand complex was

mixed with SDS solution, the free ligand underwent incorporation into the SDS micelles. As this reaction is diffusion-controlled, all absorption changes represent a k_d-dependent process; therefore nonlinear fitting of the kinetic trace provides the k_d value.

3.2.6. Topoisomerase I assay measurements

A Topoisomerase I assay was carried out according to the method previously reported [12,13]. Briefly, 0.25 μg of pUC19 was incubated with 5 U of topoisomerase I in 0.1% bovine serum albumin (BSA) and 1× reaction buffer—composed of 35 mM Tris-HCl (pH 8.0), 72 mM potassium chloride, 5 mM magnesium chloride, 5 mM dithiothreitol (DTT), and 5 mM spermidine—at 37°C for 5 min. Various concentrations of **1**–**3** were then added, and the mixture was incubated at 37°C for 1 h. The reaction was terminated by the addition of 2 μL of 10% sodium dodecylsulfate (SDS) and 0.5 μL of 20 mg/ml proteinase K, and the solution was then incubated at 37°C for 15 min. Topoisomerase I was then extracted with phenol containing chloroform and isoamyl alcohol, and then with chloroform containing isoamyl alcohol. After ethanol precipitation and dissolution, topoisomerase I was analyzed by gel electrophoresis on 1% agarose in 1× TAE at 18 V for 3.5 h. The gel was stained with Gelstar (Takara Bio, Shiga, Japan) in 1× TAE for 30 min.

3.2.7. Circular dichroism (CD) measurements

Various concentrations (5–50 μM) of **1**–**3** were added to 100 μM/base pair CT-DNA in 10 mM MES buffer (pH 6.25) containing 100 mM NaCl and 1 mM EDTA at 25°C. CD spectra were taken at a scan rate of 50 nm/min on a Jasco J-820 spectropolarimeter (Tokyo, Japan). Scan parameters were as follows: response = 2 s, data interval = 0.1 nm, sensitivity = 100 mdeg, band width = 2 nm, and scan number = 4.

3.2.8. Computer modeling

Molecular models of the cNDI-DNA complexes were constructed by MOE 2011.10 (http://www.chemcomp.com/). Compounds **1** or **2** was placed on the binding site of the DNA duplex, and energy minimization of the complex was carried out. Molecular dynamics calculation of the mineralized complex was further carried out until **1** or **2** was stabilized in the binding site. Finally, energy minimization of the complex was obtained, as shown in Fig. 6. These calculations were performed using the force field of MMFF94x.

3.3. Result and discussions

3.3.1. Binding studies of cNDIs- dsDNAs: UV-Vis titrations

Spectroscopic titration of cNDIs with dsDNAs was carried out. The interaction showed maximum absorption at 383 nm and a large hypochromic effect with a small redshift, indicative of binding between the cNDIs and the dsDNAs (Fig. 3.3). An example of the spectrophotometric titration of **1** with CT-DNA is illustrated in Fig. 3.2A. The observed hypochromic effect indicated strong intercalative binding of cNDIs between dsDNAs. Optical data of the cNDIs are shown in Table 3.2. An isosbestic point observed at 395 nm supports the prediction of a two-state system involving bound and free cNDIs. Absorbance at a specific wavelength indicated the participation of both free and bound cNDIs when titrated with a fixed concentration of DNA. Scatchard plots were prepared using absorption changes at the specific wavelength 383 nm upon the addition of various concentrations of dsDNA. I used the data in a range of approximately 30%–80% bound region of cNDIs and dsDNA. The Scatchard plot in Fig. 3.2B illustrates binding between the cNDIs and dsDNAs. It was analyzed using the McGhee-von Hippel equation [17] (Eq.

3.1) for non-cooperative ligand binding.

$$\frac{v}{C} = K(1 - nv)\left(\frac{1-nv}{1-(n-1)v}\right)^{n-1} \quad (3.1)$$

v is the stoichiometry (the number of ligand molecules bound per moles of base pair), C is the free ligand concentration, K is the observed binding constant (K_b), and n is the number of base pairs excluded by the binding of a single ligand molecule. The solid line in 3.2B indicates a good fit of the experimental values to those predicted by the McGhee-von Hippel equation. Scatchard analysis using the spectra change of cNDIs upon the addition of dsDNAs showed binding constants ranging from 1.0–53.4×10^5 M^{-1}, and the observed binding order was poly[d(G-C)]$_2$ > CT-DNA > poly[d(A-T)]$_2$. The expected value of n was four, as cNDIs interact with dsDNAs by bis-intercalation of four base pairs, whereas the threading intercalator **3** followed the nearest-neighbor exclusion principle [17], in which it was bound with dsDNAs by intercalation of two base pairs. I expected a violation of the nearest-neighbor exclusion principle by the cNDIs because they are large, cyclic macromolecules; a single cNDI molecule may cover more than two DNA base pairs and bind with dsDNA in bis-intercalative mode. Previous reports [12,13] on the binding of NDI derivatives to DNAs have shown similar trends of spectral change and support the binding constant for **3** observed here. Previously, our group reported that the interaction between **1** and duplex oligonucleotides revealed a higher binding constant (3.7 × 10^6 M^{-1}) and melting temperature than did the interaction between **3** and duplex oligonucleotides [12]. I further studied **1**–**3** with different types of dsDNA that carried AT- or GC-rich sequences to determine the sequence specificity of binding**.** Compounds **1** and **2** showed similar trends of binding behavior with the different types of dsDNA**.** Compounds **1** and **2** showed comparatively higher binding affinity to dsDNAs than **3** (Table 3.1) because of the binding flexibility of **3**. The NDI moiety of **3** may intercalate

between dsDNA base pairs, and does not depend on major and minor groove binding. On the other hand, cNDI intercalated with the major and minor grooves of dsDNA making a rigid catenane complex [9]. Our observations revealed that long-chain **1** has a higher binding affinity to dsDNAs than short-chain **2**. According to computer modeling, short-chain **2** may have a steric strain effect in its binding with dsDNA. In addition, Sato et al. previously reported that the introduction of a methyl or alkyl group results in a higher binding constant because of the substituent effect [18]. Our group has already reported that other types of short-chain cNDI derivatives may have a greater affinity for G-quadruplex DNA than for DNA duplex because of the staking interaction between the short-chain cNDI derivatives and G-quadruplex DNA [13]. Compound **1** displayed the highest affinity for poly[d(G-C)]$_2$, with a binding constant of 5.34×10^6 M^{-1}, which is approximately 9 times higher than the binding constant of its interactions with CT-DNA and Poly[d(A-T)]$_2$ (Table 2). There is a strong tendency for cNDIs to bind with GC base pairs because of the rigidity, depth, and width of the GC groove. Nucleophilic guanine may also have a strong affinity for protonated cNDI molecules [19]. I assumed that cNDIs may strongly intercalate 5′-GpC-3′ sequences by insertion of the naphthalene diimide moiety and benzene ring into the 5′-GC/CG-3′ step, creating a catenane structure with dsDNA [20]. Preferential interactions of NDI ligands with GC polymers have been observed previously, confirming that the binding affinity of NDIs varies with DNA sequence [21]. Additionally, the double-stranded DNA structure is known to be highly dynamic in solution, with base pairs opening and reforming rapidly at room temperature. cNDIs may be able to exploit this millisecond “breathing” behavior of dsDNA by sliding between the temporarily disrupted DNA base pairs to form a pseudo-catenane or bis-intercalation complex structure [22]. Under natural conditions, DNA dynamic breathing

is also referred to as "partial base flipping" [23,24]. Recently, Nakatani et al. reported that a single-molecule ligand can, in fact, induce nucleotide base flipping [25]. Overall, the present study is consistent with previous investigations of the interaction between cNDIs and dsDNAs, which have included bis-intercalators such as bisacridine and bisdaunamycine [26,27]. The binding of cNDIs to dsDNAs (Fig. 3.14) is structurally similar to cNDI-dsDNA structures previously described by other groups [9].

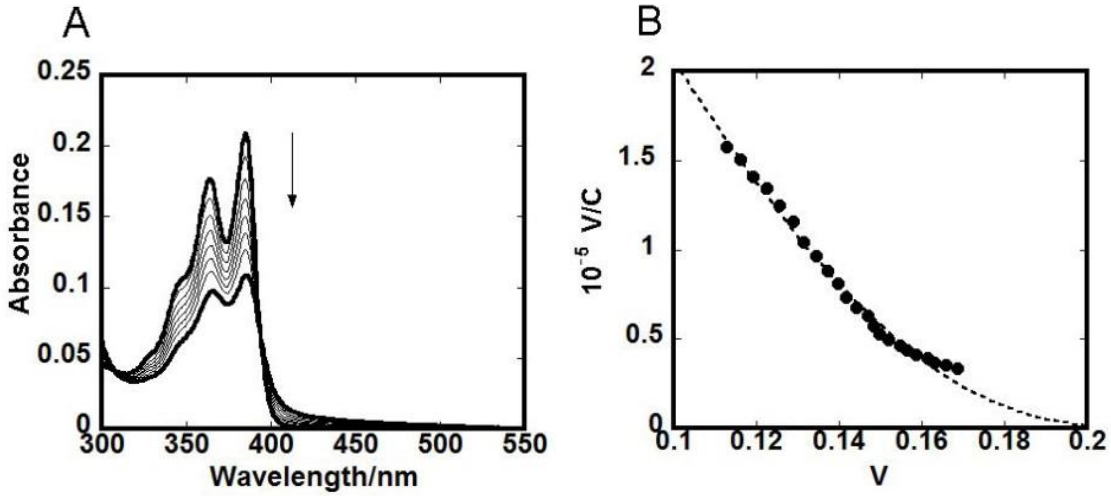

Fig. 3.2. Spectral shifts of 6.7 μM of **1** on titration with 0, 5, 10, 15, 20, 25, 30, 40 and 50 μM Calf thymus DNA (A) (from top to bottom). Scatchard plots for the binding of **1** to Calf thymus DNA (B). Experiments were performed at 25°C in 10 mM MES buffer pH 6.25 containing 100 mM NaCl and 1 mM EDTA.

Table 3.1 Binding parameters of **1-3** with CT-DNA, Ploy $[d(A\text{-}T)]_2$ and Poly $[d(G\text{-}C)]_2$

	1		**2**		**3**	
DNAs	$10^{-6}K_b/M^{-1}$	n	$10^{-6}K_b/M^{-1}$	n	$10^{-6}K_b/M^{-1}$	n
CT-DNA	0.7± 0.01	4.5	0.12± 0.005	4.9	0.34±0.006	3.4
Poly $[d(A\text{-}T)]_2$	0.6± 0.055	3	0.10± 0.004	5	0.28±0.001	3
Poly $[d(G\text{-}C)]_2$	5.34± 0.6	4	0.5 ± 0.013	3.5	0.84±0.026	2.2

Condition: 10 mM MES (pH6.25), 1 mM EDTA, and 0.1 M NaCl.

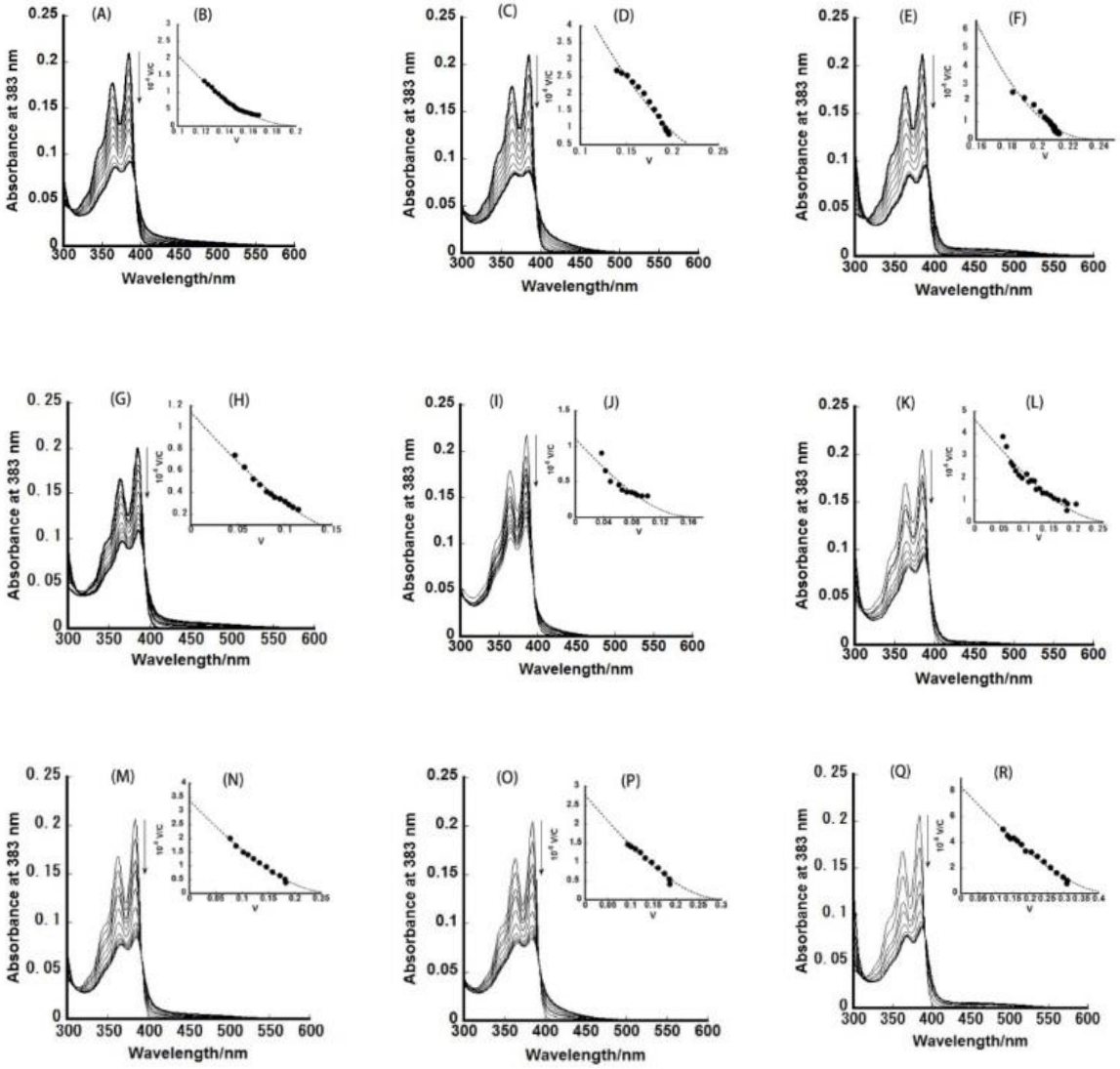

Fig. 3.3. UV-Vis absorption spectra of 6.7 µM **1** (A, C, E), **2** (G, I, K) or **3** (M, O, Q) in the absence and presence of titrant calf thymus DNA (A, G, M), Poly (dA-dT)$_2$ (C, I, O) and Poly (dG-dC)$_2$ (E, K, Q) with 0, 5, 10, 15, 20, 25, 30, 40 and 50 µM respectively. Binding affinities were estimated using the scatchard plot of **1** (B, D, F), **2** (H, J, L) or **3** (N, P, R) using the titrant calf thymus DNA (B, H, N), Poly (dA-dT)$_2$ (D, J, P) and Poly (dG-dC)$_2$ (F, L, R). Experiments were performed at 25°C in 10 mM MES buffer pH 6.25 containing 100 mM NaCl and 1 mM EDTA.

Table 3.2 Summary of the optical properties of free and DNA bound **1-3**.

DNAs	CT-DNA			Poly [d(A-T)]$_2$			Poly [d(G-C)]$_2$		
ligads	**1**	**2**	**3**	**1**	**2**	**3**	**1**	**2**	**3**
λ*max* (free)/nm	383	383	383	383	383	383	383	383	383
λ*max* (bound)/nm	387	386	388	387	386	387	388	385	388
λ*iso*/nm	395	395	393	394	396	392	392	393	391
H/%	60	60	62	47	49	60	61	61	61

λ*iso:* Wavelength at the isosbestic point; H: Hypochromicity, measured by using the formula,H%=Absorbance at 383 nm (free) - Absorbance at 383 nm (bound)/ Absorbance at 383 nm (free) × 100 [28].

3.3.2. Thermodynamic analysis

The interaction between a drug and biomolecule may involve hydrophobic forces, electrostatic interactions, van der Waals interactions and hydrogen bonds. According to data on enthalpy changes ($\triangle H$) and entropy changes ($\triangle S$), the following model of interaction between a drug and a biomolecule can be concluded: (1) $\triangle H > 0$ and $\triangle S > 0$, hydrophobic forces; (2) $\triangle H < 0$ and $\triangle S < 0$, van der Waals interactions and hydrogen bonds; (3) $\triangle H < 0$ and $\triangle S > 0$, electrostatic interactions [29]. When there is little change in temperature, $\triangle H$ can be considered constant, and its value, along with that of $\triangle S$, can be determined from the van't Hoff (Eq. 3.2) and Gibbs free energy (Eq. 3.3) equations.

$$lnK_b = -\frac{\Delta H}{RT} + \frac{\Delta S}{R} \qquad (3.2)$$

$$\Delta G = \Delta H - T\Delta S \qquad (3.3)$$

R is the gas constant and K_b is the binding constant (Table 3.4) at the corresponding temperature. Fig. 3.5 shows the spectral shift of CT-DNA upon binding of **1**. Using this absorption change, I measured the binding constant (K_b). The values of $\triangle H$ and $\triangle S$ were obtained from the slope and intercept of the linear plot (Eq. 3.2) of *lnK* against 1/T (Fig.

3.4). The value of $\triangle G$ was estimated from Eq. (3.3). Its negative value means that the binding process is spontaneous (Table 3.3). The values of $\triangle H$ and $\triangle S$ for the binding between **1-3** and CT-DNA are listed in Table 3.3. The negative values of $\triangle H$ for **3** indicates the exothermic nature of the binding process with CT-DNA and intercalation may occur favorable electrostatic interaction (Fig. 3.4). I have assumed that the binding of non-cyclic NDI with CT-DNA shows flexibility consequently energy release and binding process entalpically driven. On the Other hands, the binding of **1** and **2** with CT-DNA indicates the endothermic (Fig. 3.4). The positive enthalpy and positive entropy values of the interaction between **1** or **2** and CT-DNA indicate that hydrophobic forces played a major role in the reaction. These results are consistent with previously reported results for binding between CT-DNA and NDI derivatives [30]. When **1** or **2** interacts with CT-DNA, the driving force of the interaction clearly changes from enthalpy to entropy. The change in entropy is governed by the release of counterions and water from both DNA and the ligand, and also by changes in the local DNA structure upon ligand binding. These features simultaneously contribute unfavorable ΔH and favorable ΔS to the binding free energy and have been observed by other researchers [31,32]. Spolar et al. have also reported that the entropy change depends on the rigidity of the DNA-protein complexes [32]. Moreover, the intercalating chromophore of cNDIs consists of two aromatic ring systems that intercalate into the DNA duplex in a parallel arrangement that follows the lock and key model, making its stability entropically driven [4,32]. Binding between the bis-intercalator echinomycin and DNA has been shown to be entropically and hydrophobically driven, which is in agreement with our observations of binding between the newly designed cNDIs and CT-DNA [4,33]. According to thermodynamic data, I can state that long-chain **1** was more favorable for entropy-dependent binding than

short-chain **2.**

Table 3.3 Thermodynamic parameters of binding of **1-3** to calf thymus DNA.

Parameters	**1**	**2**	**3**
△*H*/kcal mol^{-1}	7.8±1	9.2±0.84	-6.7±0.67
△*S*/cal mol^{-1}	52.8±3.3	54.4±2.8	3±2
△*G*/kcal mol^{-1} (25 ˚C)	-7.95	-7.0	-7.59

Condition: 10 mM MES (pH6.25), 1 mM EDTA, and 0.1 M NaCl.

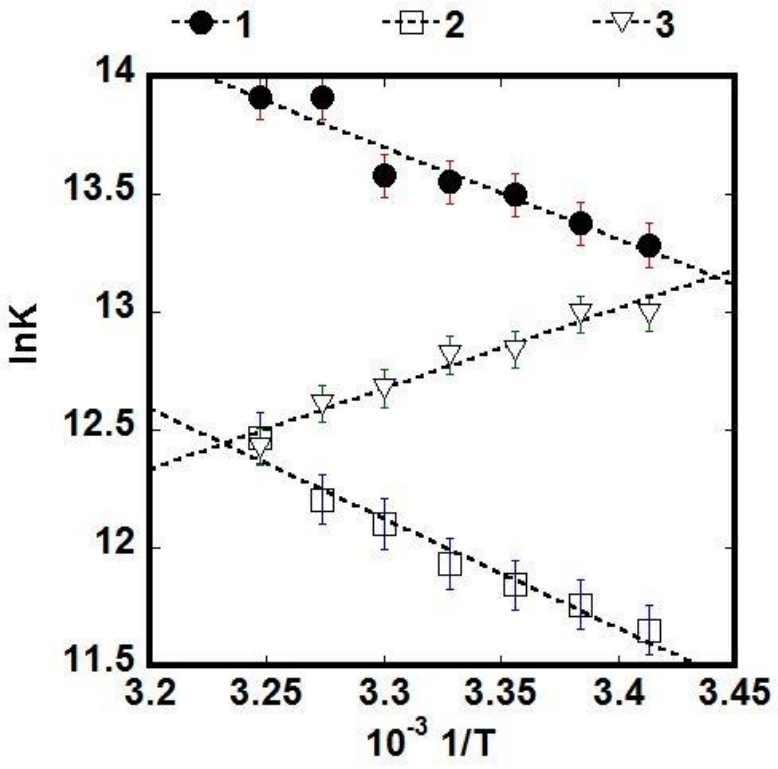

Fig. 3.4. Plots of ln*K* (the observed equilibrium constants) vs 1/T under the binding of **1-3** to calf thymus DNA.

Table 3.4 Binding constants of **1-3** interacting with calf thymus DNA at different temperature.

Temperature/°C	$10^{-5}K/M^{-1}$		
	1	**2**	**3**
20.0	5.9 (±0.24)	1.2 (±0.40)	4.5 (±0.12)
22.5	6.5 (±0.25)	1.3 (±0.40)	4.4 (±0.12)
25.0	7.0 (±0.23)	1.4 (±0.70)	3.8 (±0.11)
27.5	7.7 (±0.23)	1.5 (±0.12)	3.7 (±0.07)
30.0	7.9 (±0.50)	1.8 (±0.05)	3.2 (±0.20)
32.5	11 (±1.0)	2.0 (±0.18)	3.0 (±0.15)
35.0	11 (±1.5)	2.6 (±0.10)	2.5 (±0.20)

Condition: 10 mM MES (pH6.25), 1 mM EDTA, and 0.1 M NaCl.

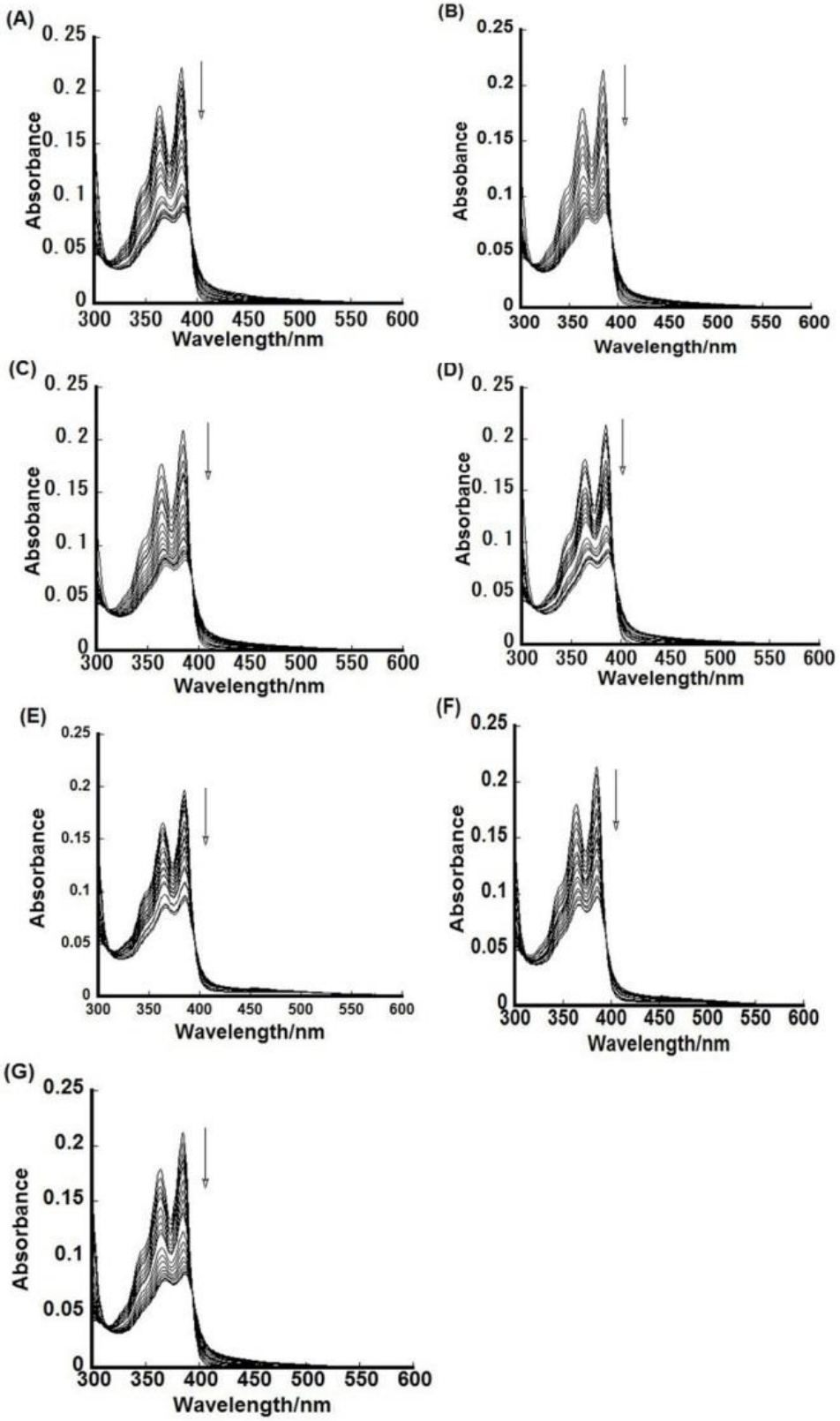

Fig. 3.5. UV-Vis absorption spectra of 6.7 μM **1** with the varied amount of calf thymus

DNA. Experiments were performed at 20°C (A), 22.5°C (B), 25°C (C), 27.5°C (D), 30°C (E), 32.5°C (F), and 35°C (G) in 10 mM MES buffer pH 6.25 containing 100 mM NaCl and 1 mM EDTA.

3.3.3. Salt effect analysis

The entropic nature of the reaction can be related to the significant role of hydrophobic interactions in the binding process. Thus the electrostatic effect is almost entirely enthalpic [29,34]. In our study, Electrostatic interaction is less important for cNDIs binding to DNA because of favorable entropy. The binding constant of cNDIs to DNA entirely depends on salt concentration even through cNDIs is neutral. Reports in the past have shown that a very high concentration of NaCl would hinder small molecules from binding with DNA [35]. Our results show that the binding parameters decreased with a gradual increase in NaCl concentration (Table 3.6). According to counterion condensation theory (Eq. 3.4) is a measure of the number of sodium ions released from DNA per bound ligand. Due to the lengthening of the DNA helix and unwinding DNA upon intercalation, increasing the phosphate gaps along the helix axis [18,31,36]. Consequently, releasing condensed counterions because of the charge density of the duplex decreases and providing an entropically favorable contribution to the binding free energy. Releasing counterions explains the dramatic salt dependencies of DNA-cNDIs complexes. High salt destabilizes DNA- cNDIs complexes. There is a large entropic gain from counterion release, if the salt concentration in solution is low and the cNDIs binds tightly to the DNA. The entropic gain from counterion release is small, if the salt concentration in solution is high and the cNDIs binds weakly. I observed that an increased salt concentration hindered the binding of **1** more significantly than that of **2**. At pH 6.25, the net charge would have been different because **1** possesses four nitrogen atoms in the

linker whereas **2** possesses only two. Moreover, at low ionic strength, a cNDI molecule binds to DNA with a large number of ion pairs, consequently increasing the free energy association through the release of a large fraction of counterions; this effect would be dramatically reduced at high ionic strength [37]. According to the polyelectrolyte theory [38], I plotted log *K* against –log [Na^+] in Fig. 3.6, and the slope was given by Eq. 3.4.

$$\frac{\delta \log K_{obs}}{\delta \log[Na^+]} = -m\Psi \qquad (3.4)$$

m is the charge on the ligand and Ψ is the proportion of counterions associated with each DNA phosphate group, normally Ψ is 0.88 for classical intercalator with double-stranded *B*-type DNA [3,34]. However, it is known that Ψ for dicationic threading intercalators show 0.6 – 0.8 [16]. The data in Table 3.5 show slopes of 0.72, 0.74 and 0.83 for **1**, **2**, and **3**, respectively. This result suggested that these dicationic cNDI derivatives behave as threading intercalator and form catenane complex with double stranded DNA.

Table 3.5 Salt effects of **1-3** in the binding affinity.

cNDI derivatives	**1**	**2**	**3**
$\delta(\log K_{abs})/ \delta(\log[Na^+])$	0.72	0.74	0.83

Condition: 10 mM MES (pH6.25), 1 mM EDTA, and 0.05-0. 125 M NaCl.

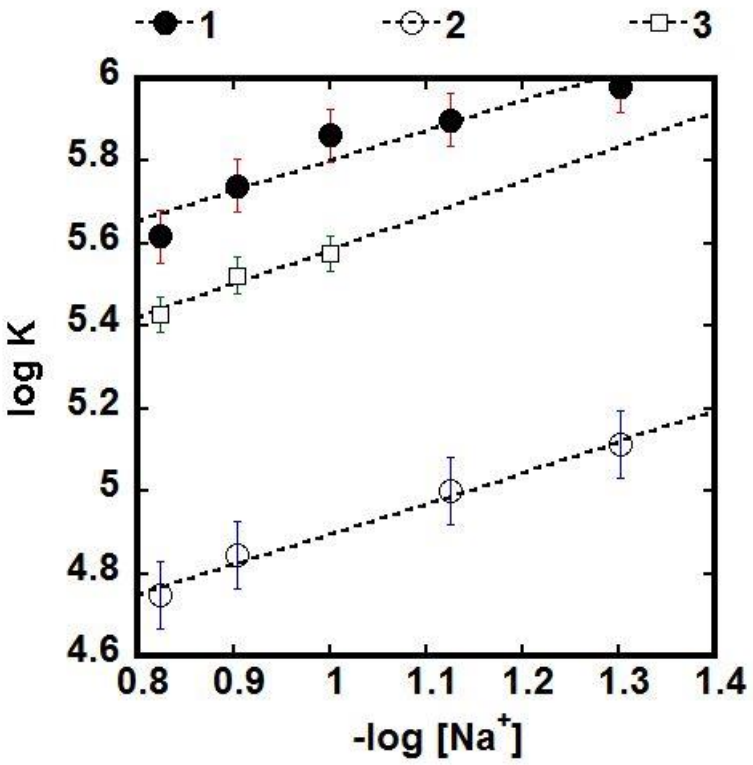

Fig. 3.6. Plots of log*K* (the observed equilibrium constants), versus –log [Na^+] under the binding of **1-3** to calf thymus DNA.

Table 3.6 Binding constants of **1-3** interacting with calf thymus DNA at different salt concentration.

[NaCl]/M	$10^{-5}K/M^{-1}$		
	1	**2**	**3**
0.05	9.56	1.3	-
0.075	7.94	1.0	-
0.1	7.29	1.3	1.30
0.125	5.50	0.7	0.95
0.15	4.15	0.56	0.56

Condition: 10 mM MES (pH6.25), 1 mM EDTA, and 0.05-0.15 M NaCl.

3.3.4. Stopped flow kinetic analysis

As suggested in our group previous report [12], **1** showed a much slower dissociation constant in its interaction with GC than **3**. In the present report, I have discussed in detail the association and dissociation kinetics of **1**–**3**.

Association: Typical examples of the association kinetic traces of the interactions of CT-DNA, Poly[d (A-T)]$_2$, and Poly[d(G-C)]$_2$ with **1**–**3** are shown in Figs. 3.7A, 3.9A and 3.10. All data were analyzed by two-exponential fitting, and the results are summarized in Table 3.7. The highest absorption by the DNA duplex-ligand complex occurred at 383 nm (Fig. 3.9A). Association constant (*ka*) was determined by the apparent rate constant (k_{app}) against DNA concentration (Fig. 3.8). Absorption decreased dramatically and underwent a slight bathochromic shift. This phenomenon has previously been observed for interactions between other naphthalene diimide derivatives and dsDNAs [16]. Association rate constants for **1–3** increased in the following order: Poly[d(A-T)]$_2$, CT-DNA, Poly[d(G-C)]$_2$. The association process of the interaction of **1** with poly[d(A-T)]$_2$ was about two and five times higher than that of **3** and **2**, respectively. The association kinetics of **1-3** with poly[d(G-C)]$_2$ were almost two times slower than with poly[d(A-T)$_2$, implying that transient breathing of the double helix influences the rate of association. Previous reports on naphthalene diimides derivatives as tri-intercalators have shown similar association constant trends [6]. Indeed, a study of the kinetics of the threading intercalator anthracyne also exhibited a similar association trend that may be related to a rate-determining DNA breathing step [39]. In addition, the association rate constant may depend on the cyclic character and the rigidity of the ligand molecule. Thus, the side chains of the ligand molecule can have large effects on DNA

interaction kinetics. Complex formation can be slowed by the disruption of a higher number of adjacent base pairs when two intercalation sites open in the double helix.

Dissociation*:* A typical example of the SDS-driven dissociation kinetic traces of interactions between CT-DNA, Poly[d(A-T)]$_2$, or Poly[d(G-C)]$_2$ and **1**–**3** is shown in Figs. 3.7B, 3.9B and 3.10. All data were analyzed by two-exponential fitting, and the results are summarized in Table 3.7. The highest absorption by the DNA duplex-ligand complex occurred at 383 nm (Fig. 3.9B). Absorption decreased dramatically and underwent a slight bathochromic shift. This phenomenon has previously been observed for interactions between other naphthalene diimide derivatives and dsDNAs [16]. Dissociation rate constants for **1**–**3** increased in the following order: Poly[d(G-C)]$_2$, CT-DNA, Poly[d(A-T)]$_2$. It is worth mentioning the very slow dissociation of **1** from the GC-rich complex, which was 100 times slower than that of **3** and 330 times slower than that of **2**. This is due to the strong binding constant of the interaction between cNDIs and GC-rich dsDNA (Table 3.1) because of the rigidity of the complex, as previously discussed. Many heterocyclic or highly polarizable intercalators exhibit a binding preference for GC base pairs with a larger asymmetric charge distribution. Although the cNDIs are symmetric, they still have significant partial atomic charges on the heterocyclic rings, and the molecule in Fig. 3.1 for example, exhibits significant GC binding specificity. These results are similar to previously reported dissociation rate constants for interactions between naphthalene diimide derivatives and CT-DNA, which were lower for GC-rich sequences than for AT-rich sequences [6]. A study of the kinetics of the threading intercalator anthracyne also noted a similar dissociation trend [39]. These effects are related to the high binding affinity of **1** and **2** for poly[d(G-C)]$_2$, resulting from

hydrophobic interactions, favorable van der Waals stacking interactions of the large naphthalene diimide ring system, and partial atomic charges on the heterocyclic rings that can provide favorable coulombic interactions, particularly with GC base pairs. Long-chain **1** showed slower dissociation from dsDNA than short-chain **2**. Researchers have already found that longer chain bis-intercalators and poly-intercalators dissociate slowly from DNA duplexes [6].

Table 3.7 Kinetic parameters for binding of **1-3** to calf thymus DNA (CT-DNA), poly [d(A-T)]$_2$, and poly [(G-C)]$_2$.

DNAs	**1**		**2**		**3**	
	$10^{-5}k_a$/M^{-1}s^{-1}	k_d/s^{-1}	$10^{-5}k_a$/M^{-1}s^{-1}	k_d/s^{-1}	$10^{-5}k_a$/M^{-1}s^{-1}	k_d/s^{-1}
Calf thymus DNA	0.57±0.03	0.1	1.2±0.11	1.1	1.24±0.14	1.1
poly [d(A-T)]$_2$	1.2±0.11	0.15	0.32±0.08	4.2	2.6±0.35	2.6
poly [d(G-C)]$_2$	0.34±0.045	0.003	0.26±0.058	1.0	0.84±0.1	0.3

Condition: 10 mM MES (pH6.25), 1 mM EDTA, 0.1 M NaCl.

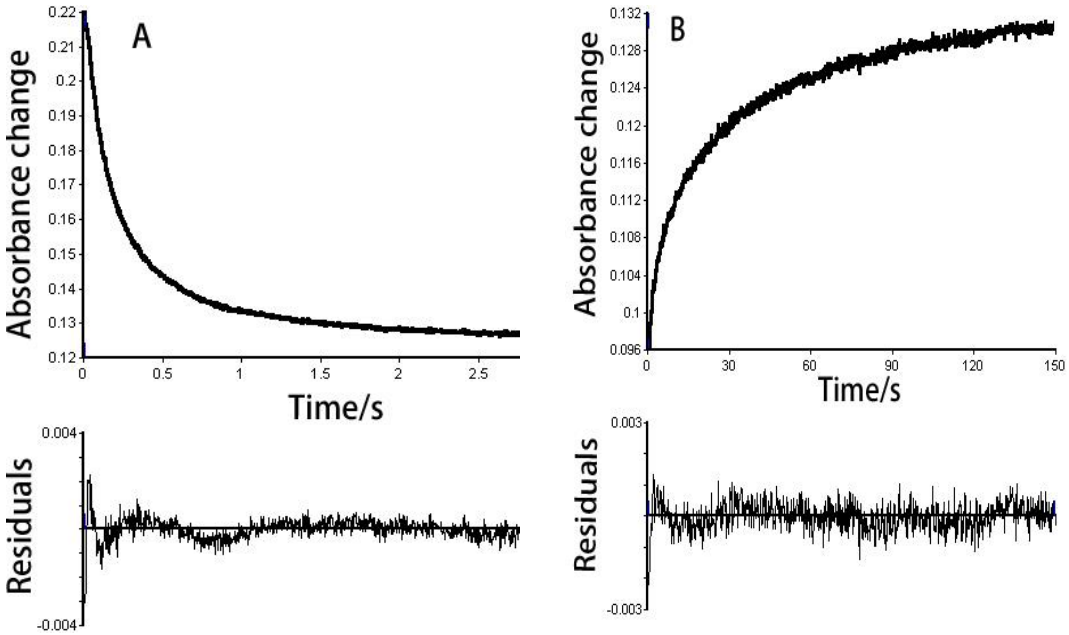

Fig. 3.7. Stopped-flow kinetic traces for the association (A) and the SDS-driven

dissociation (B) for a complex of **1** with calf thymus DNA. The smooth line represents the two-exponential fit to the data. A residual plot for the fit showed under the experimental plot. The experiments were conducted at 25 °C in 10 mM MES buffer and 1mM EDTA with 0.1 M NaCl and the concentration of **1** to DNA base pair ratio of 1:10.

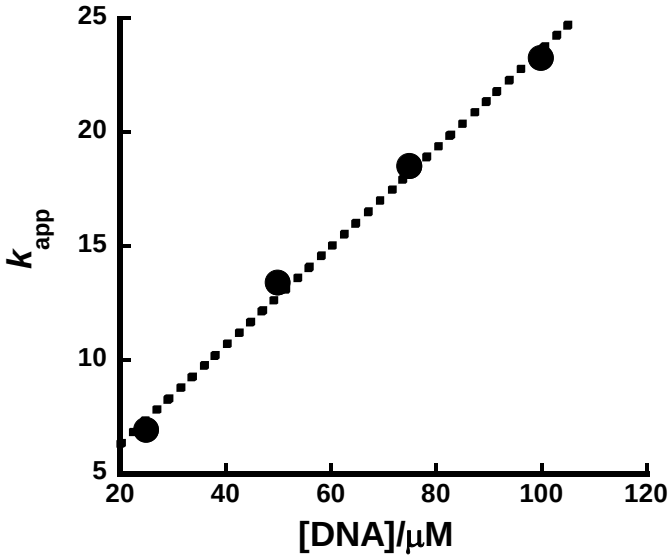

Fig. 3.8. Plot of the apparent rate constants (k_{app}) against DNA concentrations for the determination of association rate constant (k_a).

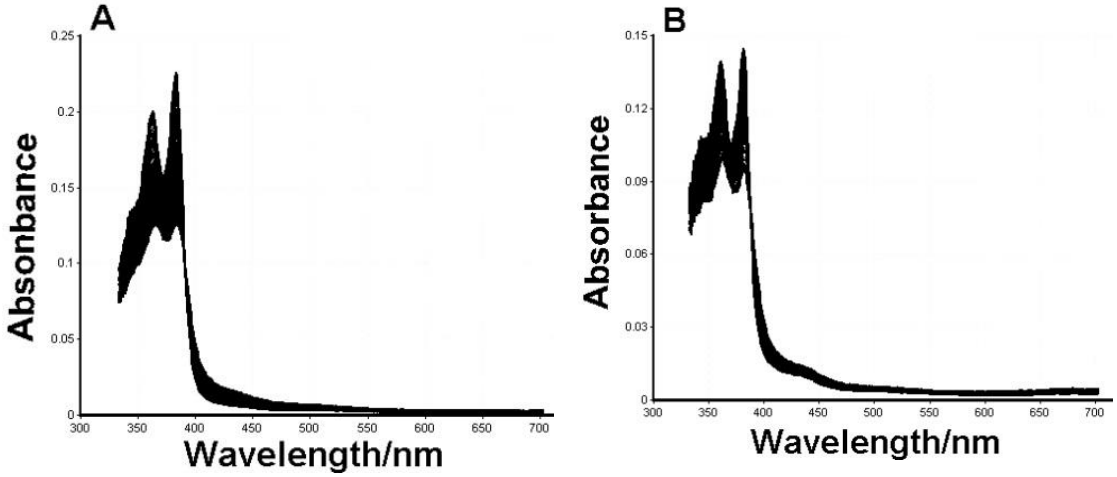

Fig. 3.9. Stopped-flow kinetic traces of absorption spectra at 383 nm for (A) association

(B) SDS-driven dissociation for a complex of **1** with calf thymus DNA. The experimental condition was under the same condition described in Fig. 3.7.

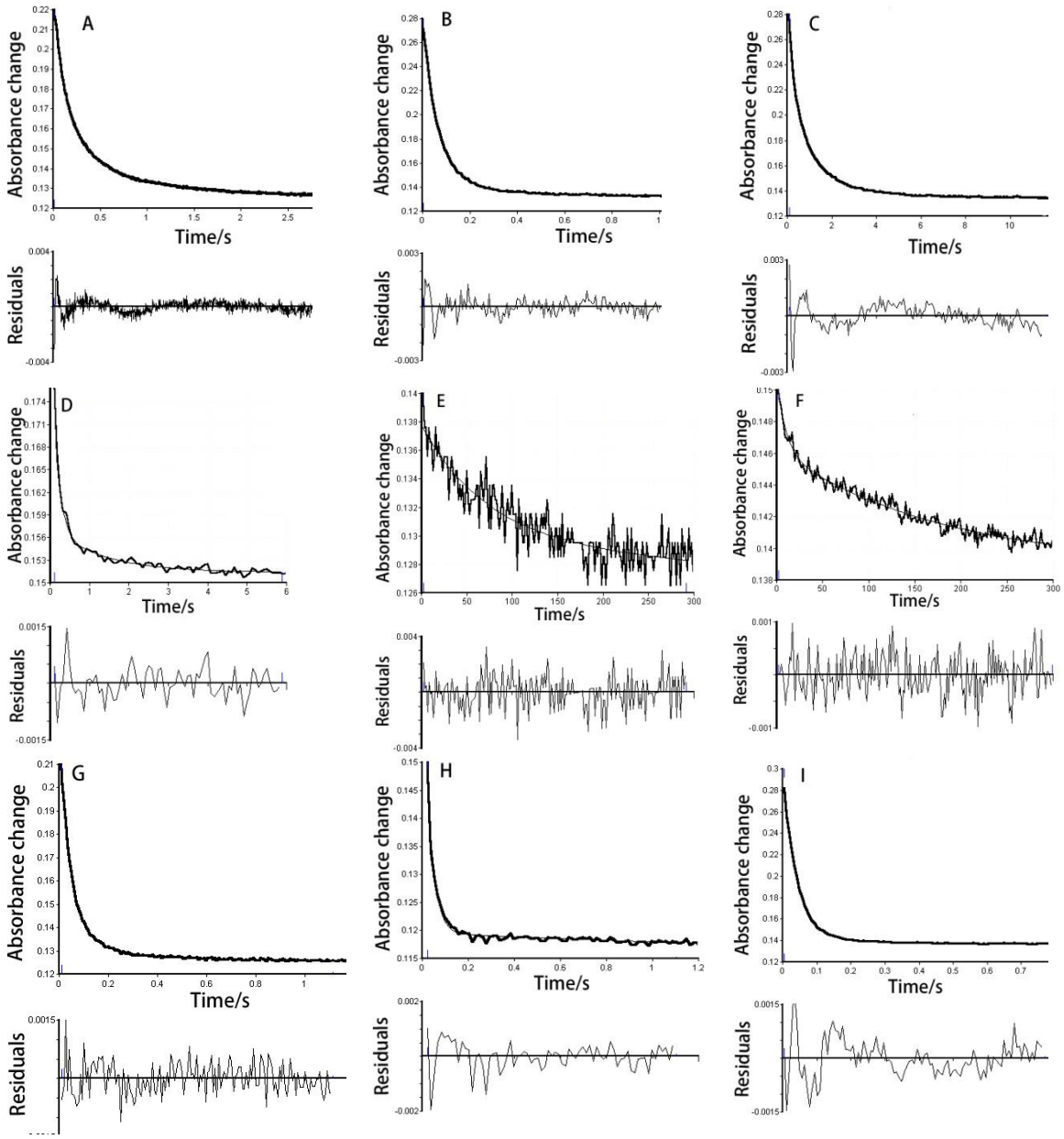

Fig. 3.10. Stopped-flow kinetics traces for association of **1** (A, B, C), **2** (D, E, F) and **3** (G,H,I) from calf thymus DNA (A, D, G), from Poly $[d(A\text{-}T)]_2$ (B, E, H) and from Poly $[d(G\text{-}C)]_2$ (C, F, I). The experiments were conducted in 10 mM MES buffer and 1 mM

EDTA (pH 6.25) containing 100 mM NaCl. [Ligand]/ [DNA/bp] =1:10.

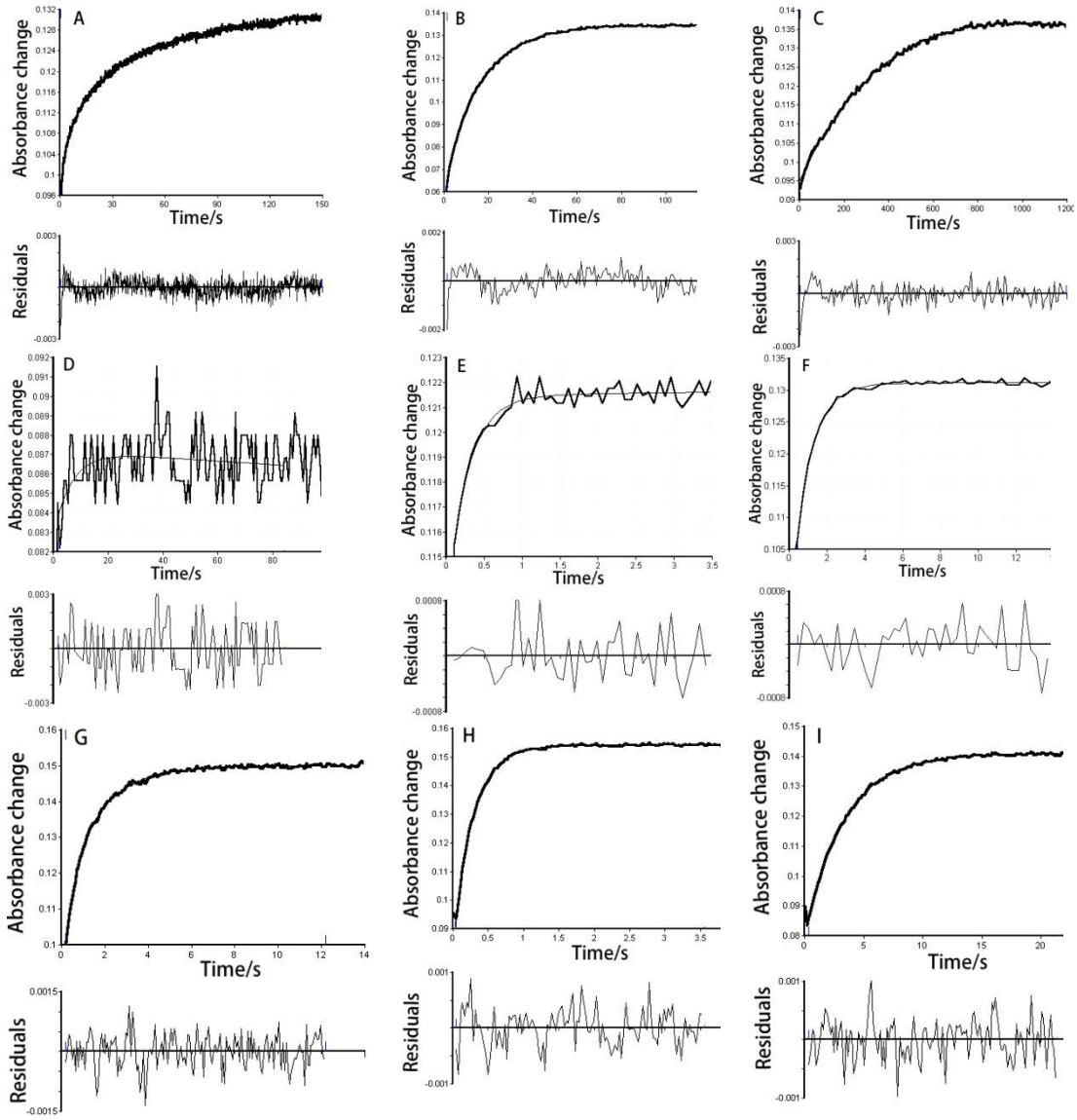

Fig. 3.11. Stopped-flow kinetics traces for SDS driven dissociation of **1** (A, B, C), **2** (D, E, F) and **3** (G, H, I) from calf thymus DNA (A, D, G), from Poly $[d(A\text{-}T)]_2$ (B, E, H) and from Poly $[d(G\text{-}C)]_2$ (C, F, I). The experiments were conducted in 10 mM MES buffer pH 6.25 containing 100 mM NaCl and 1 mM EDTA. [Ligand]/ [DNA/bp] =1:10

3.3.5. Topoisomerase I assay

Topoisomerase-based gel assays have been widely used to evaluate compounds for their ability to intercalate DNA [40]. The ability of NDI derivatives to cause re-supercoiling of plasmid DNA has been frequently reported [12,13]. The topoisomerase I assay exploits the ability of the topoisomerase I enzyme to relax supercoiled DNA (e.g., pUC19-plasmid DNA). In the presence of an intercalator, the enzyme will convert the relaxed DNA into a supercoiled state by unwinding the DNA structure. Previously, our group reported that **1** and **3** are DNA intercalators [12,13]. In the present study, plasmid DNA was treated with increasing concentrations of **2** in the presence of topoisomerase I. Complete re-supercoiling of the plasmid DNA upon interaction with **2** was readily observed, indicating its identity as a DNA intercalator (Fig. 3.12). Remarkably, Compound **1** elicited re-supercoiling more effectively than **2**. Compound **1** re-supercoiled DNA completely at a concentration of ca. 2 μM, whereas the concentration of **2** required to show a similar effect exceeded ca. 10 μM. These results are in agreement with the higher binding affinity of **1** for DNA duplexes.

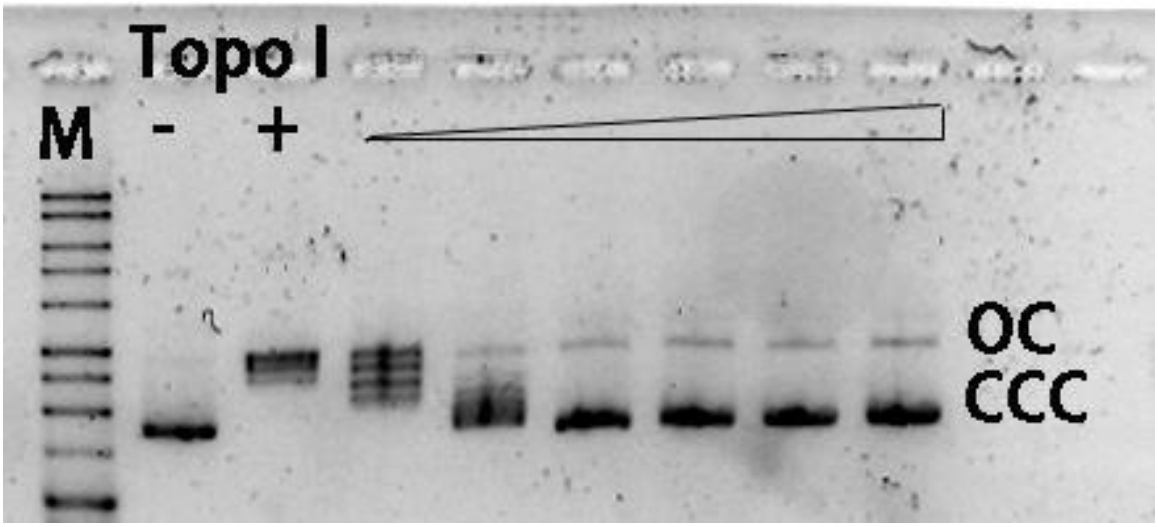

Fig. 3.12. Topoisomerase I assay for pUC19 treated with 5.0 U of enzyme. Following

incubation at various concentrations of **2** (2.0, 5.0, 10, 20, 30, 40, 50 μM from left to right) was added and the mixture incubated further. After work-up, DNA was electrophoresed Lanes M and Topo I represent 1 kb size markers and pUC19 respectively. OC and CCC refer to open circle and the covalent closed circle respectively.

3.3.6. Circular dichroism (CD) studies

Intrinsic and induced CD spectroscopy was used to further elucidate the conformational aspects of the interaction between cNDIs and CT-DNA. The characteristic CD spectrum of right-handed B-form DNA in the 200–300 nm region can provide information indicating specific structural changes in DNA upon interaction with ligands. Previously, our group reported that **1** and **3** induce a negative CD band (in the 340–440 nm region) upon interaction with CT-DNA, Poly $[d(A-T)]_2$, or Poly $[d(G-C)]_2$, indicating an intercalative binding mode [12]. Compounds **1** and **3** also showed a dramatic change in the CD spectrum in the region of 220-320 nm, indicating that the ligands affect duplex stability and conformation [12]. In the present study, I used CD spectroscopy to investigate the interaction between **2** and CT-DNA. As depicted in the CD spectrum (Fig. 3.13A), I observed a negative peak around 245 nm for free CT-DNA, due to helicity, and a positive peak around 276 nm, due to base stacking. After the addition of **2**, the positive and negative CD bands increased rapidly without any shift in the band position. I also observed a small negative band around the 320–400 nm region (Fig. 3.13B). These bands indicated that binding of CT-DNA had reached the saturation point. In light of previous reports [41], the negative CD band associated with **2**-CT-DNA complexes may indicate that **1** and **2** intercalate with the long axis of the chromophore oriented parallel or perpendicular to the long axis of the DNA base pair [11]. Compound **1** induced higher

CD spectra than **2** and **3,** in agreement with its stronger binding to DNA duplexes DNA than that of **2.**

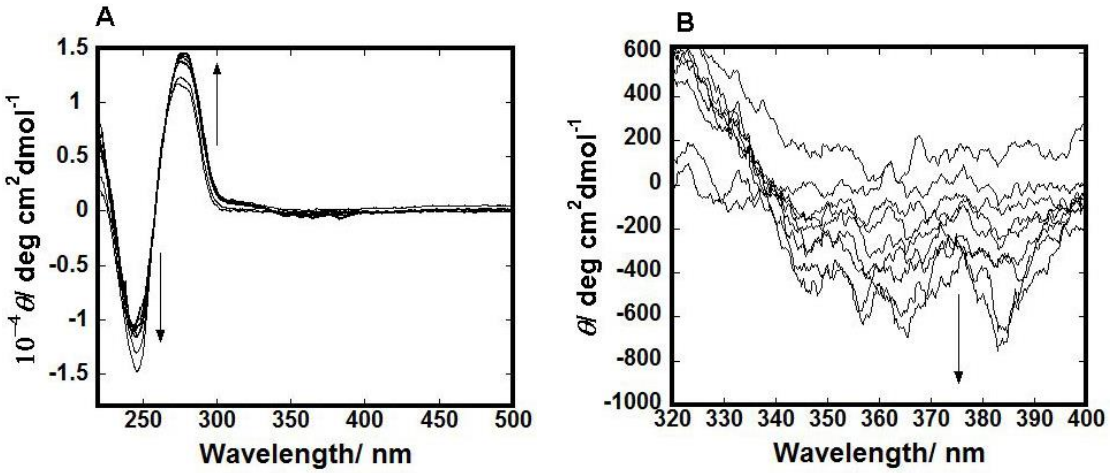

Fig. 3.13. (A) CD spectra of 100 μM DNA samples titrated with **2** (0, 5,10,15, 20, 25, 30, 40 and μM from bottom to top) at 25°C in 10 mM MES buffer and 1 mM EDTA (pH 6.25) containing 100 mM NaCl. (B) Induced CD spectra at wavelength region 320-400 nm.

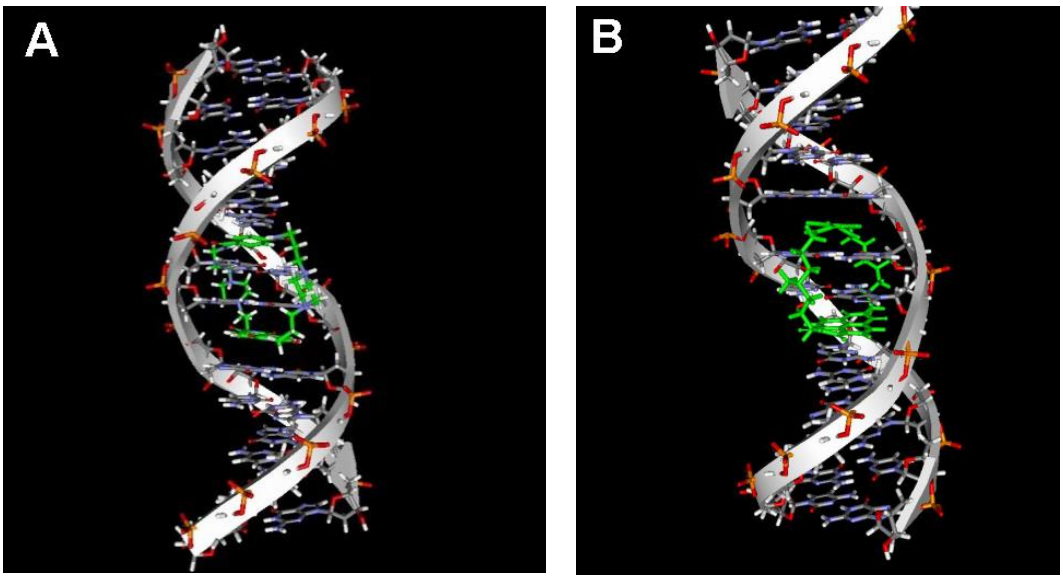

Fig. 3.14. Computer modeling of the complex of **1** (A) and **2** (A) with dsDNAs.

3.3.7. Computer modeling

Double stranded DNA was created with the Create Sequence of MOE software. Base pairs of binding site were expanded to have 3.4 Å space with slightly unwinding. After preparing the docking complex of cyclic naphthalene diimide with the DNA, the complex was minimized with a tether of nucleic bases. Computer modeling of the structures of the **1-** and **2**-dsDNA complexes is shown in Fig. 3.14. Previously, our group reported the binding mode of **1** with dsDNA. Here we propose a similar binding mode, with bis-threading intercalation or formation of a pseudo-catenate complex between **1** or **2** and dsDNA, which is consistent with a model previously published by Iverson et al. [9]. Computer modeling suggests that the **2**-dsDNA complex has a steric strain effect, due to the shorter linker chain.

3.4. Conclusions

I have developed a new type of bis-intercalator, **2**, which was synthesized by the cyclization of naphthalene diimide (NDI). Previously, our group reported in our investigation of the interaction between **1** and dsDNA [12]. Here I have compared of the interaction between **1** and dsDNA with that of **2** and dsDNA**.** The result of interaction studies of **1**–**3** with dsDNAs follows the order **1**> **2** > **3**, which suggests that the long-chain **1** has higher dsDNA binding selectivity and binds dsDNA with more favorable thermodynamics and kinetics than **2**. UV-Vis analysis showed high binding affinity of **1** to dsDNA in the range of 6×10^5–5.3×10^6 M^{-1} (approximately 10 times higher than that of **2**), with bis-intercalation of four base pairs per ligand molecule. Thermodynamic studies of **1** and **2** indicated that entropy-dependent hydrophobic interactions play a major role in their interaction with dsDNA. Compound **1** showed more entropically favorable

interactions with dsDNA than **2**. Kinetics studies of **1** and **2** indicated that **1** dissociate from GC base pairs more slowly than **2** because of its unique, pseudo-catenane, bis-intercalative binding with stairs of dsDNA. Induced CD spectra and a topoisomerase I unwinding assay further supported the more favorable bis-intercalation binding of **1** over that of **2**.

3.5. References

1. M.M. Islam, S. Fujii, S. Sato, T. Okauchi, S. Takenaka, Thermodynamics and kinetic studies in the binding interaction of cyclic naphthalene diimide derivatives with double stranded DNAs, *Bioorganic Med. Chem.* 23 (2015) 4769–4776.
2. J.B. Chaires, Drug-DNA interactions**,** *Curr Opin Struct Biol.* 8 (1998) 314-20.
3. G.M. Blackburn, M.J. Gait, D. Loakes, D.M. Williams, *Nucleic Acids in Chemistry and Biology*, 3rd Ed., RSC Publication, Thomas Graham House, Science Park, Milton Road, Cambridge CB4 0WF, UK, 2006.
4. J.B. Chaires, A thermodynamic signature for drug–DNA binding mode, *Arch. Biochem. Biophys.* 453 (2006) 26–31.
5. V.M. Guelev, M.S. Cubberley, M.M. Murr, R.S. Lokey, B.L. Iverson, Design, synthesis, and characterization of polyintercalating ligands, in: Chaires, J. B., and Waring, M. J., (Eds.), *Methods in Enzymol.* Academic Press, New York. 2001, pp 556-570.
6. R.S. Lokey, Y. Kwok, V. Guelev, C.J. Pursell, L.H. Hurley, B.L. Iverson, A New Class of Polyintercalating Molecules, *J. Am. Chem. Soc.* 119 (1997) 7202-7210.

7. G.G. Holman, M. Zewail-Foote, A.R. Smith, K.A. Johnson, B.L. Iverson, A sequence-specific threading tetra-intercalator with an extremely slow dissociation rate constant, *Nat Chem.* 3 (2011) 875-881.

8. A.R. Smith, B.L. Iverson, Threading Polyintercalators with Extremely Slow Dissociation Rates and Extended DNA Binding Sites, *Am. Chem. Soc.* 135 (2013) 12783–12789.

9. Y. Chu, D.W. Hoffman, B.L. Iverson, A Pseudocatenane Structure Formed between DNA and A Cyclic Bisintercalator, *J. Am. Chem. Soc.* 131 (2009) 3499–3508.

10. Y. Chu, S. Sorey, D.W. Hoffman, B.L. Iverson, Structural Characterization of a Rigidified Threading Bisintercalator, *J. Am. Chem. Soc.* 129 (2007) 1304-1311

11. J. Lee, V. Guelev, S. Sorey, D.W. Hoffman, B.L. Iverson, NMR Structural Analysis of a Modular Threading Tetraintercalator Bound to DNA, *J. Am. Chem. Soc.* 126 (2004) 14036-14042

12. I. Czerwinska, S. Sato, B. Juskowiak, S. Takenaka, Interactions of cyclic and non-cyclic naphthalene diimide derivatives with different nucleic acids, *Bioorg. Med. Chem.* 22 (2014) 2593–2601.

13. Y. Esaki, M.M. Islam, S. Fujii, S. Sato, S. Takenaka, Design of tetraplex specific ligands: cyclic naphthalene diimide, *Chem. Commun.* 50 (2014) 5967-5969.

14. A. Milelli, V. Tumiatti, M. Micco, M. Rosini, G. Zuccari, L. Raffaghello, G. Bianchi, V. Pistoia, J.F. Diaz, B. Pera, C. Trigili, I. Barasoain, C. Musetti, M. Toniolo, C. Sissi, S. Alcaro, F. Moraca, M. Zini, C. Stefanelli, A. Minarini, Structure activity relationships of novel substituted naphthalene diimides as anticancer agents, *Eur. J. Med. Chem.* 57 (2012) 417-428.

15. S.M. Hampel, A. Sidibe, M. Gunaratnam, J.F. Riou, S. Neidle, Tetrasubstituted nahthalene diimide ligands with selectivity for telomeric G-quadruplexes and cancer cells, *Bioorg. Med. Chem. Lett.* 20 (2010) 6459–6463.
16. F.A. Tanious, S.F. Yen, W.D. Wilson, Kinetic and Equilibrium Analysis of a Threading Intercalation Mode: DNA Sequence and Ion Effects, *Biochemistry* 30 (1991) 1813–1819.
17. J.D. McGhee, P.H. von Hippel, Theoretical aspects of DNA-protein interactions: Co-operative and non-co-operative binding of large ligands to a one-dimensional homogeneous lattice, *J. Mol. Biol.* 86 (974) 469–489.
18. Y. Sato, S. Nishizawa, K. Yoshimoto, T. Seino, T. Ichihashi, K. Morita, N. Teramae, Influence of substituent modifications on the binding of 2-amino-1,8-naphthyridines to cytosine opposite an AP site in DNA duplexes: thermodynamic characterization, *Nucleic Acids Res.* 37 (2009) 1411–1422.
19. W.C. Tse, D.L. Boger, Sequence-Selective DNA Recognition: Natural Products and Nature's Lessons, *Chem. Biol.* 11 (2004) 1607–1617.
20. Z.R. Liu , K.H. Hecker, R.L. Rill, Selective DNA Binding of (N-alkylamine) Substituted Naphthalene Imides and Diimides to G+C-rich DNA, *J. Biomol. Struct. Dyn.* 14 (1996) 331-339.
21. R.E. McKnight, Insights into the Relative DNA Binding Affinity and Preferred Binding Mode of Homologous Compounds Using Isothermal Titration Calorimetry (ITC) in: A.A. Elkordy (Eds.), *Applications of Calorimetry in a Wide Context-Differential Scanning Calorimetry, Isothermal Titration Calorimetry and Microcalorimetry,* InTech publication, Rijeka, Croatia, 2013, pp. 129-152.

22. P.H. vonHippel, N.P. Johnson, A.H. Marcus, 50 years of DNA 'Breathing': Reflections on Old and New Approaches, *Biopolymers* 99 (2013) 923–954.

23. N. Huang; K.B. Nilesh; D.M. Alexander, Protein-facilitated base flipping in DNA by cytosine-5-methyltransferase, *PNAS* 100 (1) 68–73.

24. N.K. Banavali, Partial Base Flipping Is Sufficient for Strand Slippage near DNA Duplex Termini, *J. Am. Chem. Soc.* 135 (2013) 8274−8282.

25. K. Nakatani, S. Hagihara, Y. Goto, A. Kobori, M. Hagihara, G. Hayashi, M. Kyo, M. Nomura, M. Mishima, C. Kojima, Small-molecule ligand induces nucleotide flipping in $(CAG)_n$ trinucleotide repeats *Nat. Chem. Biol.* 1 (2005) 39-43.

26. J.B. Chaires, F. Leng, T. Przewloka, I. Fokt, Y.H. Ling, R.P. Soler, W. Priebe, Structure-Based Design of a New Bisintercalating Anthracycline Antibiotic, *J. Med. Chem.* 40 (1997) 261-266.

27. G.G. Hu, X. Shui, F. Leng, W. Priebe, J.B. Chaires, L.D. Williams, Structure of a DNA-Bisdaunomycin Complex, *Biochemistry* 36 (1997) 5940-5946.

28. N. Shahabadi, A. Fatahi, Multispectroscopic DNA-binding studies of a tris-chelate nickel(II) complex containing 4,7-diphenyl 1,10-phenanthroline ligands, *J. Mol. Struct.* 970 (2010) 90–95.

29. N. Shahabadi, A. Fatahi, Multispectroscopic DNA-binding studies of a tris-chelate nickel(II) complex containing 4,7-diphenyl 1,10-phenanthroline ligands, *J. Mol. Struct.* 970 (2010) 90–95.

30. I. Haq, Thermodynamics of drug–DNA interactions, *Arch. Biochem. Biophys.* 403 (2002) 1-15.

31. H. Becker, B. Norden, DNA Binding Properties of 2,7-Diazapyrene and Its *N*-Methylated Cations Studied by Linear and Circular Dichroism Spectroscopy and Calorimetry, *J. Am. Chem. Soc.* 119 (1997) 5798-5803.

32. R.S. Spolar, M.T. ReordJr, Coupling of Local Folding to Site-Specific Binding of Proteins to DNA, *Science* 263 (1994) 777-784.

33. F. Leng, J.B. Chaires, M.J. Waring, Energetics of echinomycin binding to DNA, *Nucleic Acids Res.* 31 (2003) 7202-6197.

34. I. Haq, J.E. Ladbury, B.Z. Chowdhry, T.C. Jenkins, and J.B. Chaires, Specific Binding of Hoechst 33258 to the d(CGCAAATTTGCG)$_2$ Duplex: Calorimetric and Spectroscopic Studies, *J. Mol. Biol.* 271 (1997) 244-257.

35. W.D. Wilson, F.A. Tanious, Kinetic analysis of drug-nucleic acid binding modes: absolute rates and effects of salt concentration in: Neidle, S. and Waring, M. (Eds), *Molecular Aspects of Anticancer Drug–DNA Interactions*. CRC Press, MacMillan, London, 1994 Vol. 2, pp. 243–269.

36. M.T. Record, C.F. Anderson, T.M. Lohman, Thermodynamic analysis of ion effects on binding and conformational equilibrium of proteins and nucleic-acids roles of ion association or release, screening and ion effects on water activity, *Q.Rev. Biophys.* 11 (1978) 103–178.

37. R.L. Jones, A.C. Lanier, R.A. Keel, W.D. Wilson, The effect of ionic strength on DNA-ligand unwinding angles for acridine and quinoline derivatives, *Nucleic Acids Res.*, 8 (1980) 1613–1624.

38. W.D. Wilson, C.R. Krishnamoorthy, Y.H. Wang, J.C. Smith, Mechanism of Intercalation: Ion Effects on the Equilibrium and Kinetic Constants for the Interaction

of Propidium and Ethidium with DNA, *Biopolymers* 24 (1985) 1941-1961.

39. F.A. Tanious, T.C. Jenkis, S. Neidle, W.D. Wilson, Substituent Position Dictates the Intercalative DNA-Binding Mode for Anthracene-9,l0-dione Antitumor Drugs, *Biochemistry* 31 (1992) 11632-11640.
40. P. Peixoto, C. Bailly, M.H. David-Cordonnier, Topoisomerase I-mediated DNA relaxation as a tool to study intercalation of small molecule into supercoiled DNA, *Methods Mol. Biol.* 613 (2010) 235-256.
41. M. Monnot, O. Mauffret, E. Lescot, S. Fermandjian, Probing intercalation and conformational effects of the anticancer drug 2-methyl-9-hydroxyellipticinium acetate in DNA fragments with circular dichroism, *Eur. J. Biochem.* 204 (1992) 1035-1039.

Chapter IV

A Selective G-Quadruplex DNA-Stabilizing Ligand Based on a Cyclic Naphthalene Diimide Derivative

Contents of this chapter have been published in the Molecules Journal (M.M. Islam, S. Fujii, S. Sato, T. Okauchi, S. Takenaka, Molecules, 20 (2015) 10963-10979). The materials of the chapter have been reproduced with the permission of the Molecules Journal [1].

4.1. Introduction

Guanine-rich DNA sequences which mainly originate in important regions of the oncogene promoters, telomere, mRNA, ribosomal DNA (rDNA), and thrombin-binding aptamer (TBA) can form G-quadruplex structures [2-4]. G-quadruplex DNAs, formed at the telomeric end, can inhibit telomere elongation by telomerase, which are activated in 80%–85% cancer cells, leading to inhibition of telomerase activity [2,5]. G-quadruplex DNAs is known to be formed at promoter regions of the human oncogene that can regulate gene expression at the transcriptional level [4]. DNA aptamers bind to thrombin and inhibit thrombin-catalyzed fibrin, resulting in blood clotting [3]. Thus, guanine-rich sequences have become a very promising target for the development of new anticancer drugs and therapeutic applications, which was attracted a lot of research interest during the last few decades and a few of the resulting compounds have entered into preclinical or clinical trials [4].

It has been reported that guanine-rich oligonucleotides could form G-quadruplexes via Hoogsteen hydrogen bonding among four guanine bases arranged in a square planar configuration [5]. G-quadruplex DNA shows diverse structural polymorphism; G-quadruplex DNA can be either parallel or antiparallel, even both conformations (termed hybrid) in some cases [6,7]. This G-quadruplex DNA can fold as a mixture of several different quadruplex forms depending on DNA sequence and extrinsic cation which offers a platform to induce and stabilize the quadruplexes by using small organic molecules [6,7]. This common structural feature poses challenges for the design of ligands with considerable selectivity toward one type of quadruplex over other G-quadruplex structures [7].

Small molecules that stabilize the G-rich single-strand DNA overhang into G-quadruplex can be considered as potential anticancer and therapeutic agents [4]. A number of G-quadruplex-binding small molecules have been reported in the last few decades [4,8,9]. Several diverse structural ligands, including telomestain, oxazole, cationic TMPyP4, anthraquinone, perylene, acridine, and ethidium derivatives have been investigated to evaluate their ability to interact with G-quadruplex DNA and observe their biological functions [4,8,9]. There are a number of macrocyclic structures that have been developed in the last few years as G-quadruplexes DNA binding ligands such as BQQ1, telomestain, oxazole, porphyrin, *etc.* [10], which is a well-established technique to improve the development of G-quadruplex DNA selective drugs. A common feature of these G-quadruplex-binding molecules is the presence of an extended aromatic ring system that allows binding through π-π overlap of terminal G-tetrads [6,10]. Large flat aromatic planar molecules stack on G-tetrads and show high binding selectivity [7]. Non-planar molecules that stack with G-quadruplexes are very rare and bindings are moderate [7]. Some of these G-quadruplex-binders include porphyrin derivatives, oxazoles, perylene derivatives and similar systems [11] that have fused π-ring systems within the molecule and showed various binding selectivity with the G-quadruplexes' DNA structure. Nowadays, the researchers are focusing on developing G-quadruplex DNA structure-specific and selective binding ligands [7,10] which are important for drug development, cancer research and therapeutic application studies.

Naphthalene diimides (NDIs) are very potent G-quadruplex-binding ligands with high cellular toxicity, which is able to effectively stabilize the terminal G-quartet of a G-quadruplex by stacking interactions [12,13]. Over the last few years a number of NDI-based compounds have been developed in part by exploiting the available NDI-G-quadruplexes structures [14-22]. In our previous studies, our group has already reported interaction studies of some cyclic NDI derivatives and h-telo 22 G-quadruplex DNA, which can inhibit telomerase activity at low concentration [11,23]. In our present work, I synthesized new compound **2** by cyclization with the linker chain of a tertiary amino group and amide group through benzene to compare the binding selectivity with our previously reported compound **1** [11] (Figure 4.1). Compound **2** is expected to show reduced binding to dsDNA and increased binding affinity for G-quadruplexes DNA because of its shorter linker substituents. I have also sought to compare the binding selectivity among the various structures of G-quadruplex DNA. I have characterized the binding selectivity and stability of **2** to G-quadruplexes' DNA present in the promoter region (c-myc and c-kit), thrombin binding aptamer (TBA) and human telomeric region (a-core and a-coreTT) by UV-Vis spectroscopy, circular dichroism (CD) spectroscopy, thermal melting studies, TRAP assay and FRET-melting assay [24] experiments.

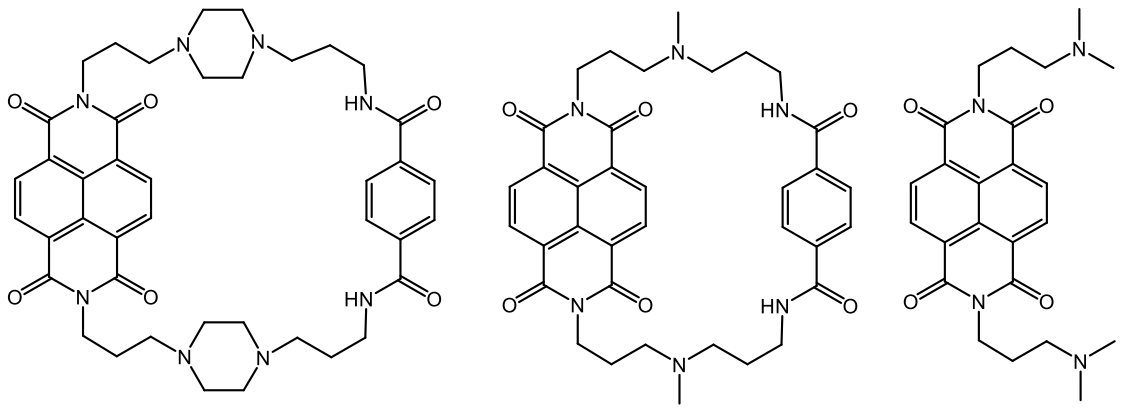

Fig. 4.1. Chemical structures of **1**, **2** and **3** (**1** taken from [11]).

4.2. Experimental Procedure

4.2.1. Materials

The seven G-rich oligonucleotides: a-core (5′-AGGG(TTAGGG)$_3$-3′), a-coreTT (5′-AGGG (TTAGGG)$_3$TT-3′), TBA (5′-GGTTGGTGTGGTTGG-3′), c-kit (5′-AGGGAGGGCGCTGGGAG GAGGAGGG-3′), c-myc (5′-TGAGGGTGGGGAGGGTGGGGAA-3′) and dsDNA composed of two complementary strands: (5′-GGGAGGTTTCGC-3′) and (5′-GCGAAACCTCCC-3′) were purchased from Genenet Co. (Fukuoka, Japan) and used without further purification. The following extinction coefficients were used for quantification of nucleic acid solutions (unit of ε was M^{-1} cm^{-1}): 114,000 for 5′-GGGAGGTTTCGC-3′; 108,600 for 5′-GCGAAACCTCCC-3′; 228,500 for a-core (5′-AGGG (TTAGGG)$_3$-3′); 245,100 for a-coreTT (5′-AGGG(TTAGGG)$_3$TT-3′); 143,300 for TBA (5′-GGTTG GTGTGGTTGG-3′); 260,100 for c-kit (5′-AGGGAGGGCGCTGGGAGGAGGAGGG-3′); 229,900 for c-myc (5′-TGAGGGTGGGGAGGGTGGGGAA-3′). Before use, oligonucleotide solutions in 50 mM Tris-HCl buffer (pH 7.4) containing 100 mM NaCl or KCl were heated to 95 °C and annealed by slowly cooling to room temperature. Guanine-rich telomere oligonucleotide sequence (5′-d-GGGTTAGGGTTAGGGTTAGGG3′), dual label with FAM (fluorescent donor) and TAMRA (fluorescent acceptor) at the 5′ and 3′ end, called ‘F21T’, respectively, were purchased from Sigma-Aldrich (St. Louis, MO, USA). The synthesis procedure of **2** was described in detail in a previous article [25]. Compound **3** was synthesized as described previously [26]. The 2.0 M KCl, and 5.0 M NaCl aqueous solutions were obtained from Life Technologies (Carlsbad, CA, USA). 1.0 M Tris-HCl (pH 7.4) buffer was obtained from Sigma-Aldrich. GoTaq Hot Start polymerase was purchased from Promega (Madison, WI, USA). TRAPese kit was obtained from EMD Millipore (Billerica, MA, USA).

4.2.2. UV-Vis Titration Experiments

Absorption spectra were measured on a U-3310 spectrophotometer (Hitachi, Tokyo, Japan) with a 1 cm path-length quartz cell and were recorded in the 200–600 nm

range at 25 °C. UV-Vis absorption titrations were carried out by the stepwise addition of 200 μM/strand of G-quadruplexes DNA or dsDNA solution to a UV-cell containing 5.0 μM solutions of **2** or **3**. The measurements were performed in a 50 mM Tris-HCl buffer (pH 7.4) containing 100 mM NaCl or KCl. Binding data obtained from spectrophotometric titration of increasing concentrations of drug to a fixed concentration of DNA was cast into the form of a Scatchard plot of ν/C against ν. The Scatchard plot was analyzed by the Scatchard equation: $\nu/C = K(n–\nu)$ [27], where ν is the stoichiometry (the number of ligand molecules bound per moles of base pair), C is the free ligand concentration, K is the observed binding constant, and n is the number of base pairs excluded by the binding of a single ligand molecule. For duplex oligonucleotides saturation of binding curves was not achieved, so K values were estimated using Benesi-Hildebrand method $1/\Delta Abs = 1/(l\Delta\varepsilon\,[ligand]) + 1/(nKl\Delta\varepsilon\,[ligand]) \times (1/DNA)$ [28] with the assumption that the ligand/oligonucleotide complex with 1:1 stoichiometry is formed (Table 4.1), where Δε is a molar absorptivity change of ligand and l is 1 cm. Scatchard plots were prepared using absorption changes at the specific wavelength 383 nm upon the addition of various concentrations of dsDNA. Scatchard plots were prepared using the data in a range of approximately 30%–80% bound region of **2** and dsDNA. The binding data were analyzed with KaleidaGraph software, using the Levenberg-Marquardt algorithm to determine parameters K_b and n.

4.2.3. Circular Dichroism (CD) Measurements

Various concentrations (5.0 to 50 μM) of **2** or **3** were added to 1.5 μM/base pair G-quadruplexes DNA in a 50 mM Tris-HCl buffer (pH 7.4) containing 100 mM NaCl or KCl at 25 °C, and CD spectra taken at a scan rate 50 nm/min on a J-820 spectropolarimeter (Jasco, Tokyo, Japan). Other conditions were: response 2 s, data interval 0.1 nm, sensitivity 100 mdeg, band width 2 nm, and scan number 4 times.

4.2.4. Thermal Melting Experiments

Melting curves of G-quadruplexes DNA or dsDNA were measured on a Hitachi 3300 spectrophotometer (heating rate of 0.5 °C/min to 90 °C) or Jasco J-820 spectrophotometer

(response, 100 mdeg; response, 8 s; data collecting interval, 0.5 °C; bandwidth, 2 nm) equipped with a temperature controller, respectively. The melting curves based on circular dichroism (CD) at 290 nm of a-core, a-core TT, and TBA, 262 nm of c-kit and c-myc or 260 nm of dsDNA were measured in 50 mM Tris-HCl (pH 7.4) containing 100 mM NaCl or KCl (for c-kit 20 mM KCl and for c-myc 5 mM KCl). A mixture of 1.5 μM a-core, a-core TT, TBA, c-kit, c-myc, dsDNA and 3.0 μM of **2** or **3** was placed in a cell of 1 cm in light path length (total 3 mL). Ligand-DNA ratio was set at 2:1.

4.2.5. TRAP Assay Experiments

Telomeric repeat amplification protocol (TRAP) assay was performed using published procedure [11,23]. TRAPeze Telomerase Detection Kit from EMD Millipore was used. Briefly, TS forward primer was elongated by telomerase in TRAP buffer (20 mM Tris-HCl pH 8.3, 1.5 mM $MgCl_2$, 63 mM KCl, 0.05% Tween 20, 1.0 mM EGTA) containing 0.05 mM dNTPs, 0.4 μM TS primer, 0.4 μM primer Mixed (RP primer, K1 primer, TSK1 primer) and 2.0 units of GoTaq Hot Start polymerase. The mixture was added to freshly prepared **2** solution from 0.1 to 4.0 μM (0, 0.1, 0.25, 0.5, 0.75, 1.0, 2.0, 3.0, 4.0 μM) and a positive control containing no ligand. Firstly, the elongation step was carried out for 60 min at 30 °C and it was followed by 5 min incubation at 95 °C. Secondly, 35 cycles of PCR were performed (94 °C, 30 s; 62 °C, 1 min; 72 °C, 1 min). Telomerase extension products were analyzed on a denaturing 12.5% polyacrylamide vertical gel prepared in 5 × TBE buffer (89 mM Tris base, 89 mM borate, and 1 mM EDTA, pH 8.0). The electrophoresis were run in 0.7 × TBE buffer for 2 h at 200 V. After electrophoresis gel was stained in 1 × GelStar Nucleic Acid Stain (Takara Bio, Shiga, Japan) in 1× TBE buffer for 30 min and photographed.

4.2.6. FRET-Melting Assay

Fluorescence-based melting competition assays was performed using a previously published procedure [24]. In more recent experiments, a real-time PCR apparatus (MX3000P, Stratagene, La Jolla, CA, USA; or Sigma-Aldrich SYBR Green or DNA

engine Opticon, MJ Research, Waltham, MA, USA) is used, allowing the simultaneous recording of 32–96 independent samples as first proposed by S. Neidle and co-workers [24]. The protocol used for our experiments is the following: a first step of equilibration at the lowest temperature (5 min at 25 °C) and a stepwise increase of 1 °C every minute for 72 cycles to reach 95 °C. The buffer 100 mM Tris-HCl (pH 7.4) containing 150 mM NaCl or KCl and 0.4 μM **2** was used for all experiments. The thermal denaturation profile of the oligonucleotide F21T (0.2 μM) and G-quadruplexes DNA (a-coreTT, TBA, c-kit and c-myc) (1.0 or 3.0 μM) were measured in the presence of **2** (0.4 μM). The ratio of F21T and G-quadruplexes DNA was used 1:5 or 1:15 at 0.4 μM **2**. Fluorescence-based melting assays competition measurements were performed with F21T dual label with FAM (fluorescent donor) and TAMRA (fluorescent acceptor) at the 5′ and 3′ end from Sigma-Aldrich at a heating rate of 1 °C/min. The recording is performed after 1 min stabilization. Typically three replicate experiments were performed, and average values are reported. Finally, the amount of ligand bound to the DNA was quantified by fluorescence after the digestion of the oligonucleotide (λ_{ex} and λ_{em} were set to 490 and 520 nm for oligonucleotides, respectively).

4.2.7. Computer Modeling

Molecular modeling of these complexes was constructed by MOE 2011.10 (http://www.chemcomp.com/). Compound **2** was placed on the binding site of mixed hybrid types G-quadruplex DNA (a-core) and energy minimization of these complexes was carried out. The molecular dynamics calculation of these mineralized complexes was further carried out until **2** was located in the binding site as stable condition. Finally, energy minimization of the complexes was obtained as shown in Fig. 4.11. These calculations were used the force field of MMFF94x.

4.3. Results and Discussion

4.3.1. UV-Vis Absorption Titration

To obtain the binding constant and the number of bound molecules for the interaction of **2** and **3** with different DNA forms such as human telomere (a-core and a-coreTT) [5,29,30], promoter region (c-kit and c-myc) [31-33] and thrombin-binding aptamer (TBA) [34,35] their absorption spectra were investigated (Fig. 4.3). Fig. 4.2A shows a representative spectrophotometric titration of **2** with human telomeric G-quadruplex DNA (a-core) in K^+ ion. It shows a maximum absorption at 384 nm. Addition of increasing amounts of G-quadruplex DNAs to **2** resulted in large hypochromicities (45%–60%) and a noticeable small red shift (3–8 nm) was observed. These spectral features are suggestive of end-staking binding rather than groove binding (Fig. 4.2). I observed isosbestic points at 392 nm and 395 nm of **2** for G-quadruplex DNAs and duplex DNA, respectively. The presence of isosbestic points indicated the equilibrium between the bound and free ligand. For comparison, I also investigated the interaction of **2** with dsDNA. Upon the addition of increasing amounts of dsDNA to **2**, smaller hypocromic shifts (25%–30%) and red shifts (2–4 nm) were observed than for G-quadruplexes DNA, suggesting this compound is not a good dsDNA binder (Fig. 4.2B). The Scatchard plot representing the binding between **2** and a-core (KCl) is presented in Fig. 4.2C. The Scatchard plot was analyzed by the McGhee-von Hippel Scatchard equation [27]. The solid line in Fig. 4.2C represents the best fit of the experimental value to the McGhee-von Hippel equation. For dsDNA saturation of binding curves was not achieved; therefore, estimation of *K* values using the Scatchard equation was impossible. However, *nK* values were estimated using the Benesi-Hildebrand method [28]. Ligand binding affinity to dsDNA does not depend on the nature of the metal cation, such as sodium and potassium ions. In the presence of sodium and potassium ions compound **3** binds to dsDNA approximately 20 times stronger than **2**.

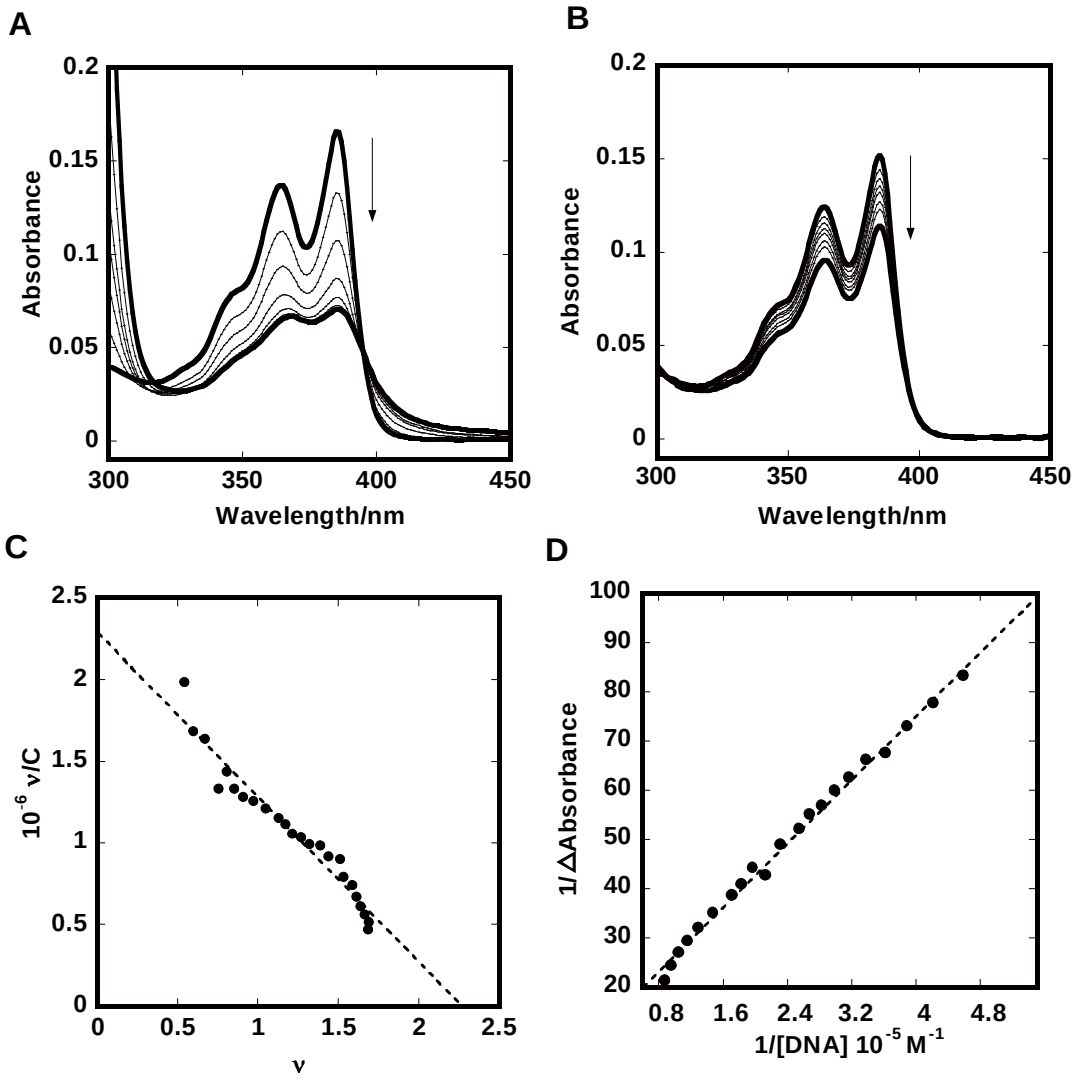

Fig. 4.2. Spectral shifts of 5 μM **2** on titration with 0, 1.4, 2.9, 4.4, 5.8, 8.7 and 14 μM a-core (**A**) or 0, 2.0, 5.0, 10, 20, 30, and 40 μM dsDNA (**B**) in 50 mM Tris-HCl (pH7.4) and 100 mM KCl. Scatchard plots for binding of **2** to a-core (**C**) and Benesi-Hildebrand plot for binding of **2** to dsDNA (**D**).

The intrinsic binding constants (*K*) of **2** and **3** to G-quadruplexes DNA and dsDNA are summarized in Table 4.1. Our group has already reported that **1** carrying a benzene moiety as longer linker chain showed higher binding affinity to either G-quadruplexes DNA or dsDNA than **3** [11]. In our present study, our group also found similar binding constant trends for G-quadruplexes DNA in the range of 10^6–10^7 M^{-1} with n = **2**, which shows almost five times higher binding affinity of **2** compared with the non-cyclic derivative **3**. Comparing with **1** [11], **2** showed almost three times higher

binding affinity to a-core and 70 times weaker binding to dsDNA. Compound **2** showed approximately 200 higher selectivity to G-quadruplexes DNA than the previously reported **1** [11]. The comparison suggests that the shorter cyclic linker chain **2** showed higher specific binding to G-quadruplex DNAs than the previously reported longer linker chain compound **1** [11].

Table 4.1 Binding parameters and melting temperatures of **2** and **3** with a-core, a-core TT, c-kit, c-myc, TBA and dsDNA.

DNAs	**2**		**3**		**Tm/°C**	**ΔTm/°C**	
	10^{-6} K/M^{-1}	n	10^{-6} K/M^{-1}	n	DNAs	**2**	**3**
a-core (K^+)	10 ± 0.5 [a]	1.5	1.6 ± 0.2 [a]	1.4	69 [c]	15	5
a-core (Na^+)	1.0 ± 0.04 [a]	2.2	0.73 ± 0.09 [a]	1.0	57 [c]	-	1
a-core TT (K^+)	6.1 ± 0.4 [a]	1.8	1.9 ± 0.3 [a]	1.3	63.5 [c]	18	-
TBA (K^+)	3.5 ± 0.2 [a]	1.4	0.49 ± 0.04 [a]	1.1	50.5 [c]	11	-
c-kit (K^+)	1.9 ± 0.18 [a]	1.4	0.74 ± 0.05 [a]	1.7	54 [d]	11	-
c-myc (K^+)	4.0 ± 0.3 [a]	1.7	1.5 ± 0.2 [a]	1.6	70 [e]	15	-
dsDNA (K^+)	0.037 [b]	-	0.60 ± 0.04 [a]	2.8	49 [c]	0.3	12
dsDNA (Na^+)	0.037 [b]	-	0.60 ± 0.08 [a]	3.0	49 [c]	0.3	12

Condition: Binding constant (*K*): 50 mM Tris-HCl (pH 7.4) and 100 mM NaCl or KCl; [a]: Scatchard analysis (*K*); [b]: Bensi-Hildebrand analysis (*nK*); Thermal melting: [ligand]:[DNA] = 2:1, 50 mM Tris-HCl (pH 7.4); [c]: 100 mM NaCl or KCl; [d]: 20 mM KCl; [e]: 5.0 mM KCl.

In comparison with our previous report [11], the linker chain of **2** and **1** may play an important role in the binding with G-quadruplexes DNA over dsDNA. The amide chains of **2** and **1** might be more effective in reducing binding with dsDNA because of the NDI moiety site blocks the aliphatic chain from intercalating in the benzene part. Moreover, the benzene part itself also prevents binding of **2** and **1** from threading intercalations with dsDNA. However, as our group has reported earlier [25], **2** and **1** showed affinity to calf thymus DNA (CT-DNA), Poly[d(A-T)]$_2$ and Poly[d(G-C)]$_2$ due to hydrophobic interactions between cyclic NDI derivatives and dsDNA. Compound **2** showed lower binding affinity to CT-DNA, poly[d(A-T)]$_2$ and poly[d(G-C)]$_2$ than **1**

perhaps because of steric reasons, whereas, according to the computer modeling, the NDI moiety site of cyclic NDI derivatives incorporated to end staking onto the G-quartet. I have observed that **2** showed higher selectivity to G-quartet than **1** because the tertiary amino chain in the linker chain of **2** may have more compatibility to bind specifically with the G-quartet plane than the piperazine linker chain of **1**.

In the presence of sodium ions the binding affinities of both ligands to basket-type tetraplex structures were much lower than G-quadruplexes in potassium solution. Our group already explained that this might be due to the fact that basket type a-core crosses its oligonucleotide chain over the G-quartet diagonally and disrupts access of **2** to the G-quartet plane [11].

In our present study, all the G-quadruplexe DNA showed higher binding constants (K) with **2** than dsDNA. In potassium ion solution, **2** exhibited the highest binding affinity for mixed hybrid type a-core [29] with $K = 1 \times 10^7\ M^{-1}$, whereas diminished the binding affinity to dsDNA with $nK = 3.7 \times 10^4\ M^{-1}$. The binding data indicated that **2** has a 270-fold preference for a-core over dsDNA. Table 4.1 shows the binding constants (K) are $K = 6.1 \times 10^6\ M^{-1}$ for a-coreTT (hybrid type-2) [30], $K = 1.9 \times 10^6\ M^{-1}$ for c-kit (parallel propeller type) [32], $K = 4.0 \times 10^6\ M^{-1}$ for c-myc (parallel type) [32], $K = 3.5 \times 10^6\ M^{-1}$ for TBA (antiparallel chair type) [35] with **2**, which represent a 165-, 51-, 108- and 95-fold binding preference over dsDNA ($K = 3.7 \times 10^4\ M^{-1}$), respectively. The ratio of ligand per dsDNA used for binding was $n = 3$, a reasonable result considering that a typical intercalator covers two base pairs upon binding to dsDNA, in addition to the expected relative difficulty in binding at terminal sites. The binding number of a ligand with G-quadruplexes DNA was estimated to be $n = 2$, which may agree with an end-stacking binding of **2** to the external G-quartet planes of quadruplexes.

According to the above result, new compound **2** showed G-quadruplexes DNA structure-specific binding. Compound **2** showed the highest affinity to a-core DNA, which exhibits mixed type hybrid (hybrid-1 and hybrid-2) structures in K^+ [25] and possessed more than two drugs staking plane and binding loops. Computer modeling showed that **2** was stacked and bound to a mixed hybrid structure at various G-quadruplex

staking planes, whereas a-coreTT exhibited hybrid-2 [30] type structures which have two G-tetrads staking planes and two binding sites. For this reason I observed that **2** showed the highest affinity with a-core. TBA exhibited an antiparallel chair type [34,35] structure which has G-quartet staking planes and binding loops, while c-kit and c-myc exhibited parallel type [32] propeller structures which possess two G-quartet staking planes, but binding loops are unusual for **2**. According to the binding data, new compound **2** was revealed to be a most preferable and specific binder to telomeric G-quadruplexes DNA than promoter regions' G-quadruplex DNA as well as thrombin binding aptamer. The binding study results are consistent with thermal melting studies where a-core showed the highest stabilization with **2**. The binding site size (*n* values) obtained from binding studies of G-quadruplexes and **2** are consistent with the Job plot analysis from CD studies (Fig. 4.5).

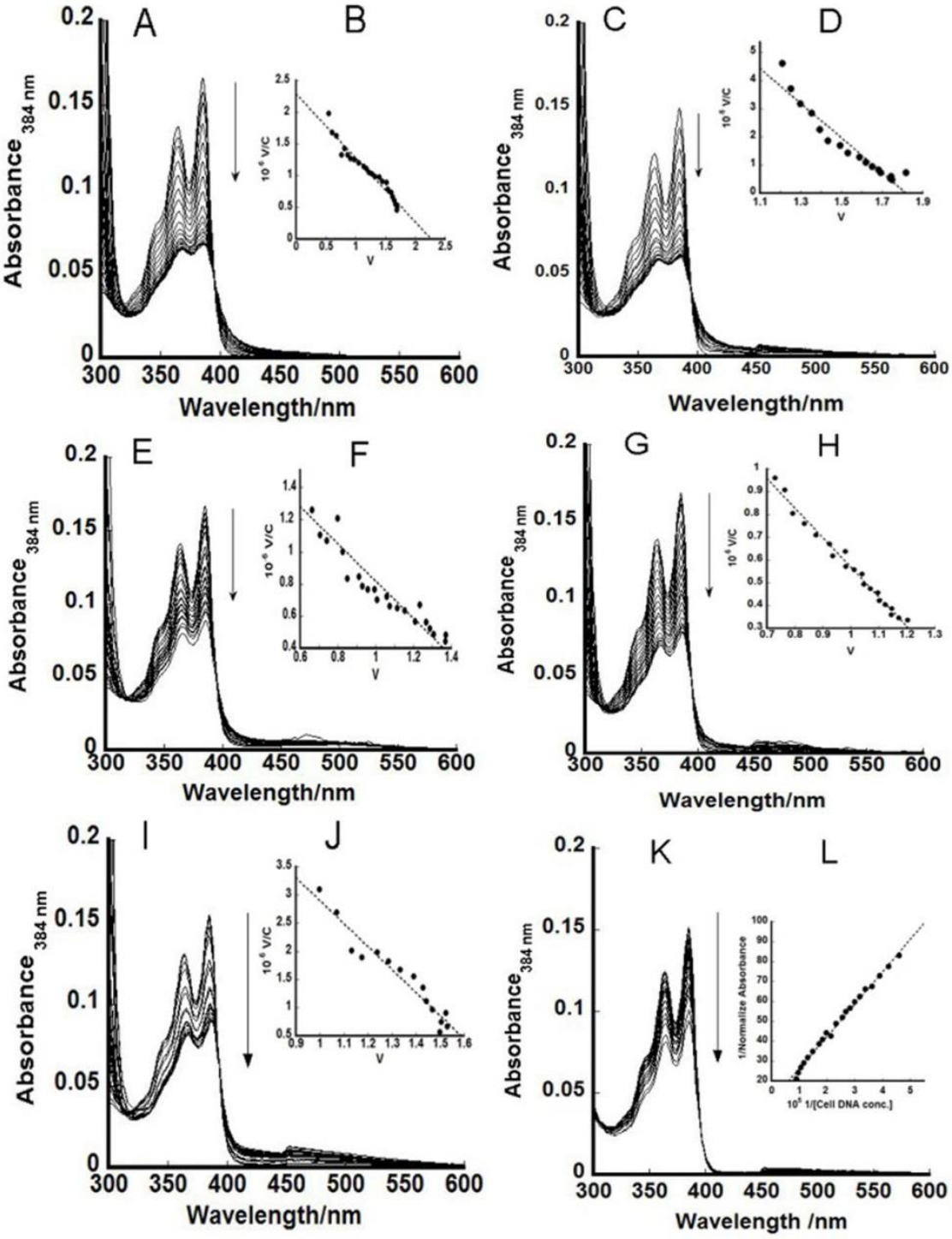

Fig. 4.3. UV-Vis absorption spectra of 5.0 μM **2** in the absence and presence of a-core (**A**), a-coreTT (**C**), TBA (**E**), c-kit (**G**), c-myc (**I**) and dsDNA (**K**) with 0.5, 1.0, 1.5, 2.0, 2.5, 3.0, 4.0, 5.0, 10 and 20 μM respectively. Binding affinities were estimated using the scatchard plot of **2** with a-core (**B**), a-coreTT (**D**), TBA (**F**), c-kit

(**H**), c-myc (**J**) and Benesi-Hildebrand plot of **2** with dsDNA (**L**). Experiments were performed at 25°C in 50 mM Tris-HCl (pH 7.4), 100 mM KCl.

4.3.2. Circular Dichroism (CD) Studies

The CD is a powerful method to differentiate the parallel, anti-parallel, and mixed-type secondary structure of G-quadruplex DNA. Compound **2** was interacted to investigate the effect of the binding mode on the conformation of the G-quadruplexes, which is shown in Fig. 4.4. The CD spectrum of human telomere (a-core) G-quadruplex DNA showed a negative peak at 240 nm, a shoulder peak at 265 nm and a positive peak at 290 nm (Fig. 4.4A) in buffer containing 100 mM KCl, supportive of a mixed hybrid type (hybrid-1 and hybrid-2) G-quadruplex structure [36,37]. The small positive peak at 265 nm was transformed increasingly into a negative peak at 260 nm together with an increase of the positive peak at 290 nm upon the addition of **2**, suggesting the induction of a hybrid type structure. After addition of **2**, a-core structure, conformation changed a little from a mixed hybrid type to hybrid-1 type [38]. In our previous study, our group reported that in the presence of Na^+ ions, telomeric DNA exists in an antiparallel basket-type conformation. Upon addition of **2**, this antiparallel basket-type structure was also retained [11].

The CD spectrum of human telomere (a-coreTT) G-quadruplex in buffer containing 100 mM KCl exhibits a negative peak at 240 nm, a shoulder peak at 265 nm and a positive peak at 290 nm (Fig. 4.4B) supportive of a hybrid-2 type G-quadruplex structure [36,37]. The small positive peak at 265 nm is transformed increasingly into a negative peak at 260 nm together with an increase of the positive peak at 290 nm upon the addition of **2**, suggesting the induction of a hybrid type structure. After the addition of **2**, a-core structure conformation changed a little from hybrid-2 type to hybrid-1 type [38].

In the presence of 100 mM KCl thrombin-binding aptamer (TBA, Fig. 4.4C) exhibited a positive peak at 290 nm, and a negative band at 250 nm, supportive of an anti-parallel chair type G-quadruplex structure [35,39]. Upon the addition of **2**, the negative

peak transformed increasingly into at 260 nm together with an increase of the positive peak at 290 nm, suggesting that the binding of **2** apparently does not disturb the structure of TBA, which is consistent with previous reports [39].

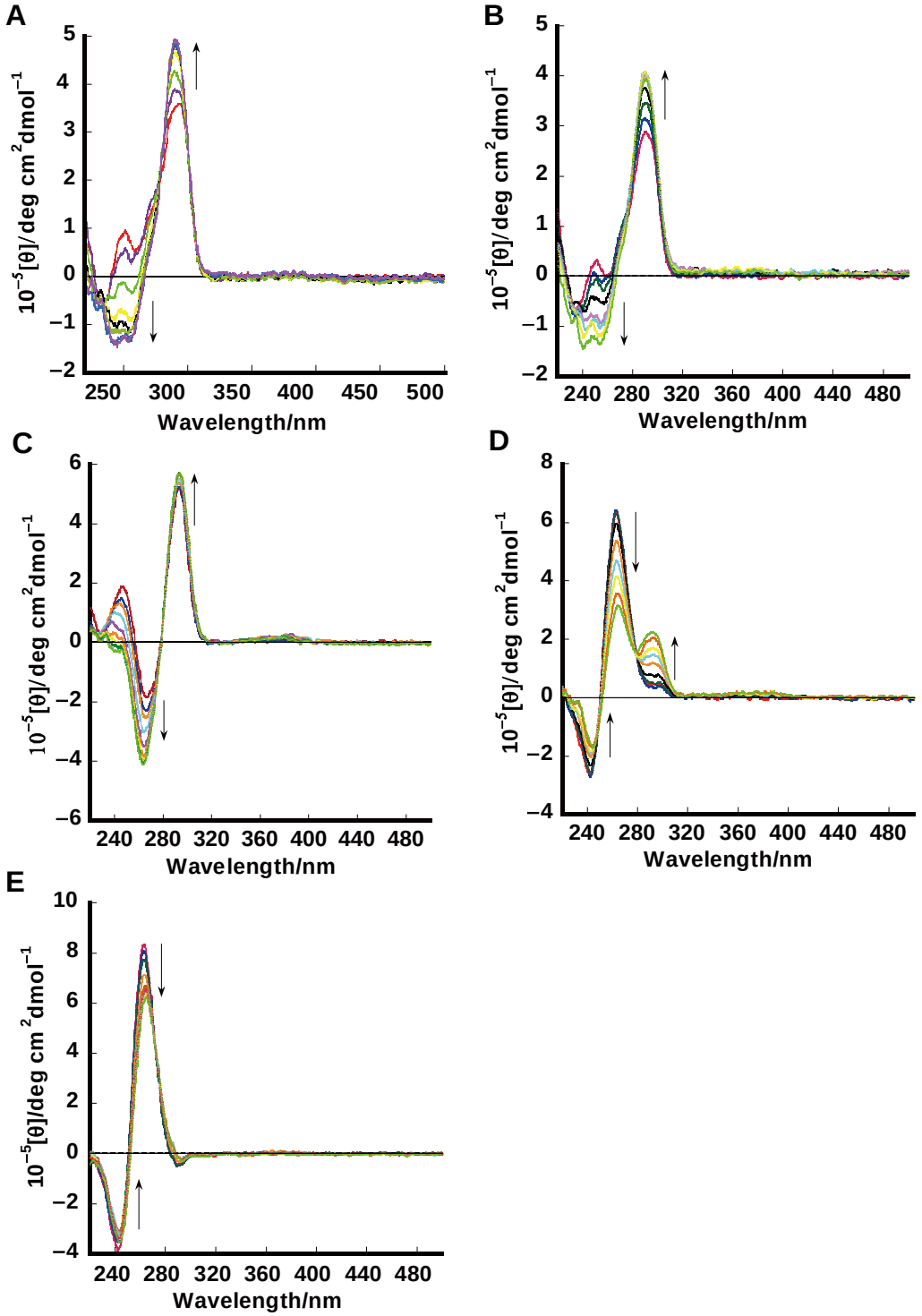

Fig. 4.4. CD spectra of 1.5 μM of a-core (**A**); a-coreTT (**B**); TBA (**C**); c-kit (**D**); c-myc (**E**) in 50 mM Tris-HCl (pH 7.4), 100 mM KCl in addition of **2** (0, 0.38, 0.75, 0.80, 2.25,

and 3.00 μM) at 25 °C.

Both c-myc and c-kit G-quadruplex (Fig. 4.4D,E) exist in the presence of K^+ ions as a parallel structure, which has a characteristic positive peak centered around 262 nm, a negative peak at 241 nm and a small shoulder peak at 290 nm [40,41]. After the addition of **2** to c-myc and c-kit G-quadruplex, a decrease of the CD peaks at 241 nm and 262 nm was observed, with no other significant change in the spectrum and the parallel structure was not changed, which suggests ligand-dependent disruption of staking of G-quadruplex DNA. Upon the addition of **2**, the c-kit structure shoulder peak at 290 nm increased little. This effect has also been observed previously by many research groups [42].

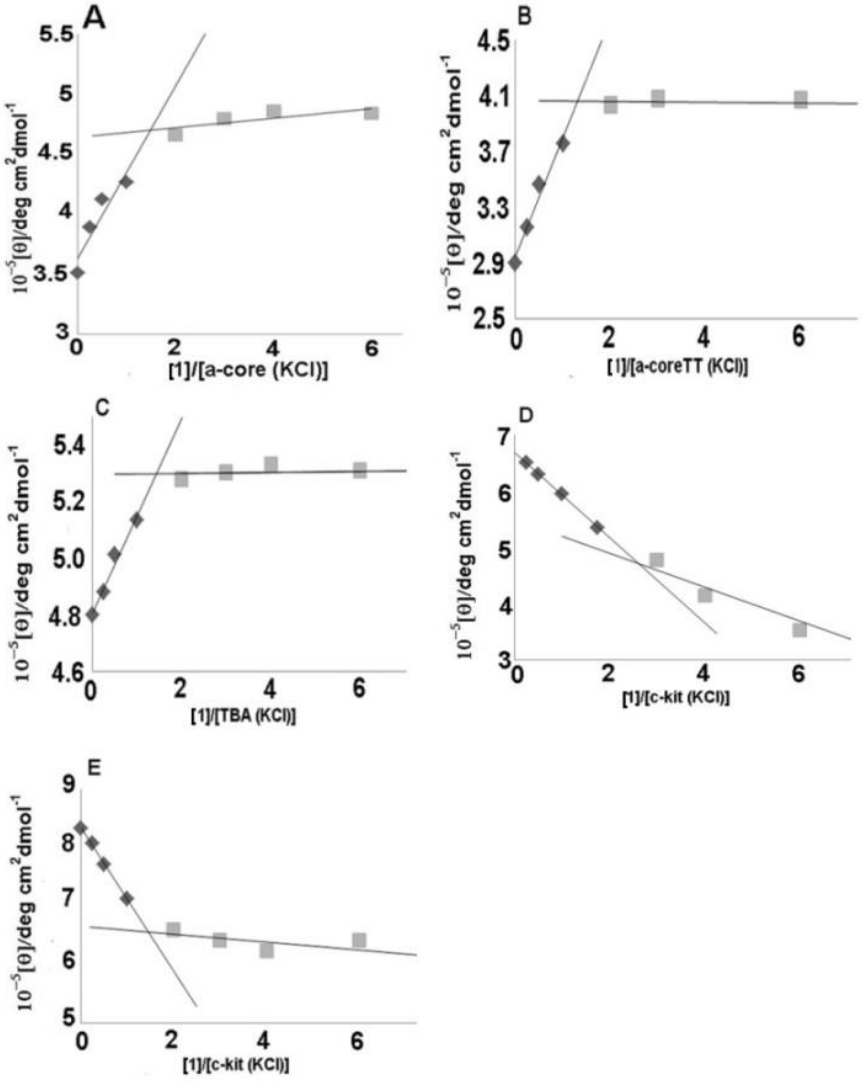

Fig. 4.5. Analysis (by Job plot) of CD spectra of **2** with a-core (A), a-coreTT (B), TBA

(C), c-kit (D), c-myc (E). Molar ellipticity values at 290 nm (a-core, a-coreTT, and TBA) and 263 nm (c-kit and c-myc) were plotted against increased ligand-DNA molar ratio. Experiments were performed at 25 °C in 50 mM Tris-HCl buffer pH 7.4 containing 100 mM KCl. The intersection of data indicated the binding stoichiometry of **2** and G-quadruplexes DNA [43]. I have observed binding stoichiometry n = 1.7 for a-core (A), n = 1.5 for a-coreTT (B), n = 1.8 for TBA (C), n = 2.5 for c-kit (D), n = 1.7 for c-myc (E). These results are consistent with the stoichiometry from UV-Vis binding studies.

The Job plot analysis by CD studies (Fig. 4.5) showed that CD studies of G-quadruplexes and **2** are consistent with binding studies where similar binding site sizes (*n* values) are obtained.

4.3.3. Thermal melting Studies

Thermal stabilization of various G-quadruplexes DNA and dsDNA in the presence of **2** was studied using the CD melting and UV-Vis melting experiment (Fig. 4.6). Thermal melting of hybrid type telomeric quadruplex DNA (a-core and a-coreTT) was monitored at 290 nm in the presence of K^+ [30].

The T_m value was observed around 69 °C for a-core without **2** (Fig. 4.6A). I observed that the interaction of **2** with telomeric DNA quadruplex enhanced the stability by 15 °C for a-core and 18 °C for a-core TT, which was approximately 3 °C higher for a-core TT than a-core G-quadruplexes DNA (Table 4.1). Researchers already reported that thermal melting increased after addition of base to oligonucleotides [43]. In our previous report [11], I observed from the absorption spectra that **1** had the lowest binding affinity to a-core of the sodium ion solution. Furthermore, dsDNA was monitored by UV-Vis melting studies. After the addition of a 2-fold concentration of **2**, only a slight increase (up to 0.3 °C) in thermal stability was observed (Table 4.1 and Fig. 4.7). These results underscore the fact that **2** selectively stabilizes telomeric quadruplex DNA as well as promoter and thrombin binding aptamer G-quadruplex DNA over dsDNA. In comparison with our previous report [11], compound **2** showed high stabilizing effect to a-core and very weak stabilizing effect to ds DNA.

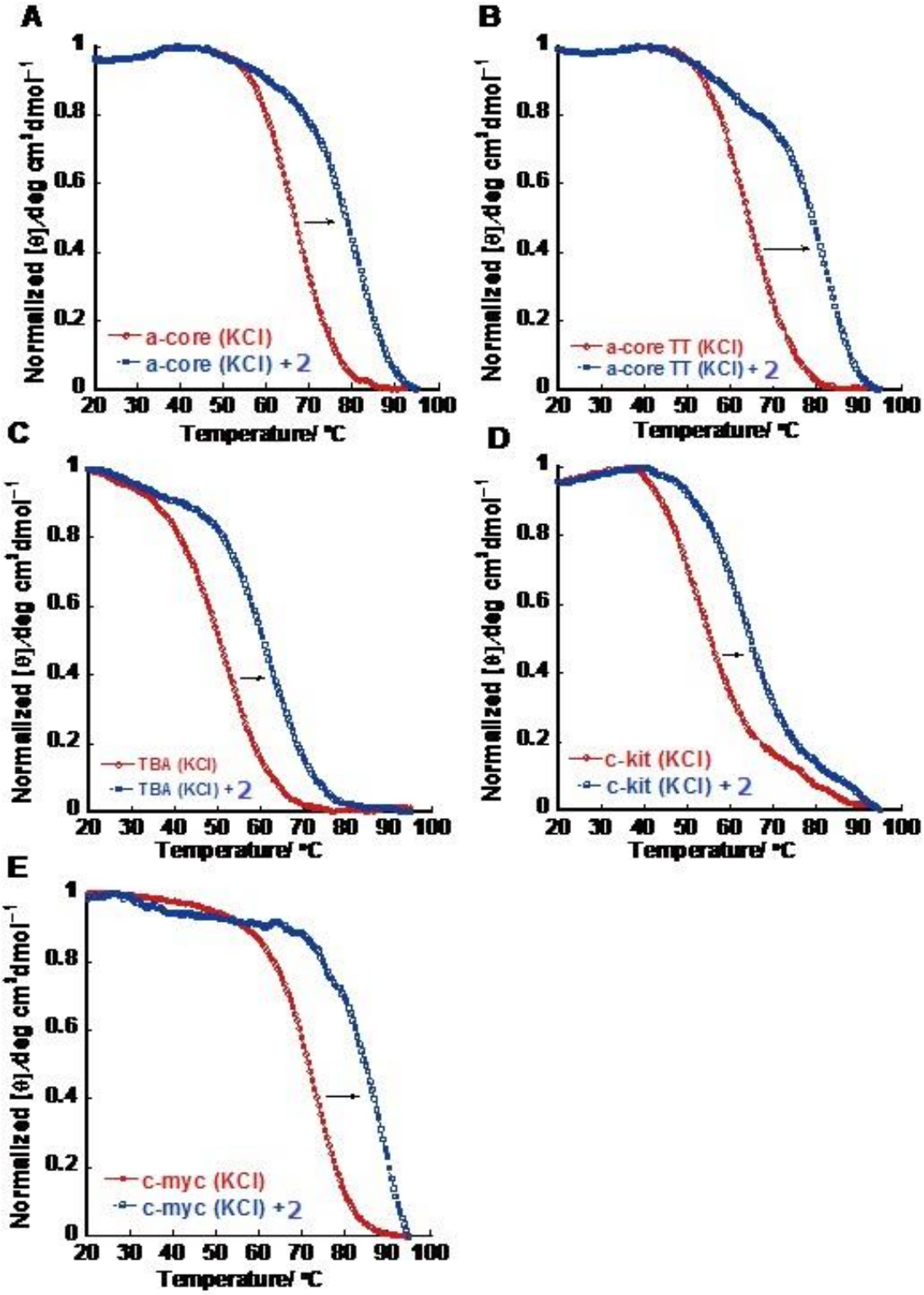

Fig. 4.6. Melting profiles for a-core (**A**); a-core TT (**B**); TBA (**C**); c-kit (**D**); c-myc (**E**) in the absence or presence of **2** in 50 mM Tris-HCl (pH 7.4); 100 mM KCl (**A**–**C**); 20 mM KCl (**D**); 5.0 mM KCl (**E**) and [ligand]:[DNA] = 2:1.

The melting temperatures of antiparallel chair type thrombin binding aptamer quadruplex DNAs (TBA) were monitored at 290 nm. Compound **2** increased the T_m of TBA by 11 °C (Table 4.1). These results are consistent with previously published articles [35,39]. The melting temperatures of parallel promoter quadruplex DNAs such as c-kit and c-mice were monitored at 263 NM [41,42]. In the case of the highly stable parallel c-kit and c-myc quadruplex DNA was highly stable at high salt concentration and a stable baseline curve was not achieved even above 90 °C, so it is not possible to measure an accurate T_m in this case, so I measured T_m for c-kit and c-myc at low salt concentration. Compound **2** increased the T_m of c-kit by >11 °C at 20 mM K^+ ion and the T_m of c-myc by >15 °C at 5 mM K^+ ion solution (Table 4.1). This type of performance of c-kit and c-myc is consistent with previously published articles [41,42]. According to the above result, I can conclude that **2** preferably stabilizes telomeric quadruplex DNA than promoter and thrombin binding aptamer G-quadruplex DNA. CD melting results are consistent with binding and competition assay studies, where **2** showed preferable binding to human telomeric G-quadruplex.

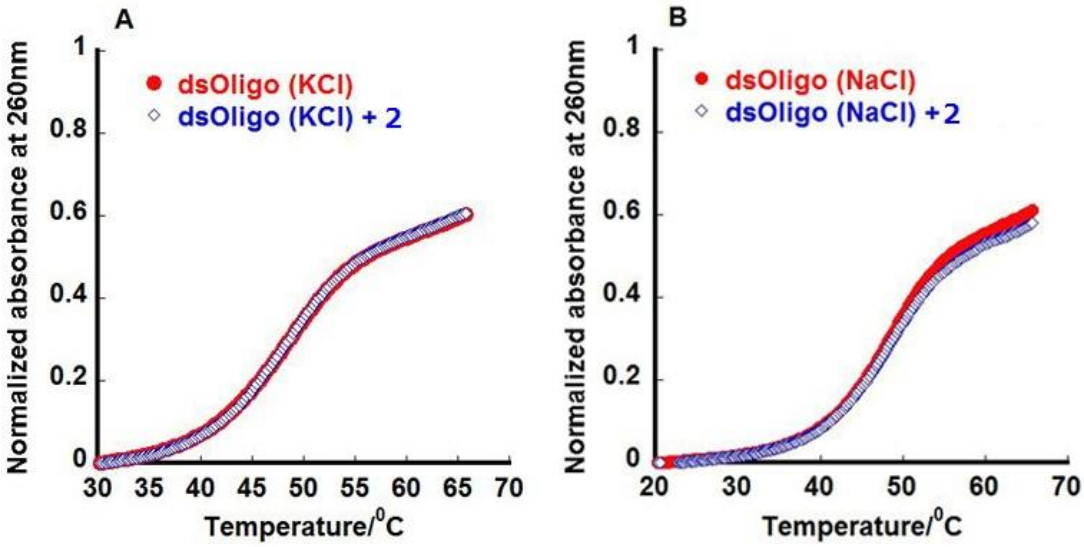

Fig. 4.7. UV-Vis melting profiles for dsDNA (KCl) (**A**) and dsDNA (NaCl) (**B**) in the absence or presence of **2** in 50 mM Tris-HCl (pH 7.4) and 100 mM KCl or 100 mM NaCl, [ligand]:[DNA] = 2:1.

4.3.4. TRAP Assay

Once the G-quadruplexes DNA stabilization was established for **2**, it was important to test whether the molecule inhibits telomerase activity. To evaluate the abilities of these compounds to inhibit telomerase, the telomeric repeat amplification protocol (TRAP assay) [11,23] was carried out using various amounts of **2** (Fig. 4.8). The assay clearly shows that **2** is a potent inhibitor of telomerase with activity in the submicromolar range (IC_{50}) 0.9 μM. This result suggests that the TS-primer extends the length to form a tetraplex structure and **2** binds to it and stabilizes its structure to inhibit the telomerase reaction. The values obtained from the TRAP assay are comparable to those of previously reported derivatives [11,23]. A number of small ligands have been discovered to inhibit the function of telomerase by stabilizing G-quadruplexes DNA structures [8]. The excellent IC_{50} for telomerase inhibition by **2** (0.9 μM) comes from its binding constant ($K > 10^7\ M^{-1}$). It is suggested that this macrocyclic compound **2** may deserve biological assays with cancer cell lines to represent a suitable candidate drug target to DNA quadruplexes.

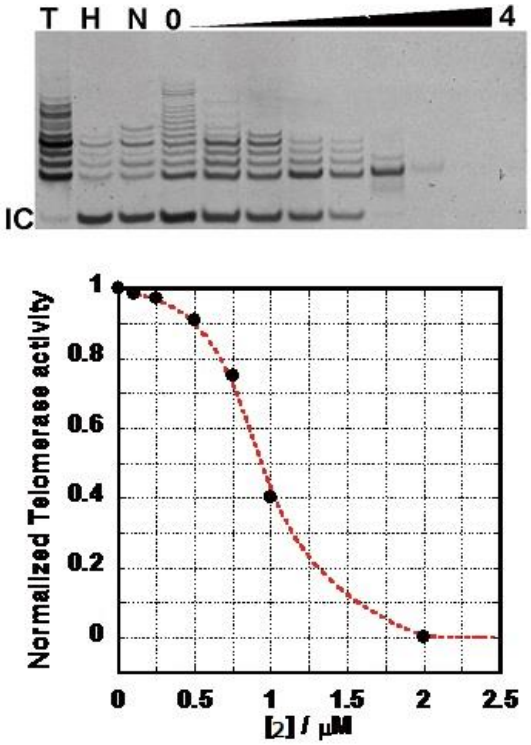

Fig. 4.8. Telomerase inhibition by **2**. The gel shows the effect of increasing concentrations of **2** (0, 0.1, 0.25, 0.5, 0.75, 1.0, 2.0, 3.0, 4.0 μM) on telomerase activity. Concentrations

of 2.0–4.0 μM **2** lead to the disappearance of all PCR products. IC_{50}s were determined as follows: ligand concentration under half telomerase activity with no ligand.

4.3.5. FRET-Melting Assay

The sequence and structural selectivity of different DNA binding agents has been previously explored by use of a thermodynamically rigorous competition assay procedure introduced by Ren and Chaires [24,45]. In this method, different nucleic acid structures are assayed against a common ligand solution. This is a simple method to evaluate specificity toward quadruplexes [46]. It has been already reported that F21T showed a Tm value around 50 °C [24] that increased by 11 °C after incorporation of **2** with F21T. Comparison with other G-quadruplexes DNA is shown in Fig. 4.9 and Fig. 4.10. Compound **2** displays a strong preference for binding to F21T quadruplex structure which corresponds to the human telomeric G-rich motif than other quadruplexes DNA structures.

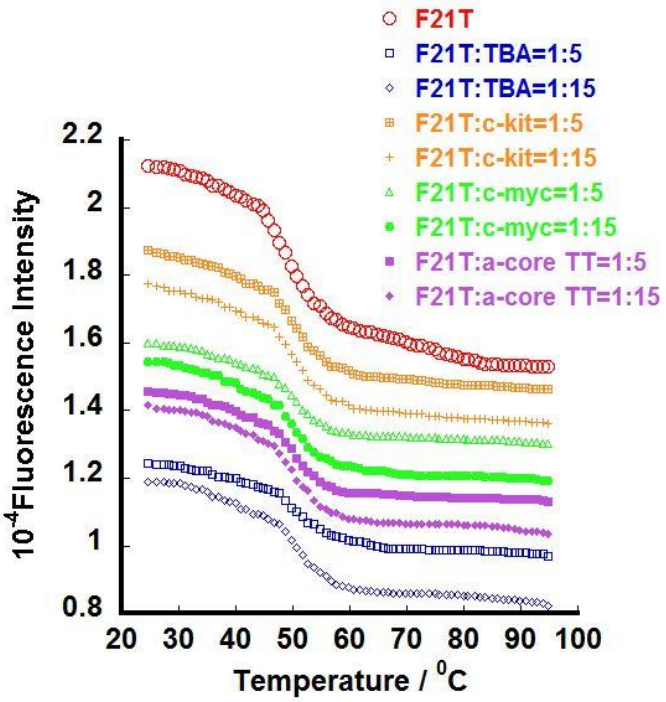

Fig. 4.9. FRET-melting assay of human telomeric DNA (a-coreTT), promoter region's G-quadruplex (c-kit & c-myc) and thrombin-binding aptamer (TBA) with

F21T (0.2 μM) in the presence of **2** (0.4 μM). Experiments were performed in 100 mM Tris-HCl buffer (pH 7.4) containing 150 mM KCl.

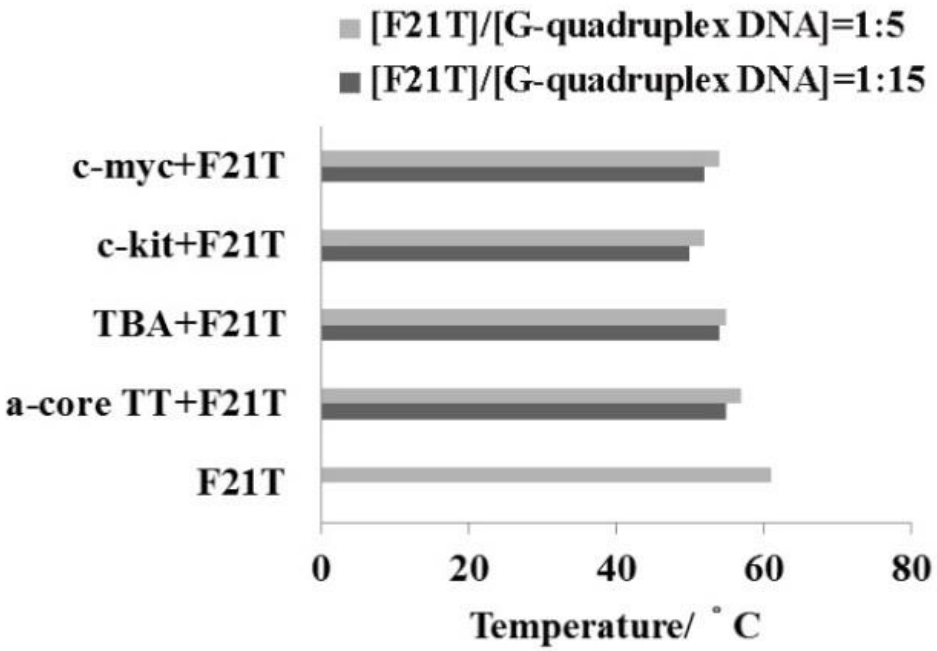

Fig. 4.1. FRET-melting assay of human telomeric DNA (a-coreTT) (1.0 or 3.0 μM), promoter region's DNA (c-kit & c-myc) (1.0 or 3.0 μM) and thrombin-binding aptamer (TBA) (1.0 or 3.0 μM) with F21T (0.2 μM) in the presence of **2** (0.4 μM). Experiments were performed at 25 °C in 100 mM Tris-HCl buffer pH 7.4 containing 150 mM KCl.

4.3.6. Computer Modeling

The computer-modeling structures consisting of **2** with mixed hybrid types G-quadruplex DNA (a-core) are shown in Fig. 4.11. In this article, I proposed a model involving an end stacking binding mode between **2** and mixed hybrid types G-quadruplex DNA (a-core), which are consistent with our previously published article [23]. The computer modeling showed that **2** stacked and bound to different G-quartet plane of mixed hybrid types G-quadruplex DNA (a-core).

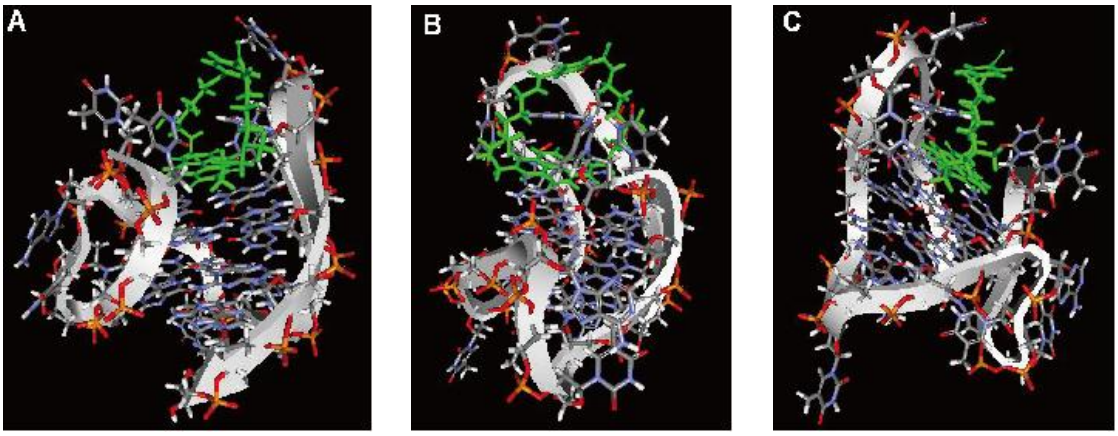

Fig. 4.11. Computer modeling of **2** interactions with mixed hybrid G-quadruplex DNA structure (**A**–**C**).

4.4. Conclusions

I have synthesized a new type of ligand **2**, carrying a benzene moiety as linker chain and studied its interaction with different types of G-quadruplexes DNA. I have compared this study with our group's previously reported **1** [11] which has a long linker chain than **2**. Compound **2** exhibited high binding affinity in the range of 10^6–10^7 M^{-1} to G-quadruplexes DNA and reduced binding affinity to dsDNA. The binding data (Table 4.1) indicated that **2** has 270-fold preferential binding for a-core, 165-fold for a-coreTT, 51-fold for c-kit, 108-fold for c-myc, 95-fold for TBA over dsDNA. The binding stoichiometry of **2** for G-quadruplex is 2:1, suggesting a staking binding mode. Compound **2** revealed 200-fold higher binding selectivity compared with our previously reported **1** [11]. I have observed that **2** revealed preferable binding to mixed hybrid types structure of telomeric G-quadruplex DNA (a-core) over parallel types of promoter region's G-quadruplex DNA (c-kit and c-myc) and antiparallel chair types of thrombin binding aptamer (TBA). The CD spectra showed that **2** stabilized G-quadruplexes DNA structure. Upon the addition of **2** to a-core the CD spectra showed little change indicating a mixed hybrid structure and little changed to the hybrid-1 type G-quadruplex structure [38]. Thermal melting measurements indicated that **2** highly stabilized the G-quadruplexes DNA structure. Compared with our previous report [11], **2** increased ΔT_m by 5–8 °C. I have

performed competitive assays in order to determine the binding selectivity among the G-quadruplexes DNA, and **2** showed highly preferable stabilization of human telomeric G-quadruplex sequence (F21T). This novel compound **2** can also inhibit the telomerase activity at low submicromolar concentrations. These results indicated that **2** is an important class of G-quadruplex stabilizing ligand compared with dsDNA.

4.5. References

1. M.M. Islam, S. Fujii, S. Sato, T. Okauchi, S. Takenaka, A Selective G-Quadruplex DNA-Stabilizing Ligand Based on a Cyclic Naphthalene Diimide Derivative, *Molecules*, 20 (2015) 10963-10979.
2. S. Neidle, *Therapeutic Applications of Quadruplex Nucleic Acid*, 1st ed.; Academic Press: London, UK, 2012; pp. 1–15.
3. A. Avino, C. Fabrega, M. Tintore, R. Eritja, Thrombin binding aptamer, more than a simple aptamer: Chemically modified derivatives and biomedical applications. *Curr. Pharm. Des.* 18 (2012) 2036–2047.
4. T. Ou, Y. Lu, J. Tan, Z. Huang, K. Wong, L. Gu, G-Quadruplexes: Targets in Anticancer Drug Design, *Chem. Med. Chem.* 3 (2008) 690–713.
5. J. Dai, M. Carver, D. Yang, Polymorphism of human telomeric quadruplex structures, *Biochimie* 90 (2008) 1172–1183.
6. J.L. Huppert, Four-stranded nucleic acids: Structure, function and targeting of G-quadruplexes, *Chem. Soc. Rev.* 37 (2008) 1375–1384.
7. Haider, S.M. Neidle, S. Parkinson, G.N. A structural analysis of G-quadruplex/ligand interactions, *Biochimie* 93 (2011) 1239–1251.
8. D. Monchaud, M.P. Teulade-Fichou, A hitchhiker's guide to G-quadruplex ligands, *Org. Biomol. Chem.* 6 (2008) 627–636.
9. J.T. Davis, G-Quartets 40 Years Later: From 5′-GMP to Molecular Biology and Supramolecular Chemistry, *Angew. Chem. Int. Ed. Engl.* 43 (2004) 668–698.
10. Nielsen, M.C.; Ulven, T. Macrocyclic G-Quadruplex Ligands, *Curr. Med. Chem.* 17 (2010) 3438–3448.

11. I. Czerwinska, S. Sato, B. Juskowiak, S. Takenaka, Interactions of cyclic and non-cyclic naphthalene diimide derivatives with different nucleic acids, *Bioorg. Med. Chem.* 22 (2014) 2593–2601.
12. S.M. Hampel, A. Sidibe, M. Gunaratnam, J. Riou, S. Neidle, Tetrasubstituted naphthalene diimide ligands with selectivity for telomeric G-quadruplexes and cancer cells, *Bioorg. Med. Chem. Lett.* 20 (2010) 6459–6463.
13. C. Marchetti, A. Minarini, V. Tumiatti, F. Moraca, L. Parrotta, S. Alcaro, R. Rigo, C. Sissi, M. Gunaratnam, S.A. Ohnmacht, S. Neidle, A. Milelli, Macrocyclic naphthalene diimides as G-quadruplex binders, *Bioorg. Med. Chem.* 23 (2015) 3819-3830.
14. G. Prato, S. Silvent, S. Saka, M. Lamberto, D. Kosenkov, Thermodynamics of Binding of Di- and Tetrasubstituted Naphthalene Diimide Ligands to DNA G-Quadruplex, *J. Phys. Chem. B* 119 (2015) 3335–3347.
15. G.W. Collie, R. Promontorio, S.M. Hampel, M. Micco, S. Neidle, G.N. Parkinson, Structural Basis for Telomeric G-Quadruplex Targeting by Naphthalene Diimide Ligands, *J. Am. Chem. Soc.* 134 (2012) 2723–2731.
16. M. Micco, G.W. Collie, A.G. Dale, S.A. Ohnmacht, I. Pazitna, M. Gunaratnam, A.P. Reszka, S. Neidle, Structure-Based Design and Evaluation of Naphthalene Diimide G-Quadruplex Ligands As Telomere Targeting Agents in Pancreatic Cancer Cells, *J. Med. Chem.* 56 (2013) 2959–2974.
17. M. Nadai, F. Doria, M.D. Antonio, G. Sattin, L. Germani, C. Percivalle, M. Palumbo, S.N. Richter, M. Freccero, Naphthalene diimide scaffolds with dual reversible and covalent interaction properties towards G-quadruplex, *Biochimie* 93 (2011) 1328–1340.
18. F. Doria, A. Oppi, F. Manoli, S. Botti, N. Kandoth, V. Grande, I. Manet, M.A. Freccero, Naphthalene diimide dyad for fluorescence switch-on detection of G-quadruplexes, *Chem. Commun.* 51 (2015) 9105–9108.
19. F. Doria, M. Nadai, M. Folini, M. Scalabrin, L. Germani, G. Sattin, M. Mella, M. Palumbo, N. Zaffaroni, D. Fabris, *et al.*, Targeting Loop Adenines in G-Quadruplex by a Selective Oxirane, *Chem. Eur. J.* 19 (2013) 78–81.

20. F. Doria, M. Nadai, M. Folini, M.D. Antonio, L. Germani, C. Percivalle, C. Sissi, N. Zaffaroni, S. Alcaro, A. Artese, et al., Hybrid ligand-alkylating agents targeting telomeric G-quadruplex Structures, *Org. Biomol. Chem.* 10 (2012) 2798–2806.
21. M.D. Antonio, M. Folini, S.N. Richter, C. Bertipaglia, M. Mella, C. Sissi, M. ManlioPalumbo, M. Freccero, Quinone Methides Tethered to Naphthalene Diimides as Selective G-Quadruplex Alkylating Agents, *J. Am. Chem. Soc.* 131 (2009) 13132–13141.
22. M. Nadai, F. Doria, L. Germani, S.N. Richter, M. Freccero, A Photoreactive G-Quadruplex Ligand Triggered by Green Light, *Chem. Eur. J.* 21 (2015) 2330–2334.
23. Y. Esaki, M.M. Islam, S. Fujii, S. Sato, S. Takenaka, Design of tetraplex specific ligands: Cyclic naphthalene diimide, *Chem. Commun.* 50 (2014) 5967–5969.
24. A.D. Cian, L. Guittat, M. Kaiser, B. Sacca, S. Amrane, A. Bourdoncle, M.P. Teulade-Fichou, P. Alberti, L. Lacroix, J.L. Mergny, Fluorescence-based melting assays for studying quadruplex ligands, *Methods* 42 (2007) 183–195.
25. M.M. Islam, S. Fujii, S. Sato, T. Okauchi, S. Takenaka, Thermodynamics and Kinetic Studies in the Binding Interaction of Cyclic Naphthalene Diimide Derivatives with Double Stranded DNAs, *Bioorganic Med. Chem.* 23 (2015**)** 4769–4776.
26. F.A. Tanious, S.F. Yen, W.D. Wilson, Kinetic and Equilibrium Analysis of a Threading Intercalation Mode: DNA Sequence and Ion Effects, *Biochemistry* 30 (1991) 1813–1819.
27. J.D. McGhee, P.H. vonHippel, Theoretical aspects of DNA-protein interactions: Co-operative and non-co-operative binding of large ligands to a one-dimensional homogeneous lattice, *J. Mol. Biol.* 86 (1974) 469–489.
28. H.A. Benesi, J.H. Hildebrand, A Spectrophotometric Investigation of the Interaction of Iodine with Aromatic Hydrocarbons, *J. Am. Chem. Soc.* 71 (1949) 2703–2707.
29. A. Ambrus, D. Chen, J. Dai, T. Bialis, R.A. Jones, D. Yang, Human telomeric sequence forms a hybrid-type intramolecular G-quadruplex structure with mixed parallel/antiparallel strands in potassium solution, *Nucleic Acids Res.* 34 (2006) 2723–2735.
30. R. Hansel, F. Lohr, S.F. Trantirkova, E. Bamberg, L. Trantirek, V. Dotsch, The parallel G-quadruplex structure of vertebrate telomeric repeat sequences is not the preferred folding topology under physiological conditions, *Nucleic Acids*

Res. 39 (2011) 5768–5775.

31. J.X. Dai, M. Carver, L.H. Hurley, D.Z. Yang, Solution structure of a 2:1 quindoline-c-MYC G-quadruplex: Insights into G-quadruplex-interactive small molecule drug design, *J. Am. Chem. Soc.* 133 (2011) 17673–17680.
32. A.T. Phan, V. Kuryavyi, S. Burge, S. Neidle, D.J. Patel, Structure of an Unprecedented G-Quadruplex Scaffold in the Human c-kit Promoter, *J. Am. Chem. Soc.* 129 (2007) 4386–4392.
33. A. Arora, S. Maiti, Effect of Loop Orientation on Quadruplex-TMPyP4 Interaction, *J. Phys. Chem. B* 112 (2008) 8151–8159.
34. R.F. Macaya, P. Schultze, F.W. Smith, J.A. Roet, J. Feigon, Thrombin-binding DNA aptamer forms a unimolecular quadruplex structure in solution, *Proc. Natl. Acad. Sci. USA* 90 (1993) 3745–3749.
35. M. Toro, R. Gargallo, R. Eritja, J. Jaumot, Study of the interaction between the G-quadruplex-forming thrombin-binding aptamer and the porphyrin 5,10,15,20-tetrakis-(*N*-methyl-4-pyridyl)-21,23*H*-porphyrin tetratosylate, *Anal. Biochem.* 379 (2008) 8–15.
36. A.T. Phan, V. Kuryavyi, K.N. Luu, D.J. Patel, Structure of two intramolecular G-quadruplexes formed by natural human telomere sequences in K+ solution, *Nucleic Acids Res.* 35 (2007) 6517–6525.
37. K.N. Luu, A.T. Phan, V. Kuryavyi, L. Lacroix, D.J. Patel, Structure of the Human Telomere in K+ Solution: An Intramolecular (3 + 1) G-Quadruplex Scaffold, *J. Am. Chem. Soc.* 128 (2006) 9963–9970.
38. Y. Du, D. Zhang, W. Chen, M. Zhang, Y. Zhou, X. Zhou, Cationic N-confused porphyrin derivative as a better molecule scaffold for G-quadruplex recognition, *Bioorganic Med. Chem.* 18 (2010) 1111–1116.
39. S. Nagatoishi, Y. Tanaka, K. Tsumoto, Circular dichroism spectra demonstrate formation of the thrombin-binding DNA aptamer G-quadruplex under stabilizing-cation-deficient conditions, *Biochem. Biophys. Res. Commun.* 352 (2007) 812–817.
40. J. Dash, P.S. Shirude, S.D. Hsu, S. Balasubramanian, Diarylethynyl Amides That Recognize the Parallel Conformation of Genomic Promoter DNA G-Quadruplexes, *J. Am. Chem. Soc.* 130 (2008) 15950–15956.

41. C. Wei, Y. Wang, M. Zhang, Synthesis and binding studies of novel di-substituted phenanthroline compounds with genomic promoter and human telomeric DNA G-quadruplexes, *Org. Biomol. Chem.* 11 (2013) 2355–2364.
42. V. Dhamodharan, S. Harikrishna, C. Jagadeeswaran, K. Halder, P.I. Pradeepkumar, Selective G-quadruplex DNA Stabilizing Agents Based on Bisquinolinium and Bispyridinium Derivatives of 1,8-Naphthyridine, *J. Org. Chem.* 77 (2012) 229–242.
43. R. Kieltyka, P. Englebienne, N. Miotessier, H. Sleiman, Quantifying Interactions Between G-quadruplex DNA and Tranition-Metal Complexes in: P. Baumann, (Eds.), *G-quadruplex DNA Methods and Protocols*, 1st ed.; Humana Press: New York, NY, USA, 2010; pp. 221–256.
44. K.L. Hayden, D.E. Graves, Addition of Bases to the 5′-end of Human Telomeric DNA: Influences on Thermal Stability and Energetics of Unfolding, *Molecules* 19 (2014) 2286–2298.
45. P. Ragazzon, J.B. Chaires, Use of competition dialysis in the discovery of G-quadruplex selective ligands, *Methods* 43 (2007) 313–323.
46. M.P.T. Fichou, C. Carrasco, L. Guittat, C. Bailly, P. Alberti, J.L. Mergny, A. David, J.M. Lehn, W.D. Wilson, Selective Recognition of G-Quadruplex Telomeric DNA by a Bis(quinacridine) Macrocycle, *J. Am. Chem. Soc.* 125 (2003) 4732–4740.

Chapter V

Conclusions and Perspectives

Contents of this chapter have been published in the Bioorgamic & Medicinal chemistry Journal and Molecules Journal (M.M. Islam, S. Fujii, S. Sato, T. Okauchi, S. Takenaka, Bioorganic Med. Chem. 23 (2015) 4769–4776 and M.M. Islam, S. Fujii, S. Sato, T. Okauchi, S. Takenaka, Molecules, 20 (2015) 10963-10979). The materials of the chapter have been reproduced with the permission of the Bioorgamic & Medicinal chemistry Journal and Molecule Journal [1,2].

The stabilization of a specific DNA sequences with small molecule is leading to the development of therapeutics. These small molecules bind with target DNA sequences and regulate the gene expression [3-6]. Recently, DNA secondary structure such as G-quadruplexes DNA stabilizing with small ligand molecules is now considered as a promising target for the development of anticancer drugs [3]. But the selectivity of ligands binding to G-quadruplexes DNA still now are controversial. So, the designing and development of more specific ligands for G-quadruplexes DNA stabilization are crucial.

In my doctoral thesis, I have presented two different types of cNDIs (**1**,**2**) as a new DNA interactive compounds which I dealt with during my doctoral research. In particular, my effort have been directed towards synthesis and design of two new cNDIs, one cyclic linker chain was designed by piperazine and amide group through the benzene ring named

as cNDI **1**. Another type of cyclic linker chain was designed by tertiary amine and amide group through the benzene ring named as cNDI **2**.

Subsequently, in order to evaluate the activity of the newly synthesized molecules, I have studied their ability in binding and stabilizing different types of DNA such as dsDNA (calf thymus DNA (CT-DNA), poly[d(A-T)]$_2$, or poly[d(G-C)]$_2$) and G-quadruplex DNA (a-core and a-core TT as a human telomeric DNA, c-kit and c-myc as DNA sequence at promoter region, or thrombin binding aptamer (TBA)) structure as well as their selectivity towards G-quadruplexes DNA with respect to duplex DNA. To these aims, several experimental techniques have been used such as UV-Vis spectroscopy, Circular Dichroism (CD) spectroscopy, Stopped-flow kinetics, Topoisomerase I assay, Thermal melting stability, FRET-melting assay, TRAP assay and computer modeling studies.

Firstly**,** I have studied the comparison of the interaction of studies between **1** and **2** with dsDNA**.** Using UV-Vis studies, I have found high binding affinity of **1** to dsDNA in the range of 6×10^5-5.3×10^6 M^{-1} with covering four base pairs of DNA per molecule, which are approximately 10 times higher than **2**. The binding studies of **1** with poly[d(G-C)]2 indicated approximately 5 times higher than **3**, where **3** covered two base pairs of DNA as threading intercalator. Thermodynamic studies of **1** and **2** indicated the endothermic and entropy dependent hydrophobic interaction played major role in the reaction. Compound **1** showed more entropically favorable than **2**, whereas **3** showed exodothermic and enthalpy dependent binding to CT-DNA played main role in the interactions. The analysis of salt ion effect showed that the high salt concentration reduced

the binding of cNDIs with CT-DNA. Kinetics studies of **1** and **2** indicated that **1** slowly dissociated from GC base pair than **2**, which comes from the unique bis-intercalative binding mode like a catenane formation with stairs of double stranded DNA. The CD spectra indicated that **2** can induce the CT-DNA structure. The Topoisomerase I unwinding assay of circular dsDNA further supported favorable bis-intercalation binding of **1** than **2**.

Secondly, I have studied the interaction of **2** and **3** with different types of G-quadruplexes DNA and compared this study with our previously reported **1** [7] which have long linker chain than **2**. Compound **2** revealed high binding affinity in the range of 10^6-10^7 M^{-1} to G-quadruplexes DNA whereas reducing the binding affinity with dsDNA. Compound **2** revealed 6 times higher binding constant than **3** with a-core G-quadruplex DNA. The binding data indicated that **2** has 270 times preferable binding for a-core, 165 times for a-core TT, 51 times for c-kit, 108 times for c-myc, 95 times for TBA over dsDNA. The binding stoichiometry of cNDI-G-quardruplex is 2:1, suggesting an end staking binding mode. Compound **2** revealed 200 times binding selectivity over our previously reported **1** [7]. I have observed that **2** showed better binding to telomeric mixed hybrid types of a-core G-quadrulex DNA over promoter region's parallel types of c-kit and c-myc G-quadrulex DNA and thrombin binding aptamer (TBA) antiparallel chair types of G-quadrulex DNA. The CD spectra showed cNDI molecule induced G-quardruplexes DNA structure which also indicated the end staking interaction between cNDIs and G-quadruplexes DNA. Upon the addition of **2** to a-core G-quadruplex DNA, CD spectra conformation little changed indicating mixed hybrid structure a little changed to hybrid-1 types G-quadruplex DNA structure [8]. Thermal melting measurement

indicated that **2** highly stabilized with the G-quardruplexes DNA structure. Comparing with **1** [5], **2** increased ΔT_m by 5-8 $^{\circ}$ C. The FRET melting assay was measured to determine the competitive binding among the G-quardruplexes DNA, the result showed **2** highly preferable stabilization to F21T which is the generated from the human telomeric G-quardruplex DNA sequences. This novel **2** can also inhibit the telomerase activity at low sub-micro-molar (0.9 μM) concentration. The results indicated that **2** is an important class of G-quadruplex stabilizing ligands compared with dsDNA.

The interesting result from biochemical, biophysical and biological points of view, encourage further development of cNDIs derivatives to find out more specific binding G-quadruplexes ligands. These newly design cNDIs deserve for further analysis of the mechanisms of action inside the cancer cell lines by these compounds, due to G-quadruplexes binding drug candidate and the possible pharmacological applications.

Reference

1. M.M. Islam, S. Fujii, S. Sato, T. Okauchi, S. Takenaka, Thermodynamics and kinetic studies in the binding interaction of cyclic naphthalene diimide derivatives with double stranded DNAs, *Bioorganic Med. Chem.* 23 (2015) 4769–4776.

2. M.M. Islam, S. Fujii, S. Sato, T. Okauchi, S. Takenaka, A Selective G-Quadruplex DNA-Stabilizing Ligand Based on a Cyclic Naphthalene Diimide Derivative, *Molecules*, 20 (2015) 10963-10979.

3. R.R. Tidwell, D.W. Boykin, Dicationic DNA minor groove binders as antimicrobial agents in: M. Demeunynck, C. Bailly, W.D. Wilson, (Eds.), *Small Molecule DNA and*

RNA Binders, Wiley-VCH Verlag GmbH & Co. KGaA, Weinheim, Germany, 2004, pp. 414-460.

4. P.G. Baraldi, A. Bovero, F. Fruttarolo, D. Preti, M.A. Tabrizi, M.G. Pavani, R. Romagnoli, DNA minor groove binders as potential antitumor and antimicrobial agents, *Med. Res. Rev.* 24 (2004) 475-528.
5. B.A.D. Neto, A.A.M. Lapis, Recent developments in the chemistry of deoxyribonucleic acid (DNA) intercalators: Principles, design, synthesis, applications and trends, *Molecules* 14 (2009) 1725-1746.
6. R. Palchaudhuri, P.J. Hergenrother, DNA as a target for anticancer compounds: methods to determine the mode of binding and the mechanism of action, *Curr. Opin. Biotechnol.* 18 (2007) 497-503.
7. I. Czerwinska, S. Sato, B. Juskowiak, S. Takenaka, Interactions of cyclic and non-cyclic naphthalene diimide derivatives with different nucleic acids, *Bioorg. Med. Chem.* 22 (2014) 2593–2601.
8. Y. Du, D. Zhang, W. Chen, M. Zhang, Y. Zhou, X. Zhou, Cationic N-confused porphyrin derivative as a better molecule scaffold for G-quadruplex recognition, *Bioorganic Med. Chem.* 18 (2010) 1111–1116.

The author

Md. Monirul Islam has studied his doctoral course from October, 2012 to September, 2015 at the biological chemistry laboratory with professor Takenaka's group in the department of applied chemistry. He has completed undergraduate and master's course in the department of biotechnology and genetic engineering in 2009 and 2010 respectively. In the future, his interested research fields are nucleic acid chemistry, biological chemistry and drug development.